STUDIES ON OCEAN SURFACE LAYER RESPONSES TO ATMOSPHERIC FORCING IN THE NORTH INDIAN OCEAN

Thesis submitted in
partial fulfilment of the requirements
for the award of

DOCTOR OF PHILOSOPHY

in

Oceanography

UNDER FACULTY OF MARINE SCIENCES

by

JOSSIA JOSEPH K.

Department of Physical Oceanography
Cochin University of Science and Technology
Cochin 682 016

October 2011

DECLARATION

I hereby declare that the thesis entitled, "**Studies on ocean surface layer responses to atmospheric forcing in the North Indian Ocean**" is an authentic record of the research work carried out by me under the supervision and guidance of Dr A N Balchand, Professor, Department of Physical Oceanography, Cochin University of Science and Technology, in partial fulfilment of the requirements for the award of the Ph.D. degree in the Faculty of Marine Sciences and no part thereof has been presented for the award of any other degree in any University / Institute.

Cochin-16 Jossia Joseph K
October 2011

CERTIFICATE

This is to certify that this thesis titled, "**Studies on ocean surface layer responses to atmospheric forcing in the North Indian Ocean**" is an authentic record of the research work carried out by Ms. Jossia Joseph K. under my supervision and guidance at the Department of Physical Oceanography, Cochin University of Science and Technology, in partial fulfilment of the requirements for the Ph. D. degree of Cochin University of Science and Technology under the Faculty of Marine Sciences and no part thereof has been presented for the award of any degree in any University.

Cochin-16
October 2011

Dr. A N Balchand
Department of Physical Oceanography
(Supervising Guide)

ACKNOWLEDGEMENT

It is with great zeal and humility I acknowledge all support and help received from great many people, whose contributions in many ways are immeasurable and invaluable for the completion of this research work of mine and without which this study could never have been accomplished.

At the outset, I wish to express my deep sense of gratitude and thanks to supervising guide Dr. A. N. Balchand, Professor and Head, Department of Physical Oceanography, Cochin University of Science and Technology, for the valuable guidance, untiring support and encouragement extended throughout the period of my research work. His ideas and expertise in the subject helped a lot in defining the scope of this study, developing its structure and contributed greatly in improving the manuscript of this research. I could never have completed this study without his relentless support and patience and I was fortunate enough to receive his guidance in abundance at every stage of this research work.

I am extremely thankful to Dr. M. G. Joseph, Scientist, NPOL, and my project guide, for his guidance, suggestions and inspiring discussions. I gratefully acknowledge his role in moulding this research work. Dr. P. V. Hareeshkumar, Scientist, NPOL nurtured my interest in this field and his constant advice inspired me a lot to take up this study. I express my sincere gratitude to his support and encouragement.

It is with great pleasure and immense gratitude that I wish to acknowledge the fruitful discussions I had with Dr. P. V. Joseph, Director (Retd.), IMD and Prof. V. P. Narayanan Nampoori, Professor, International School of Photonics, CUSAT. I would also thank Dr. R. Sajeev and Dr. Benny N. Peter for their encouragement and support. Thanks to Mr. P. K. Saji, for his valuable suggestions and for providing the materials for part of this study. I am indebted to all my beloved teachers who have enlightened my life with their knowledge and wisdom. I record my sincere thanks to the office staffs of Department of Physical Oceanography, for all the help rendered.

I am grateful to Dr. S. Kathiroli, Director, National Institute of Ocean Technology, Chennai, for the encouragement and for the facilities provided during the period of

the research work. With great pleasure and immense gratitude, I wish to acknowledge the encouragement and support extended by Prof. M. Ravindran, Founder Director, NIOT. My special thanks to Mr. K. Premkumar, Former Program Director, National Data Buoy Program, for his encouragement, support and advice during his term at NDBP. Special note of thanks and obligations to Dr. G. Latha and Mr. P. R. Rajesh, my reporting officers, who greatly helped me to carry out this research work, even under busy work schedules and tighter deadlines.

Within these few words I acknowledge the support and encouragement received from the Ocean Science Group during my tenure at NPOL. Mr. V. Chander, Former Director, Dr. R. R. Rao, Head, Ocean Science Group and Dr. C. V. K. Prasada Rao, Principal Investigator are greatly acknowledged for giving me the opportunity to work under SAC project in NPOL. Dr. Basil Mathew, Dr. Nimmi R Nair, Dr. K.V. Sanilkumar, Dr. N. Mohankumar, Mr. Gopakumar, Dr. M.R. Santhadevi, Dr. M.G. Radhakrishanan, Mr. P.V. Nair, Dr. J. Swain, Dr. O. Vijayakumar, Dr. P. Madhusudanan, Mr. V. V. James and Mrs. Hema are also acknowledged for their caring encouragement and moral support. I thank the reviewers for their constructive comments and criticisms. I am very much thankful to my colleagues Aruna, Jitu and my friends Baheeja, Seema and Rose for their friendship and support.

I am also very much indebted to my friends at CUSAT for their wits, wisdom and support throughout the period of this work. Dr. M. S. Madhusoodanan, Dr. K. Ajith Jospeh, Dr. K. Rasheed, Dr. Venu G. Nair, Dr V. Madhu and Mrs. M. G. Sreedevi are greatly acknowledged for their constant support and encouragement. I place on record with thanks, the support and help rendered by the office staff of my Department at CUSAT. My sincere thanks to Abhilash, Anand, Asharaf, Johnson, Lorna, Neema, Prasanth, Rajesh, Rajith, Sajith, Sandhya, Sanjana, Smitha, Sooraj and Suchithra. Their understanding and friendship is a memorable period in my life.

I am specially benefited by the support from NDBP team during my tenure at the division. It is my duty to thank for their sincere efforts, dedication and hard work. Many untold sacrifices were made by them to maintain the moored buoy network in Indian Seas which provided the critical data for this research work. I greatly acknowledge Dr. Harikrishnan, Rajesh, Venkatesh, Sundar, Siva and Savithri for

their moral support, encouragement and friendship. Mr. Velmurugan is greatly acknowledged for the constant support in documenting the results. I convey my special acknowledgement to Saravanan, Rajavel, Arul, Gowtham, Senthil, Selva, Vimala, Sailani and Chithra for their indispensable help.

My parents are the beacon of light that shines thru my life, I am grateful to God for blessing me with such wonderful parents. I thank them for their selfless love, encouragement, support and patience throughout my life as well in my studies. I thank my loving sisters Mini, Anitha, Julie and Almie who have always been a source of strength to me. I am thankful to my brothers James, Benny, Justine and Jose for their love, support and encouragement. Many thanks to my in-laws for their love and support.

In a different note, I thank my husband, Siby, for his encouragement, support and constructive criticism that motivated me to think beyond the subject. His insistence on simplicity and quality has greatly helped me to improve the presentation. His gifted sense of humour, active support and silent care are greatly cherished, which made the final stages of this work more enjoyable.

I would like to thank each and everyone who were part of this academic pursuit of mine and helped me to completely write the last lines of this thesis.

Above all, I thank almighty God for all His blessings.

CONTENTS

CHAPTER I

Introduction

The oceans and the atmosphere are closely linked to form one of the most dynamic component of the climate system. The surface layer is the region of the ocean that is in constant contact with the atmosphere, and through which all air-sea interaction takes place. Energy is transferred from the atmosphere to the ocean surface layer that influences the upper ocean characteristics and in turn, energy from the ocean is fed back to the atmosphere affecting the atmospheric circulation, the weather and the climate. The passage of a tropical cyclone over any warm tropical ocean is one of the best examples of air-sea interaction, which stimulates several modes of oceanic variability. The behaviour of the ocean during normal atmospheric conditions and that during extreme weather conditions exemplifies the role of atmospheric forcing in determining the resultant characteristics of the ocean. The energy and momentum transfer from wind to water, and its transfer to remote locations and further to deep oceans, vary in time and space and this plays an important role in determining the dynamics of the upper ocean.

The Indian Ocean is the smallest of the major oceans and is considered by many investigators to be the most complex and the least understood oceanographically. Interestingly, this area is most dynamic because of the changing wind patterns associated with the Indian monsoons. The periodic reversals in the winds and associated changes in the current pattern of the upper ocean in this semi enclosed basin makes it unique compared to the Atlantic or Pacific Oceans. The limited northward extent, presence of warmest Sea Surface Temperature (SST) in the

southeastern Arabian Sea warm pool, the Indian Ocean Dipole, tele-connections with ElNiño/LaNiña, etc. further adds to the unique nature of the North Indian Ocean. Many of the physical phenomena which are well understood in other oceans remain to be explored in detail for North Indian Ocean and thus it makes a perfect basin to study the various aspects of upper ocean response to the passage of cyclone, in particular and its spatio-temporal variability. The present study addresses the details of oceanic response and its variability associated with passage of cyclones.

1.1 Cyclones

A warm-core, non-frontal, synoptic-scale low-pressure system, originating over tropical and sometimes subtropical waters, with an organized deep convection, and a closed surface wind circulation about a well-defined center is referred as cyclone. Once formed, a tropical cyclone is maintained by the extraction of heat energy from the ocean at relatively higher temperature and promotes heat export to the low temperatures of the upper troposphere. Depending on sustained surface winds, the system is classified as tropical disturbance, tropical depression, tropical storm, or tropical cyclone within category 1- 5. The cyclone is accompanied by thunderstorms, and circulation of winds near the Earth's surface, which is clockwise in the southern hemisphere and counter-clockwise in the northern hemisphere.

Research at Colorado State University has proved the importance of the surrounding environment with horizontal and vertical wind shear playing significant roles in thermodynamic processes which determine the formation of a tropical cyclone (Gray, 1979). There are six environmental factors that influence the formation of a tropical cyclone - a critical value of earth's vorticity, low-level relative vorticity, vertical wind shear, minimum SST of 26-27^{o}C, potentially unstable troposphere and mid-troposphere humidity. Almost all these factors are satisfied in tropical oceans at any time especially during the summer. Among these, the changes in low level vorticity and vertical wind shear leads to favourable cyclonic conditions.

Cyclones mainly draw their energy from the warm water of the tropics and latent heat of condensation thereof. Sufficient depth in mixed layer, apart from a minimum SST,

is also required, since as the tropical cyclone gains energy from the ocean and favoures upwelling. If the upwelled water is too cool, the ocean may no longer be capable of sustaining the development process in atmosphere. Thus, a stationary cyclonic disturbance will not often develop if the depth of the warm surface layer is too shallow.

The passage of a tropical cyclone over the warm tropical ocean stimulates several modes of oceanic variability. Price *et al.* (1994) reported that the ocean's response occurs in two stages-forced stage and relaxation stage. The forced stage response is the local response excited by the strong wind stress during the passage of cyclone, includes the mixed layer currents (Sanford *et al.*, 1987) and substantial cooling of the mixed layer and sea surface (Black, 1983; Stramma *et al.*, 1986; Ginis and Dikinov, 1989) and this consists of a geostropic current and an associated trough in sea surface height. The relaxation response is the non local baroclinic response to the wind stress curl following the passage of cyclone. The time scale of the forced stage response is the cyclone's residence time (half day). The relaxation stage response is comparatively longer (5-10 days), which is the e-folding of mixed layer currents (Price, 1983 and Gill, 1984).

1.2 Oceanic response to the cyclone passage

The oceanic response to the passage of a cyclone depends on a number of air-sea parameters with maximum response to intense, slow moving cyclones. Price (1981), Shay *et al.* (1992), Price *et al.* (1994), Dickey *et al.* (1998), Jacob *et al.* (2000) and Morey *et al.* (2006b) studied in detail the upper ocean temperature response to the passage of cyclones. Marked asymmetry in SST response is reported about the cyclone track, with maximum response on the right side. However the rightward bias is less for slow moving cyclones compared to that for rapidly moving cyclones (Price, 1981). Price *et al.* (1994) reported the details of various factors that determine the structure and amplitude of the upper ocean currents generated by cyclone passage, also in two stages. The strong wind stress in forced stage generates mixed layer currents with a time scale equal to the residence period of the cyclone. During

relaxation stage, the energy of the mixed layer currents are dispersed as near inertial frequency currents that penetrate into the thermocline, in response to the wind stress curl of the cyclone (Geisler, 1970 and Gill, 1984). Similar to that of SST, significant rightward bias is observed in mixed layer currents caused by the asymmetry in wind field. The wind stress vector rotates clockwise on the right side of the track and remains nearly parallel with the mixed layer currents and generates inertial currents which propagate to a greater distance and depth (Jacob *et al.*, 2000).

1.2.1 SST and mixed layer cooling

The SST response depends on the mixed layer thickness with larger response in thinner mixed layer and in steep upper thermocline temperature gradient (Price, 1981 and Morey *et al.*, 2006b). There is marked asymmetry in the general wind field on both sides of the track with clockwise rotation of the wind vector on right side and anticlockwise rotation on left side of the track in northern hemisphere (Cardone *et al.*, 1977 and Price, 1981). The wind stress and stress curl are in near-resonant coupling with mixed layer currents on the right side of the track and forces high mixed layer velocities. This results in significant drop of SST, caused by the strong entrainment and near inertial mixed layer currents on right side of the cyclone track (Federov *et al.*, 1979; Pudov *et al.*, 1979 and Price, 1981).

Morey *et al.* (2006a) studied the upper ocean response to surface heat and momentum fluxes associated with a major hurricane Dennis (July 2005) in the Gulf of Mexico. He reported with the help of a numerical model that surface heat fluxes are primarily responsible for widespread reduction (0.5° to 1.5°C) of SST and momentum fluxes are responsible for stronger surface cooling (2°C) near the center of the storm. Mahapatra *et al.* (2007) reported a shift in the region of maximum surface cooling to the left of the cyclone track in the coastal region of the landfall owing to the importance of coastal dynamics and bottom topography.

There is strong cooling in the mixed layer directly beneath the cyclone track due to intense upwelling. The upwelling considerably enhances the entrainment under slowly moving hurricanes and reduces the rightward bias of the SST response. The pressure

gradients set up by the upwelling and the horizontal advection play an important role in dispersing energy from the mixed layer after the passage of cyclone (Chang and Anthes, 1978 and Price, 1981). The cooling directly beneath the cyclone track is in two stages- direct cooling and post storm cooling. The direct cooling is much lesser than post storm cooling and the magnitude decreases with depth. The cooling depends on many factors including ocean structure beneath the storm (i.e. location), storm speed, time of year and storm intensity (Cione and Uhlhorn, 2003).

1.2.2 Inertial Oscillations

On a non-rotating earth, in the absence of any force the water in motion will move in the same direction at the same speed unless otherwise it is opposed by an external force. But in a rotating earth, the moving water will experience Coriolis force. In the northern hemisphere (southern hemisphere) the Coriolis force deflects the water parcel to the right (left) at right angles to the direction of motion which will result in the water parcel to move in a circle. These oscillations continue even after the forcing stops as a consequence of inertia and is referred as inertial oscillation.

The inertial oscillation is considered as the manifestation of unforced ocean dynamics. It is the balance between the rate of change of velocity and Coriolis force (Gill, 1982). Webster (1968) reported that inertial currents occur at all depths in the ocean with velocities ranging from 10 to 80 cm/s. The amplitude varies depending on the strength of generating mechanisms and they decay due to friction when the forcing stops (Pond and Pickard, 1986). Generally inertial oscillations are observed after the passage of cyclones. The direction of rotation is clockwise (anticyclonic) in northern hemisphere and is anticlockwise (cyclonic) in southern hemisphere.

The inertial period (T) is a function of Coriolis force (f), which in turn varies with latitude and hence it increases towards the equator.

$T = 2\pi/f$ where $f = 2\Omega\sin(\Phi)$, 'Ω' (7.292 x 10^{-5} rad/s) is the angular velocity of the earth and 'ϕ'is the latitude of observation. The radius of the circle is: $r = V/f$ where '*V*' is the inertial current speed.

The forcing perturbations and the availability of energy in the ocean system is expected to generate inertial oscillations. Wind forcing is a major initiator of the inertial oscillation (Pollard, 1970; Pollard and Millard, 1970; Weller, 1982 and Poulian *et al.,* 1992). The horizontal temperature gradients in the ocean interacting with the vertical mixing may also generate sustained inertial oscillations (Pedlosky and Stommel, 1993). Lien *et al.* (1996), Brink (1989), Shay and Chang (1997), Firing *et al.* (1997), Saji *et al.* (2000) and Jacobs *et al.* (2001) have reported inertial oscillations after the passage of various cyclones. The inertial oscillations are initially excited primarily in the surface mixed layer and then propagate down into the thermocline and away from the forcing region (Lien *et al.,* 1996). Garret (2001) and Chiswell (2003) proved that deep inertial oscillation could penetrate only towards equator. The duration of the wind as compared with the inertial period is the most important factor, which governs the amplitude of the inertial oscillation (Gonella, 1971). The largest inertial amplitude reported so far is 1.7 m/s associated with an unusually large and strong hurricane Gloria (Price *et al.,* 1994). This maximum amplitude was found in the mixed layer to the right rear quadrant of the storm. Shenoi and Antony (1991), Rao *et al.* (1996), Saji *et al.* (2000), Hareeshkumar *et al.* (2001) and Joseph *et al.* (2007) have reported inertial oscillations in the North Indian Ocean under various meteorological conditions.

There is marked asymmetry in circulation pattern on both the sides of the cyclone track. The near inertial oscillations are stronger where the wind direction rotates clockwise, resonating with the inertial oscillations. It happens on the right side of the track in northern hemisphere and left side of the track in southern hemisphere. These inertial currents exist for a period of a few weeks, which depends on the intensity of the cyclone and the local dynamics. The inertial band account for more than 50% of the total kinetic energy in the mixed layer (Pollard, 1980 and Thomson *et al.,* 1998).

The frequency of inertial oscillation depends mainly on the local latitude, but generally the observed frequency varies from the theoretical value. Factors affecting the frequency of the inertial oscillations are latitudinal variation of Coriolis factor, which is capable of generating mean eastward or westward drift (Ripa, 1997), divergence in the quasi geostrophic flow field (Weller, 1982), vorticity in the quasi geostrophic flow field (Mooers, 1975 and Perkins, 1976), dissipation of energy through friction or other means (Pollard, 1970) and stratification and eddy viscosity of the water (Gonella, 1971). Many studies have reported a shift between the theoretical and the observed frequencies (White, 1972; Kundu, 1976; Millot and Crepon, 1981 and Saji *et al.,* 2000, Elipot, *et al.,* 2010). The observed inertial frequency less (higher) than the theoretical frequency is termed as red (blue) shift. Gonella (1971) has reported that the difference is smallest when the transfer of momentum is at a maximum due to the homogeneity of the surface layer. Thomson *et al.* (1998) have reported a blue shift of 1.3 % in the northeast Pacific. White (1972) suggested that frequency shift observed in the equatorial currents were due to a positive doppler shifting of the frequency of the inertial wave by the zonal mean flow past the moored system. The lowering of the inertial frequency is possible through the large-scale flow altering background vorticity (Mooers, 1975; Perkins, 1976 and Weller, 1982). The dissipation of inertial oscillation energy by the bottom friction or turbulent mixing downward from the surface layer is another reason for lowering of inertial frequency (Pollard, 1980). Poulian (1990) and Jacobs *et al.* (2001) reported a red shift in the observed inertial frequency in North Pacific and Korea Strait respectively. Salat *et al.* (1992) reported a red shift of 10% in the shelf-slope front off northeast Spain.

1.2.3 Surface wave

The passage of a tropical cyclone generates violent waves which are a major threat to the navigation in the open ocean and turns disastrous as it approaches the coast. The cyclonic wind induced wave height increases significantly with intensity of the cyclone. Kumar *et al.* (2001 and 2003) studied in detail the estimation of wind speed and wave height during cyclones and found that the empirical relation holds good when the wave height is more than 3 m. In another study, Kumar *et al.* (2004) analysed the wave characteristics off Visakapatnam, during the passage of a cyclone

in November 1998 and reported significant variability in wave spectra during cyclone passage. The swells generated by the cyclone travel long distance, thereby affecting the distant locations. Cyclone generated waves play a significant role in design of coastal and offshore structures (Young, 2003).

Apart from the above, the upper ocean responds in many folds to the passage of a tropical cyclone which has significant impacts on the physical, chemical and biological properties. The wind induced mixing produces significant change in chlorophyll-a concentration and salinity of the upper ocean. The increase in primary productivity associated with the cyclone passage and the subsequent increase in phytoplankton biomass has been an active field of research (Shiah *et al.,* 2000, Madhu *et al.,* 2002, Vinayachandran and Mathew, 2003 and Vinayachandran *et al.,* 2005). However, the present study has been aimed at identifying in detail the properties of reduction in SST, cooling of the mixed layer, the inertial oscillations and the modification on waves associated with the passage of tropical cyclones.

1.3 Cyclones in North Indian Ocean

The north Indian Ocean is subdivided into two tropical cyclone areas, the Arabian Sea (AS) and the Bay of Bengal (BoB). The frequency and intensity of tropical cyclone experienced in this area are less compared to other oceans, on an average six occurrences per year, which is about 6.5% of cyclone occurrences (wind speeds greater than or equal to 17m/s) in the world waters (Neumann, 1993 and McBride, 1995). The BoB is the area of higher incidence of cyclones compared to AS because of the favorable conditions and is about 5 to 6 times the frequency in the Arabian Sea (Dube *et al.,* 1997 and Chinthalu *et al.,* 2001). These disturbances move towards north, northeast or northwest based on various cyclone parameters such as seasonality, initial position, intensity, speed and size of the cyclone (Deo *et al.,* 2001).

The tropical cyclones in the North Indian Ocean exhibit significant temporal variation in which the seasonal variation is more remarked than the annual variation. The variability in cyclone genesis is associated with the location of the thermal equator as it moves north and south with seasons (Lal, 1991; Menon, 1997 and Asnani, 2005).

India Meteorological Department (IMD) has prepared a detailed atlas on the tracks and frequency of storms for the period 1877-1990. The first part describes the cyclones during the period 1877 to 1970 and the second part during the period 1971 to 1990 (IMD, 1979 and IMD, 1992). The cyclone tracks available in the Unisys website for the period 1945 to 2006 also exhibits significant inter-annual and seasonal variability in terms of the originating area, intensity, track, and landfall.

The cyclones in BoB are most destructive, when they strike the low lying coastline. The piling up of water due to the funnel shape of the coastline and the narrow continental shelf combined with the high population density along the coastal areas amplifies the damage and loss of property. Interestingly, vulnerability to storm surges is not uniform along Indian coasts in terms of height of the storm surge and frequency of occurrence. And, of course, east coast of India faces higher vulnerability than that along west coast. Among the cyclones that crossed the coasts of India, the most disastrous as indicated by were as given below:

- The cyclone that hit Calcutta in October 1737 coinciding with a violent earthquake, accounts for a toll of 3,00,000 lives accompanied by a 12m high storm surge (Lander and Guard, 1998).
- Midnapore Cyclone of October 1942 was accompanied by gale wind speed of 225 km/hr.
- Rameswaram Cyclone of December 1964 wiped out Dhanuskodi in Rameswaran Island from the map with storm surge of 3-5m.
- Bangladesh Cyclone of November 1970 took toll of about 3,00,000 people with storm surge of 4-5m (Lander and Guard, 1998).
- Andhra Cyclone of November 1977 took a toll of about 10,000 lives with maximum wind speed of 200 km/hr and storm surge of 5m (Lander and Guard, 1998).
- Orissa super cyclone of October 1999 has been estimated for maximum wind speed of 260-270 km/hr in the core area which produced a huge storm surge that

led to pile up of more than 6m of water and took a toll of nearly 10,000 people (Kalsi and Srivastava, 2006).

Many studies have been conducted recently on the various aspects of the Orissa super cyclone (October 1999), one of the most destructive cyclones in Indian history. Most of these studies address the cyclone genesis, intensification, forecasting the track, landfall and other atmospheric parameters (Rajesh *et al.*, 2005; Kalsi and Srivastava, 2006; Bhaskar Rao and Hariprasad, 2006; Loe *et al.*, 2006 and Kalsi, 2006). The upper ocean response to the passage of cyclones are addressed by Nayak *et al.* (2001), Madhu *et al.* (2002), Vinayachandran and Mathew (2003); they focused on the biological response and the impact on primary productivity. Mahapatra *et al.* (2007) studied the transformation of the upper ocean's response in the near-coastal waters to the 1999 Orissa super cyclone using a 3-dimensional model. He reported region of maximum surface cooling on the left of the cyclone track which indicates the importance of coastal dynamics and bottom topography in upper ocean response.

Rao (1986, 1987), Rao and Sivakumar(1998), Premkumar *et al.* (2000), Rao and Premkumar (1998), Shenoi *et al.* (2002), and Sengupta *et al.* (2002) reported the significant reduction in SST and mixed layer cooling associated with the passage of various cyclones in the North Indian Ocean. Sengupta *et al.* (2007) reported that pre-monsoon and post monsoon cyclones differ significantly in the reduction of SST in North Bay of Bengal. He reported that a shallow upper layer of freshwater due to river runoff and monsoon rains reduces the cooling during post monsoon cyclones.

The response of upper ocean physical and biological properties to the passage of May 2003 cyclone in the southern Bay of Bengal reports a decrease in SST up to 5°C, associated with the deepening of mixed layer by about 12m (Smitha *et al.*, 2006). Changes in the current pattern associated with cyclone passage are reported in many studies. Saji *et al.* (2000) and Joseph *et al.* (2007) reported the inertial oscillation generated by the passage of cyclones from buoy observations in the BoB.

1.4 Objectives

The time series observations along the track of a tropical cyclone are very crucial for understanding the oceanic response and its variability. However the observations in the cyclone track are limited, especially the *in-situ* time series observations. There are many studies, which report the atmospheric characteristics and upper ocean responses during the passage of cyclones in world oceans. The majority of the reports on cyclone passage in North Indian Ocean concentrate on the atmospheric parameters of tropical cyclone, its genesis, intensification and forecasting whereas the report on oceanic response are limited due to the inadequate *in-situ* observations. In this context, the North Indian Ocean requires detailed studies of this aspect, especially the spatio-temporal variability. The establishment of moored buoy network in 1997 in the Indian Seas provided a wealth of information regarding the upper ocean characteristics and this could thereon disclose the oceanic response to cyclone passage and its spatio-temporal variability. The present study is a first of its kind to understand the characteristics of inertial oscillation and its variability in North Indian Ocean utilizing moored buoy observations, as most apt choice.

The objectives of this study are:

- To understand the upper ocean response to extreme atmospheric forcing due to cyclones in the North Indian Ocean highlighting the reduction in SST, cooling of the mixed layer, inertial oscillation and the response in the wave characteristics.
- To analyse the spatio-temporal variability of cyclone frequency in North Indian Ocean with an emphasis on the inter-comparison between AS and BoB.
- To identify the relative importance of various factors that controls the upper ocean response to cyclones highlighting the cooling in SST.

1.5 Scheme of the thesis

The doctoral thesis has been arranged into six chapters. The first chapter gives a general introduction to the ocean surface layer responses on the passage of cyclones with reviews related to the significant reduction in SST, the mixed layer response, the inertial oscillations and change in wave characteristics. A detailed literature review on the above aspects depicting the studies carried out elsewhere and specifically, in the North Indian Ocean is presented in this chapter.

The details of data sets used and the various mathematical and analytical methods applied in this study are given under chapter II.

Chapter III deals with the spatio-temporal variability in cyclone frequency in North Indian Ocean. The inter-annual, intra-annual and spatial variability of tropical cyclones in the North Indian Ocean are addressed in detail. The long term observations of monthly average SST and sea level pressure are also utilized to identify the role of local dynamics in the spatio-temporal variability of cyclones.

The upper ocean response to cyclone passage in North Indian Ocean are addressed in two chapters. Chapter IV deals with the characteristics of oceanic response in AS and Chapter V describes the same in BoB. The drop in SST, the sudden increase in wave height, change in current pattern, fluctuations in wind direction, rotation in surface current direction etc. are studied in detail, utilizing the *in-situ* buoy observations during the passage of cyclones. The spatial response of the upper ocean has been studied utilizing the TMI-SST data. Detailed analysis of the variability in oceanic response and important conclusions are provided at the end of each chapter.

Chapter VI presents the conclusion of the study listing all major findings and its implications. The asymmetric response in wave characteristics is also presented. The oceanic response to cyclones in terms of intensity, relative location, proximity to track and drop in SST are analysed in detail with an emphasis on variable response between AS and BoB.

Reference list is appended.

CHAPTER II

Data and Methods of Analysis

2.1 Introduction

The study of upper ocean response to atmospheric forcing in North Indian Ocean reports the various aspects associated with the passage of cyclones and its variability. A detailed study requires long term time series data with sufficient spatial coverage. The ocean's response to a cyclone passage is a typical example where we require high frequency time series data to report the sudden fluctuations in the upper ocean. The moored buoy data, which provides values at every three hours, is a wealth of information for studies with characteristics/variability pertaining to a wide range of frequencies. However the moored buoy data is not adequate to study the spatial variability of forcing and its responses in upper ocean. Hence a combination of *in-situ* observations (moored buoy data) as well as satellite data in North Indian Ocean pertaining to the period of study is analysed to delineate the variability in atmospheric forcing and upper ocean response.

The cyclone track information available in the Unisys website during the period from 1947 to 2006 is utilized to understand the variability during the extreme wind forcing. Data analysis methods such as Progressive Vector Diagram (PVD), Power Spectrum, Rotary Spectrum and Wave spectrum along with appropriate presentation methods are utilized in this study.

2.2 Data

The moored data buoy observations and satellite data sets are used in this study to identify the response of atmospheric forcing in the upper ocean. The buoy data provides information on high frequency variability of ocean responses at a particular point whereas the satellite data sets provide the spatial variability as well as the temporal variability.

2.2.1 Moored buoy data

Time series observations of surface meteorological and oceanographic parameters from NIOT moored data buoys from September 1997 to December 2006 are utilised for this study. The moored buoys are floating platforms (Fig 2.1) designed to carry specific suit of sensors to measure meteorological and oceanographic parameters. The SEAWATCH Wavescan buoy (http://www.oceanor.no/related/Datasheets-pdf/SW06_SEAWATCH_Wavescan_Buoy_FINAL.pdf) from Oceanor-Norway is used to establish the moored buoy network in Indian Seas. These data buoys are equipped with sensors to measure air temperature, sea level pressure, wind, Sea Surface Temperature (SST), surface current and wave parameters. The buoys are also equipped with global positioning system, beacon light and satellite transceiver. These buoys are powered by batteries and are charged by solar panels during daytime. The details of wavescan buoy instrumentation and operation are provided in the website http://www.oceanor.no/systems/seawatch/buoys-and-sensor/wavescan along with the information about the operation and maintenance in Indian waters http://www.oceanor.no/systems/seawatch/Seawatch-systems/seawatch-india.

Buoy Type	: Discus
Total Weight	: 950 Kg
Diameter of hull	: 2.2 m
Buoy length - over all	: 5.85 m
Natural heave frequency	: 0.5Hz
Reserve Buoyancy	: 2000 kg

Fig. 2.1: The NIOT moored buoy and its characteristics

Oceanor 'GENI (GEneral INterface)' is an operating system onboard the wavescan buoy, which is an interface and processing unit between sensors, various processes and the satellite system (http://www.oceanor.no/related/Datasheets-pdf/SW02_Fugro_OCEANOR_GENI.pdf). GENI enables all sensors to operate at regular intervals (at every three hours), and the processed data are stored on buoy hard-disk and transmitted through satellite to the shorestation established at NIOT.

The surface wind observations are made at a height of 3m above the sea surface and are extrapolated to the standard 10m height using the power law (Panofsky and Dutton, 1984). Water temperature, conductivity and current observations are made at a depth of 2.5m below the sea surface. Some of the deep sea buoys are fitted with thermistor chain upto a depth of 122m with 15 elements at specific depths. These elements are located at 2m, 7m, 12m, 17m, 22m, 27m, 32m, 37m, 42m, 47m, 52m, 57m, 72m, 97m and 122m depths. The details of accuracy, range, resolution and make/user manual are given in Table 2.1.

Table 2.1: Moored Buoy Sensor Specifications

Parameter	Range	Accuracy	Resolution	Sampling Durn & Freq.	Sensor make and Reference
Air Temperature	-30 ^{o}C – 75 ^{o}C	± 0.1^{o}C	0.01^{o}C	10 min, 1Hz	Omega's RTD Sensor http://www.omega.com/pptst/RTD-805_RTD-806.html
Sea Level Pressure	700hPa–1100hPa	±0.1hPa	0.01hPa	1 min, 1Hz	Vaisala PTB200 barometer http://www.vaisala.com/Vaisala%20Documents/User%20Guides%20and%20Quick%20Ref%20Guides/PTB200_User_Guide_in_English.pdf
Wind Speed**	0 – 60 ms^{-1}	±1.5% FS	0.07 ms^{-1}	10 min, 1Hz	Lambrecht wind sensor - 1453 S2 http://www.merazet.pl/pliki/produkty/533_2.pdf
Wind Direction**	0 – 359^{o}	± 1^{o}	0.1^{o}	10 min, 1Hz	
Current Speed*	0 – 6 ms^{-1}	± 1cms^{-1}	0.01cms^{-1}	10 min, 1Hz	NE Sensortec UCM-60, Ultrasonic current meter http://www.sensortec.com/pdfs/UCM-60%20Product%20Sheet.pdf
Current Direction*	0 – 359^{o}	± 2^{o}	0.01^{o}	10 min, 1Hz	
Sea Surface Temperature*	-5 – +45^{o}C	± 0.005^{o}C	0.001^{o}C	10 min, 1Hz	
Wave Height	0 – 20m	5 cm	1cm	17 min, 1Hz	Seatex MRU ftp://poseidon.hcmr.gr/pub/mru4.2/Man_user_mru_r11.pdf
Wave Direction	0 – 359^{o}	± 0.05^{o}	0.01^{o}	17 min, 1Hz	

* Measurement at a depth of 2.5 m below the sea surface

** Measurement at a height of 3m above the sea surface

Various quality control procedures such as spike test, range test, stuck value test, location test etc. are carried out using the tailor made software 'ORKAN' provided by the buoy manufacturer (Reed, *et al.,* 1990 and Thrane, 1999). Orkan provides a data base with application programs for storage of time series. This helps to run a set of programs that decode, store, retrieve, process, analyze and present data in ORKAN system**.**

The data gaps of less than a day in the buoy data are filled using three point Lagrangian interpolation scheme whereas the gaps of more than a day are left as it is. The gap filled data sets with sufficient number of observations are only utilized for spectral analysis. The temperature profile available during September 1997 (DS3-A and DS5-A) and June 1998 (DS1) are utilized to study the vertical variability of temperature during the passage of cyclone. The temperature profile is also used to study the penetration of the inertial oscillation to deeper layers. Data from 12 moored buoys are utilized in this study of which 11 are deep sea buoys and one shallow water buoy (Fig. 2.2 and Table 2.2).

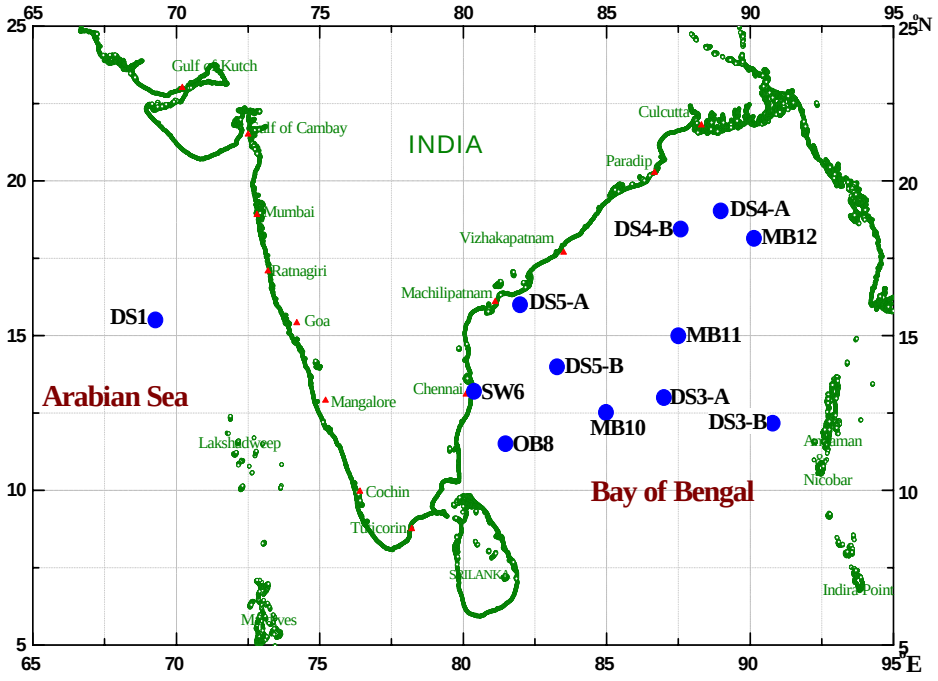

Fig. 2.2: Location map of the moored buoy network in Arabian Sea and Bay of Bengal utilized in the present study

Table 2.2: Details of data buoy locations

Sl No	Buoy-Id	*Location	Lat (^{o}N)	Long (^{o}E)	Depth (m)
1.	DS1	off Goa (1998-2007)	15.50	69.25	3800
2.	DS3-A	off Chennai (from 1997-1999)	13.00	87.0	3200
3.	DS3-B	off Chennai (from 2000-2007)	12.15	90.75	3100
4.	DS4-A	off Paradip (1997-March 1998)	19.03	88.98	1700
5.	DS4-B	off Paradip (June 1998-2007)	18.30	87.60	2200
6.	DS5-A	off Machilipatnam (1997-1998)	15.99	81.98	1050
7.	DS5-B	off Machilipatnam (2000-2007)	14.03	83.25	3200
8.	MB10	off Mahabalipuram (2003-2007)	12.51	84.98	3230
9.	MB11	off Ramaypatnam (2003-2007)	14.99	87.50	2807
10.	MB12	off Visakhapatnam (2003-2007)	18.14	90.14	2200
11.	OB8	Off Cuddalore (2003-2007)	11.50	81.47	3510
12.	SW6	off Ennore (1997-2000)	13.01	80.32	17

* Nomenclature follows the place name of the nearest location on mainland

2.2.2 ARGO data

The vertical profiles obtained through ARGO (Array for Real-time Geostrophic Oceanography) floats are excellent information regarding the vertical structure of the ocean. These floats record temperature and salinity profiles while sinking to (rising from) the predetermined depth, stays afloat for few days (5 or 10 days), rises to the surface, transmits the data to satellites and again sinks. The data is transmitted to the ground station and is immediately available via the Global Telecommunication System (GTS) and also on the internet after quality check. Data from ARGO floats during the cyclone in May 2003 and April 2006 have been utilized for the present study. The profiles are recorded at an interval of five days and 12 profiles comprising the pre cyclone, cyclone and post cyclone periods are analysed to estimate the effect of cyclone in the upper ocean dynamics. The data is downloaded from the website: http://www.incois.gov.in/argo.

2.2.3 Cyclone track data

The Joint Typhoon Warning Centre (JTWC) provides detailed information during the passage of cyclones in the North Indian Ocean. The Unisys Weather and Hurricane utilizes this information and provides cyclone track since 1945 in North Indian Ocean. The details of the cyclone tracks along with wind speed, air pressure and category of cyclone provided in the Unisys website (http://www.weather.unisys.com/hurricane) are utilized to identify the ocean response to extreme wind forcing and its variability.

Table 2.3: Saffir-Simpson Scale

Type	**Category**	**Pressure (mb)**	**Winds (knots)**	**Winds (mph)**	**Surge (ft)**
Tropical Depression	TD	-----	< 34	< 39	0
Tropical Storm	TS	-----	34-63	39-73	0-3
Cyclone	Cy-1	> 980	64-82	74-95	4-5
Cyclone	Cy-2	965-980	83-95	96-110	6-8
Cyclone	Cy-3	945-965	96-112	111-130	9-12
Cyclone	Cy-4	920-945	113-135	131-155	13-18
Cyclone	Cy-5	< 920	>136	>156	>19

The data set also provides a text based table of tracking information along with charts. The table includes position in latitude and longitude, maximum sustained winds in knots, and central pressure in milli bars. The category of cyclones is classified based on the wind speed following Saffir-Simpson Scale (Table 2.3). The cyclone translation speed is calculated at buoy locations and TMI-SST extraction point using the track details.

2.2.4 Satellite data

The Tropical Rainfall Measuring Mission (TRMM) Microwave Imager (TMI) SST is utilized in this study to understand the spatial/temporal variability of SST during the passage of various cyclones in the North Indian Ocean. The TMI-SST is available from 06 December 1997 covering a region extending from 40^{o}S to 40^{o}N at a pixel resolution of 0.25x0.25deg. Three day average values (average of 3 days with third day as the file date) of TMI-SST are downloaded from the website: http://ssmi.com/.

2.2.5 Other Data Sets

To identify the role of local dynamics in the distribution of cyclone frequency in North Indian Ocean, the monthly average values of SST and Sea Level Pressure (SLP) during the period 1947 to 2006 are utilized. The monthly average Extended Reconstructed Sea Surface Temperatures, version 3 (ERSST.v3), is available at a resolution of 2x2 degree grid since January 1854. The analysis is based on the International Comprehensive Ocean-Atmosphere Data Set (Smith *et al.,* 2008). The ASCII data is available at website: ftp://eclipse.ncdc.noaa.gov/pub/ersst/.

The Hadley Centre's monthly historical mean sea level pressure (MSLP) data set (HadSLP2) is based on rich terrestrial and marine data compilations and covers the period since 1850. A series of quality control tests were carried out on the terrestrial pressure series and marine observations from the International Comprehensive Ocean Atmosphere Data Set. The quality controlled data sets blended together and gridded over a spatial resolution of 5x5 degree. MSLP fields were made spatially complete using reduced space optimal interpolation (Allan and Ansell, 2006). The data is available at ftp://ftp.cdc.noaa.gov/Datasets.other/hadslp2/slp.mnmean.nc

2.3 Methods of analysis

The result of any research/study greatly depends on the data analysis methods adopted and it varies with the type of data sets and the intended application. The presentation of results using an appropriate plotting method is also equally important (Chambers *et al.,* 1983). Hence different spectral analysis (Jenkins and Watts, 1968) and visualization methods are utilised in this study to arrive at the pertinent result. The methods used in this study are: Progressive Vector Diagram (PVD), Power Spectrum, Wave Spectrum and Rotary Spectrum.

2.3.1 Progressive Vector Diagram (PVD)

The PVD simulates Lagrangian display from Eulerian measurements and is used to estimate the time-integrated displacement of vector measurements (Neumann and Pierson, 1966; Emery and Thomson, 1997). It exhibits the relative displacement of fixed point measurements at any point of time as if in a lagrangian measurement. The

starting location (x_o,y_o) is the origin and (u_i,v_i) represents the vector measurements at 'i^{th}' point of time at an interval of 'Δt'. The cumulative displacement (x_i, y_i) is calculated at each point of time. The time series plot of these points shifted in time by one step and converted to space units (m or km) provides the progressive vector diagram. The time series observations of surface current is presented with the first observation starting from the origin and then progresses according to the direction and speed of each observation.

2.3.2 Spectral Analysis

Spectral analysis is used to partition the variance of a time series as a function of frequency (Jenkins and Watts, 1968). The present study utilizes Power spectrum to estimate the frequency distribution in the temperature profile of moored buoys and Rotary cross spectral analysis to estimate the inertial oscillation observed in the surface current data. The wave spectrum is used to delineate the variable response in wave field associated with cyclone passage.

2.3.2.1 Power Spectrum

The power spectrum provides the estimate of power (energy per unit time) of the data distributed over a range of given frequency bins (Press *et al.,* 1992). The discrete Fourier transform of an N-point sample of the function *c(t)* at equal intervals are carried out which provide the following coefficients

$$C_k = \sum_{j=0}^{N-1} c_j e^{2\pi ijk/N} \quad k = 0, \ldots, N-1$$

the periodogram estimate of the power spectrum is defined at N/2 + 1 frequencies as

$$P(0) = P(f_0) = \frac{1}{N^2}|C_0|^2$$

$$P(f_k) = \frac{1}{N^2}\left[|C_k|^2 + |C_{N-K}|^2\right] \qquad k=1,2,.....(N/2-1)$$

$$P(f_c) = P(f_{N/2}) = \frac{1}{N^2}|C_{N/2}|^2$$

where f_k is defined only for the zero and positive frequencies

$$f_k = \frac{k}{N\Delta} = 2f_c\frac{k}{N} \qquad k=0,1,2,.....(N/2)$$

By Parseval's theorem the above equation is normalized so that the sum of the *'N/2+1'* values of *'P'* is equal to the mean squared amplitude of the function c_j (Emery and Thomson, 1997). As a solution to the problem of leakage, data windowing is implemented in spectrum analysis. The inbuilt functions of FFT and power spectrum using Welch's window in MATLAB are used to compute the power spectrum of the time series data.

2.3.2.2 Rotary Spectrum

The rotary spectral analysis is utilized to estimate the inertial oscillation observed in the surface wind, wave and current (Gonella, 1972). The time series data is converted into an earth referenced Cartesian co-ordinate system consisting of two orthogonal components –the horizontal component and vertical component.

To carry out the rotary spectral analysis, the vector measurement (*u, v*) is split into clockwise and counterclockwise rotating circular components (A^-, θ^-; and A^+, θ^+) where A^- and A^+ are the amplitudes and θ^-, θ^+ are the relative phases respectively (Emery and Thomson, 1997).

In rotary spectral format, the current vector $\omega(t)$ can be written as the Fourier series

$$\omega(t) = \overline{u(t)} + \sum_{k=1}^{N} U_k \cos(\omega_k t - \phi_k) + i\left[\overline{v(t)} + \sum_{k=1}^{N} V_k \cos(\omega_k t - \theta_k)\right]$$

$$= \overline{u(t)} + i\overline{v(t)} + \sum_{k=1}^{N} U_k \cos(\omega_k t - \phi_k) + i V_k \cos(\omega_k t - \theta_k)$$

in which $\overline{u(t)} + i\overline{v(t)}$ is the mean velocity, $\omega_k = 2\pi f_k = 2\pi k / N\Delta t$, is the angular frequency, $t(= n\Delta t)$ is the time and (U_k , V_k) and (θ_k , Φ_k) are the amplitudes and phases, respectively, of the Fourier constituents for each frequency, for the real and imaginary components. The rotary components are derived by expanding the trigonometric functions.

The counter clockwise and clockwise rotary component amplitudes are:

$$A_k^+ = \frac{1}{2}\left\{\left[U_{1k} + V_{2k}\right]^2 + \left[U_{2k} - V_{1k}\right]^2\right\}^{1/2}$$

$$A_k^- = \frac{1}{2}\left\{\left[U_{1k} - V_{2k}\right]^2 + \left[U_{2k} - V_{1k}\right]^2\right\}^{1/2}$$

and the corresponding phase angles for time t=0, are:

$\varepsilon_k^+ = \tan^{-1}[V_{1k} - U_{2k}]/[U_{1k} + V_{2k}]$

$\varepsilon_k^- = \tan^{-1}[U_{2k} + V_{1k}]/[U_{1k} - V_{2k}]$

The one-sided spectra $(G_k^+, G_k^-) = (S_k^+, S_k^-)$ for the two oppositely rotating components for frequencies $f_k = \omega_k / 2\pi$ are:

$$S_k^+ = \frac{(A_k^+)^2}{N\Delta t}, \qquad f_k = 0,.....,1/(2\Delta t)$$

$$S_k^- = \frac{(A_k^-)^2}{N\Delta t}, \qquad f_k = -1/(2\Delta t),.....,0$$

The mean kinetic energy or the total spectrum is : $S_t = S_k^+ + S_k^-$

The corresponding rotary coefficient is, $r(\omega) = \frac{S_k^+ - S_k^-}{S_t}$,

where '*r*' ranges from '-1' (clockwise rotation) to '+1' (counter clockwise rotation) and *r*=0 represents unidirectional flow. The sign of the rotary coefficient differs from that of Gonella (1972), to link the clockwise rotation with negative rotary coefficient as explained in Emery and Thomson (1997). The value of r = ±1 indicates circular motion where the combined vector is determined by one component and the other can be neglected. The specific phase difference at the inertial peak is estimated from the rotary spectrum. Rotary spectrum is specifically used in inertial oscillation studies, where one of the rotary component –the clockwise component in the northern hemisphere and the counterclockwise component in southern hemisphere- significantly dominate the other.

2.3.2.3 Wave Spectrum

The moored data buoys are equipped with a MRU (Motion Reference Unit) for wave measurements which outputs absolute roll, pitch, compass and heave. Acceleration, velocity of linear motions and angular velocity are also available. The wave data is measured at a rate of one Hz for 17 minutes at every three hours. The processor on the buoy applies wave analysis software known as NEPTUN (Torsethaugen, and Krogstad, 1979), which uses a Fast Fourier Transform on the wave record to obtain power spectrum. In the wave spectrum, measurements between 0.04 - 0.5Hz is utilized for estimating various components (Table 2.4). Both directional and non-directional analysis was carried out to calculate a range of wave parameters.

Table 2.4: Definitions of the wave parameters

m_o, m_1.. (m_k)	Moments of the spectrum about the origin $\int_{0.04}^{0.5} f^k s(f) df$ where s(f) is the spectral density
Hm0	Estimation of Sig. Wave Height = $\sqrt{4}\ m_0$
Tm02	Estimatione of avg. wave period = $\sqrt{}\ m_0/m_2$
Mdir	Mean of the wave direction of whole spectrum

2.4 Visualization of data and results

The majority of the data sets utilised in this study belong to time series observation and most of them represent a point observation. Hence simple line diagrams are used to display the variability of the time series data and were plotted in Microcal-Origin. MATLAB, powerful software for various data analysis methods is used in data analysis and visualization of data. The spatial variability of a data set can be best represented in a contour plot and hence the Hovmöller diagrams depicting the time-longitude variability during cyclone passage were plotted using the Surfer package and Grid Analysis and Display System (GrADS).

CHAPTER III

Temporal and Spatial Variability of Cyclone Frequency in North Indian Ocean

3.1 Introduction

The north Indian Ocean is subdivided into two tropical cyclone areas, Arabian Sea (AS) and Bay of Bengal (BoB). The frequency and intensity of cyclones experienced in North Indian Ocean are less compared to other oceans (Neumann, 1993 and McBride, 1995). The BoB is the area of higher incidence of cyclones with 5 to 6 times than the frequency in AS (Dube et.al, 1997). Even with lesser percentage of occurrence compared to the global value, the cyclones in North Indian Ocean cause severe damage to life and property along the coastal belt of India. Hence, any change in cyclone characteristics (frequency, intensity etc.) has significant impact on the coastal population and industrial belt.

Cyclone variability has been an active field of research in all ocean basins. Significant changes in cyclone frequency and intensity are reported in many studies (Goldenberg *et al.,* 2001; Pielke, *et al.,* 2005 and Trenberth, 2005) but most of them addressed Pacific and Atlantic Oceans. Sudden decrease in cyclone activity during mid-1970's is reported due to the transition in atmosphere-ocean climate system and an associated change in storm tracks across large part of Northern Hemisphere (Folland and Parker, 1990; Trenberth 1990; Miller *et al.,* 1993 and McCabe *et al.,* 2001). Webster (2005) reported significant decrease in the frequency of cyclones throughout the planet excluding the

North Atlantic Ocean. He has also reported a great increase in the number and proportion of intense cyclones. Changes in the cyclone frequency and intensity associated with climate variability is reported in North Indian Ocean as well (Ali and Chowdhury, 1997; Ali, 1999; Singh *et al.*, 2001a and Singh *et al.*, 2001b), but most of them focused on the variability in BoB. This chapter addresses the spatial and temporal variability of cyclone frequency in North Indian Ocean during the study period of 1947 to 2006.

3.2 Data

The cyclone track data during the period 1947 to 2006, provided by 'Unisys Weather and Hurricane' is utilized in this study to identify the variability in cyclone frequency in North Indian Ocean. Considering the unavailability of cyclone intensity during the first half of the study period, the low pressure systems under all categories (tropical depressions, tropical storms and cyclone categories 1 to 5) is addressed as cyclones in the present study. Significant decrease in the frequency of cyclones is observed after the year 1976 and consequently the analysis is carried out as two parts-up to and after 1976. The inter-annual and intra-annual variability of cyclones significantly differs between AS and BoB and hence addressed separately.

To identify the role of increasing SST on cyclone variability, monthly SST values from Extended Reconstructed Sea Surface Temperatures (ERSST.v3) during the period 1947 to 2006 is utilized. The Hadley Centre's monthly historical mean sea level pressure (MSLP) data set (HadSLP2) during the period 1947 to 2004 is also analyzed to find out the possible relationship with cyclone frequency. The SST (at 0^oN, 6^oN, 10^oN, 14^oN and 18^oN) and SLP (0^oN, 5^oN, 10^oN, 15^oN and 20^oN) data at various latitudes are extracted along 70^oE in AS and 90^oE in BoB. The SST and SLP data are further analysed by extracting the monsoon months (June to September) to identify the possible relation with the sudden decrease in cyclone frequency during monsoon period after 1976. The average monsoon SST and annual average SST and SLP values are smoothed on a five year scale to eliminate the high frequency variations in the data set.

3.3 Inter-annual variability

The inter-annual variability of cyclones in the North Indian Ocean does not exhibit any significant natural cycles during the period under study. One striking feature is the substantial decrease in the number of cyclones in AS and BoB after the year 1976 (Fig. 3.1). However the reduction in cyclone frequency in AS is not so intense as that of BoB. Cyclone frequency indicates a reduction of 39.1% in AS after 1976 whereas that in BoB is 71.4% (Table 3.1).

The cyclone frequency in AS varies from a minimum of 0 to a maximum of 5 with an average of 2 cyclones in a year. There are 12 years without any occurrence of cyclones and maximum of 5 cyclones during the years 1972, 1975 and 1998. The highest number of occurrences is reported during periods 1959-1964, 1970-1976, 1998 and 2004. The period 1980-1991 exhibit strikingly less number of cyclones.

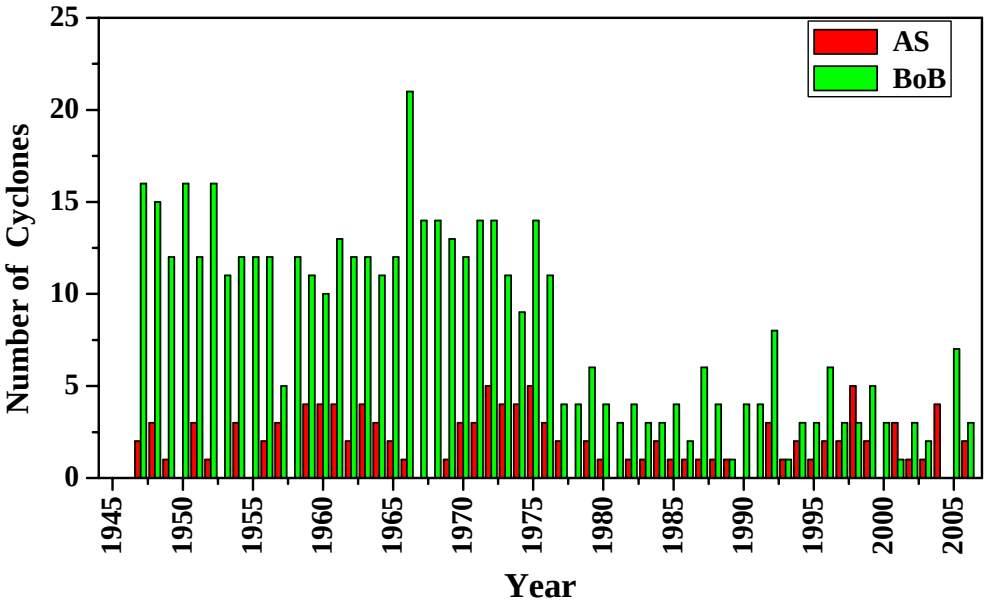

Fig. 3.1: Inter-annual variability of cyclones during the period 1947-2006

Substantial decrease in cyclone frequency is observed in BoB after the year 1976. During the first half of observation, the number of cyclone varies from a minimum of 5 (during 1957) to a maximum of 21 (during the year 1966). The second half of observation varies between a cyclone free year 2004 and a maximum of 8 during the year 1992.

There is no significant correlation between the frequency of cyclones in AS and BoB, even though the cyclone free years in AS are coincident with higher occurrence in BoB. The 60 year data does not exhibit any significant cyclic oscillation neither as a whole nor in individual basins. However, substantial decrease in cyclone frequency is observed after the year 1976.

Table 3.1: Statistics of cyclone frequency during 1947 to2006

	1947-1976		1977-2006	
	AS	BoB	AS	BoB
Total number of cyclones	70	379	43 (40%)	107 (73(%)
Annual Minimum	0	5 (1956)	0	0
Annual Maximum	5 (1972,1975)	21 (1966)	5 (1998)	8 (1992)
Annual Average	2.33	12.63	1.43	3.57
Cyclone free years	1950,1953, 1955, 1958, 1967,1968	Nil	1978,1981, 1990, 1991, 2000,2005	2004

3.4 Intra-annual variability

The intra-annual variability of tropical cyclones in North Indian Ocean is more prominent than the inter-annual variation. Considering the significant decrease in cyclone frequency after the year 1976, the data has been grouped into two classes – upto 1976 (1947-1976) and after 1976 (1977-2006). The intriguing observation in intra-annual variability is the substantial reduction in cyclone frequency during monsoon season after 1976 (Fig. 3.2).

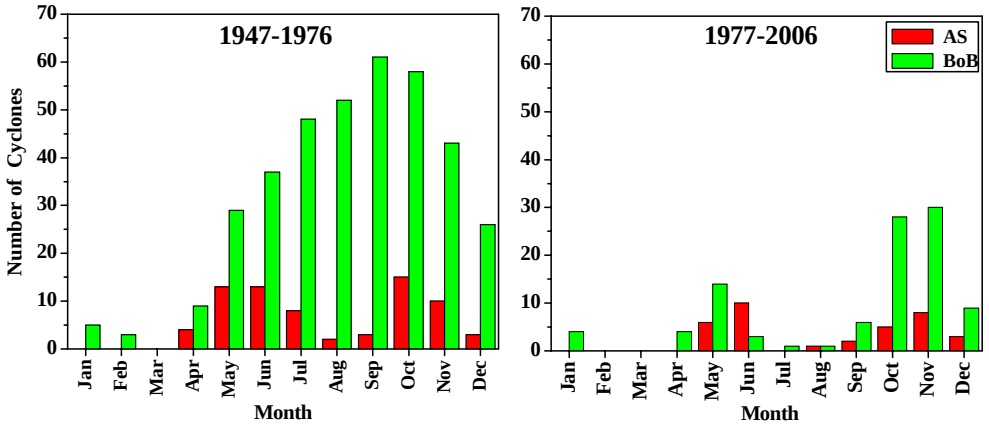

Fig. 3.2: Intra-annual variability of cyclones in AS and BoB during 1947-1976 (left panel) and 1977-2006 (right panel)

3.4.1 Variability During 1947 to 1976

The AS and BoB exhibit significant difference in intra-annual variability of cyclone frequency. The cyclone season starts in both AS and BoB during the month of April. AS exhibits two major cyclone seasons - from April to July and from October to November. The months August, September and December also exhibit a few cyclones in AS with cyclone free months during January to March. BoB exhibits a different picture with an active cyclone season during April to December with maximum frequency during September and October. The month of January and February also reports a few cyclones with a single cyclone free month March (Fig. 3.2).

The AS exhibits bimodal oscillation in annual cyclone frequency whereas that of BoB is unimodal. The months of May and June exhibit higher occurrence of cyclones in AS. The cyclone frequency in AS during the peak of monsoon season (July-September) and during December is comparatively less. A secondary peak in cyclone activity is observed during the post monsoon season (October-November). BoB exhibits a single maximum in annual cyclone frequency which starts in the month of April, increases slowly and reaches maximum in September. The frequency then decreases towards the cyclone free month March. The highest occurrence of cyclones in BoB is reported during the month of October (61 cyclones) followed by November (58 cyclones).

3.4.2 Variability During 1977 to 2006

The intra-annual variability of cyclone frequency during the period 1977 to 2006 exhibits an entirely different scenario than that of the period 1947 to1976 with nearly cyclone free period during southwest monsoon (Fig. 3.2). The discrepancy is pronounced in BoB with considerable reduction in cyclone activity during monsoon season.

AS and BoB exhibit bimodal oscillation in annual cyclone frequency, before and after the southwest monsoon. There are equal chances of cyclone occurrence in AS during both the seasons, whereas BoB indicates higher cyclone frequency during post-monsoon. The pre-monsoon peak in BoB is concentrated mainly during the month of May whereas the post monsoon peak is distributed in October and November.

There is significant reduction in cyclone frequency after 1976. Average frequency of cyclones in AS during 1947-1976 was 2.3, which reduced to 1.4 cyclones per year during 1977-2006. The cyclone frequency reduced from an average of 12.6 to 3.6 cyclones per year in BoB during the second half of the study period (Table 3.1).

3.5 Variability in origin and dissipation of cyclones

The origin and dissipating point of cyclones in North Indian Ocean exhibit large variability in space and time. Considering the significant intra-annual variability in cyclone frequency before and after 1976, the variability in cyclone genesis is also carried out under the same classification.

3.5.1 Variability During 1947 to 1976

The months of January and February have a record of few cyclones originating in BoB whereas the AS remains cyclone free. The cyclones in BoB are generated around 5^{o}N and travel large distances before dissipation, even though most of these cyclones could not make landfall (Fig. 3.3a).

The month of March is absolutely cyclone free with no trace of a single cyclone during the period from 1947 to 1976. However the cyclone season started in April with higher occurrences in BoB. Most of these cyclones were generated around 10^{o}N. The cyclones in AS moved towards northwest while that in BoB moved towards northeast and some of them made landfall before dissipation.

The month of May and June exhibit higher occurrence of cyclones in both AS and BoB. The cyclones generated over a wide region covered the entire BoB, with higher frequency in the northern bay during June. Most of these cyclones in BoB make landfall predominantly crossing land in Bangladesh/northeast coast of India. The cyclones in AS were generated between 5^{o} and 15^{o}N and centered around 70^{o}E. Most of the cyclones in AS moved towards northwest and dissipated before landfall. However, some of the cyclones made landfall in northwest coast of India/ Pakistan.

The cyclones during July and August in BoB are generated over a narrow region around 17^{o}N in the head bay (Fig. 3.3b). All these cyclones move towards northeast and make landfall around the coast of Orissa/West Bengal and traveled longer distances over land before dissipation. The occurrence of cyclones during these months in AS is rare and only a few cyclones are generated near the coast of Gujarat which moved towards east-northeast. Most of the AS cyclones dissipated before landfall.

The month of September has a few cyclones in AS which are originated around 15^{o}N. In BoB the cyclones are originated above 15^{o}N. In both AS and BoB, the cyclones moved towards northeast. The cyclones in BoB made landfall along the east coast of India and that in AS dissipated before landfall.

The month of October has comparatively higher occurrence of cyclones in both AS and BoB with the origin of the cyclone above 5^{o}N. The cyclones in AS were generated near to the coastline of India, whereas the origin of cyclones spread in the entire bay. Similar to that of September, these cyclones also moved towards northeast.

Again the origin of cyclones shifted to the region between 5^{o} to 15^{o}N in both AS and BoB during November and these cyclones moved towards northwest/northeast. Some of the cyclones dissipated before landfall. The origin of cyclones during the month of December was confined to the smaller band of 5^{o} to 10^{o}N. Only a few cyclones were generated in AS compared to that of BoB. These cyclones moved towards either north or northeast. Most of them dissipated before landfall and the remaining, immediately after the landfall.

3.5.2 Variability During 1977 to 2006

The month of January exhibits nearly same frequency of cyclones in BoB whereas AS remains cyclone free as observed earlier. The significant difference is the southward shift in the originating area in BoB. The cyclones moved northward in earlier case whereas the current period exhibits landfall towards northwest (Fig. 3.3a).

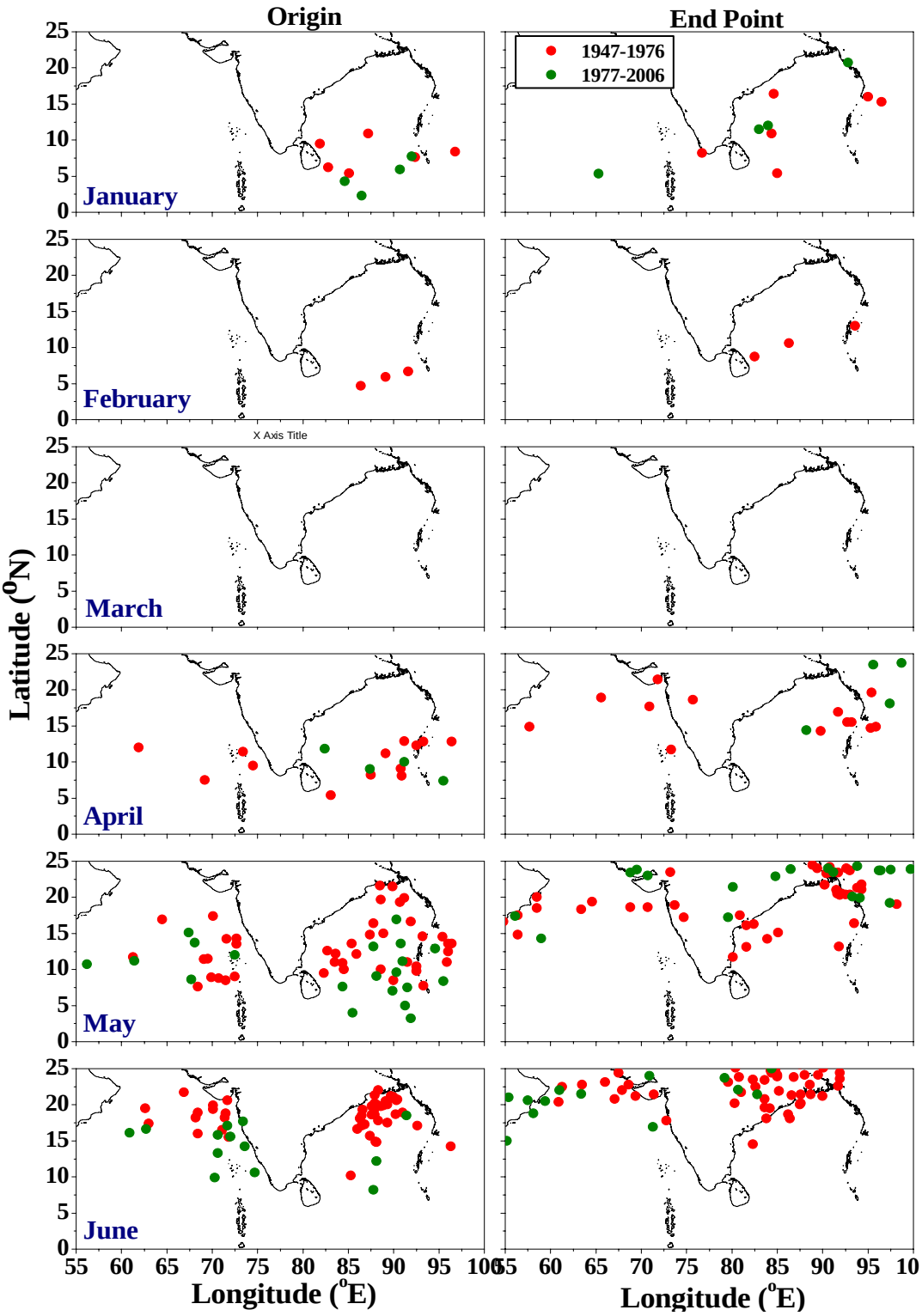

Fig. 3.3a: The intra-annual variability of origin and dissipating point of cyclones during January to June for the period **1947-1976** (•) and **1977- 2006** (•)

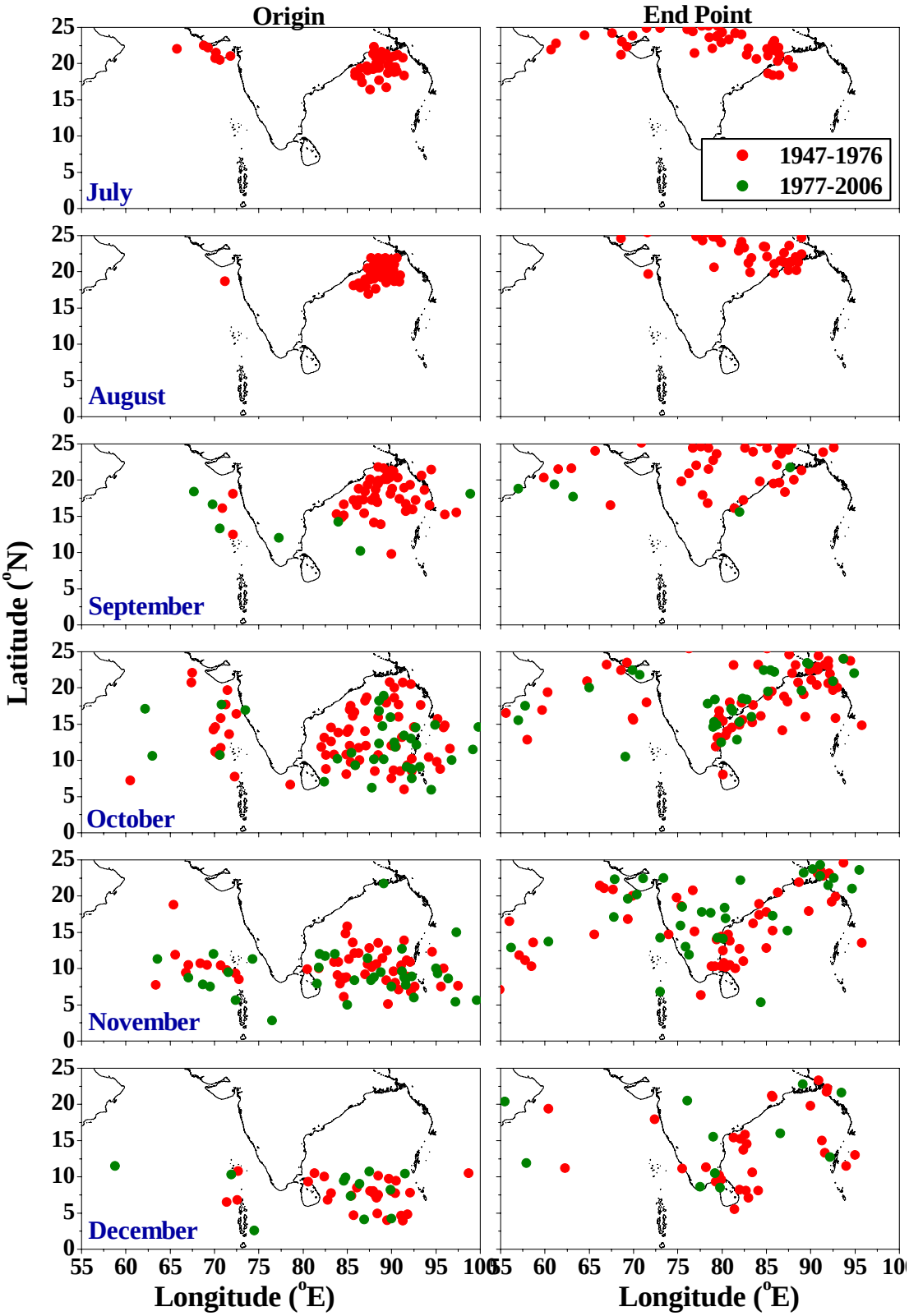

Fig. 3.3b: The intra-annual variability of origin and dissipating point of cyclones during July to December for the period **1947-1976** (•) and **1977- 2006** (•)

The first half of the study period exhibits the occurrence of a few cyclones in BoB during February, which is not observed in the recent records. The month of March exhibit cyclone free month as observed in first half. The cyclone season started in April in BoB as observed during 1947 to 1976. However the AS remained cyclone free in April. The originating area does not exhibit any significant shift during April. However most of them made land fall, whereas those during 1947-1976 failed to make land fall.

The month of May exhibits the beginning of cyclone season in AS. The cyclone frequency is less compared to the earlier observation. As observed in January, the originating area indicates southward shift in BoB and are originated far from the coast. Unlike the earlier period, most of these cyclones made landfall. The cyclone frequency in the month of June exhibits considerable decrease especially in BoB. The originating area indicates significant southward shift in both AS and BoB (Fig. 3.3b). The month of July and August are absolutely cyclone free months in both AS and BoB

The month of September indicates a few cyclones in AS and BoB with significant reduction of cyclone frequency in BoB. The month of October also exhibits considerable reduction in cyclone frequency. Even though there is no southward shift, the originating area is far from the coast and most of them made landfall during October. The months of November and December also exhibit substantial decrease in cyclone frequency in AS and BoB without any significant change in originating area. Unlike the cyclones during 1947-1976, most of these cyclones made landfall.

The cyclone genesis during the period 1977 to 2006 exhibited significant decrease in cyclone frequency. An important feature is the southward shift in originating area during January, May and June in BoB and during June in AS. However there is no significant shift during September to December. The active cyclone months May, June and October exhibited originating area far from the coast. Unlike the cyclones during 1947-1976, most of the cyclones made landfall during 1977-2006. The observation during 1947-1976 exhibits an active cyclone season during southwest monsoon whereas the recent reports exhibit extensive reduction in cyclone activity during southwest monsoon with cyclone free months July and August.

3.6 Cyclone Variability and SST

The average (annual and monsoon period) SST smoothed on a five year scale during the period 1947 to 2006 exhibit the significant increase in SST at various locations (0^o, 6^o,10^o,14^o and 18^oN) along two transects (70^oE in AS and 90^oE in BoB). In general AS exhibits higher spatial variability with strong SST gradient in annual and within monsoon period. A minimum of 27.8^{o}C at 18^oN and a maximum of 29.06^{o}C at equator is reported in annual average SST in AS whereas that of BoB exhibits weaker spatial SST gradient compared to that of AS, with a minimum of 27.93^{o}C at 18^oN and a maximum of 29.06^{o}C at the equator (Table. 3.2). The AS exhibits higher spatial gradient than that of BoB, except between 0^oN and 6^oN. In contrary, BoB exhibits significantly higher annual SST at 0^oN, followed by much lesser spatial gradient between 6^oN to 14^oN and much lower SST at 18^oN. The SST at 0^oN and 10^oN in both the basins are comparable. The difference in SST between AS and BoB at 6^oN is much higher compared to the differences at other latitudes.

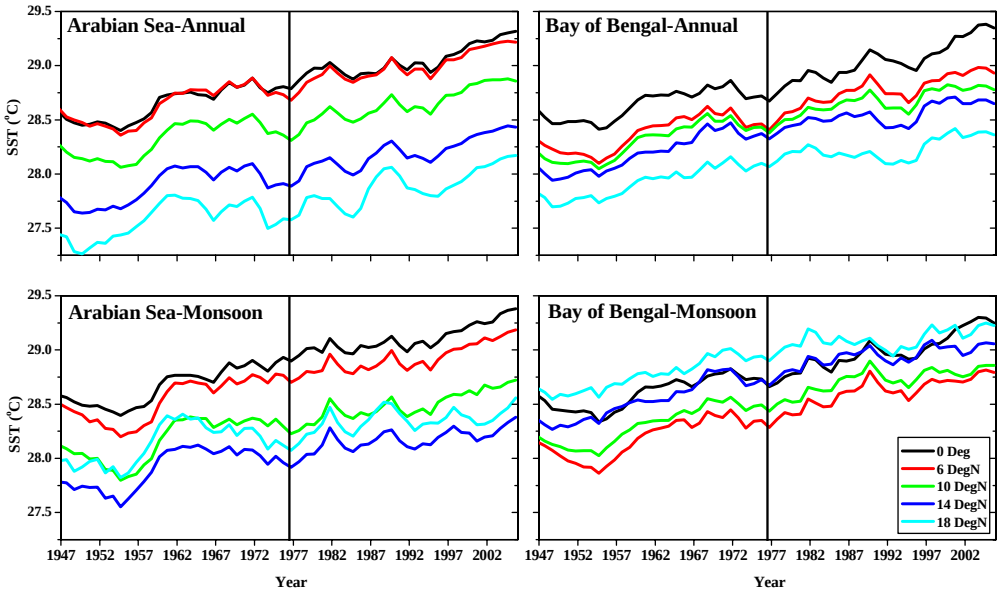

Fig. 3.4: The inter-annual variability of SST at various latitudes along two transects (70^oE in AS and 90^oE in BoB). The top panel depicts the variability of annual average SST whereas the bottom panel displays the variability of monsoon (Jun-Sep) SST. The vertical line indicates the year 1976.

The distribution of monsoon (June to September) SST in AS and BoB exhibits significant difference in heat gain and spatial variability (Fig. 3.4). BoB exhibits an intriguing

pattern with maximum SST at 18°N which decreases gradually reaching the minimum at 6°N and then increases towards the equator. Even though there is no drastic difference in SST pattern after the year 1976, the net heat gain is less at higher latitudes especially at the end of the study period. This could have contributed in the reduction of monsoon cyclones, which are originated in the higher latitudes. The distribution of monsoon SST in AS exhibits a pattern similar to that of annual distribution with maximum SST at the equator, which gradually decreases towards higher latitudes. The lesser frequency of cyclones originated at higher latitudes in AS during monsoon season could de due to the lower SST at higher latitudes compared to that of BoB.

Table 3.2: Average SST and net heat gain at various latitudes. The values in bracket indicate the corresponding values of monsoon SST

Lat. (°N)	Avg. SST (°C) (1947-76)		Avg. SST (°C) (1977-2006)		Heat Gain (°C) (1977-2006) - (1947-1976)	
	AS	BoB	AS	BoB	AS	BoB
0	28.65 (28.68)	28.64 (28.60)	29.06 (29.12)	29.06 (29.0)	0.41 (0.44)	0.42 (0.40)
6	28.64 (28.54)	28.38 (28.19)	29.0 (28.94)	28.78 (28.62)	0.37 (0.39)	0.41 (0.43)
10	28.32 (28.17)	28.31 (28.31)	28.66 (28.50)	28.67 (28.73)	0.34 (0.33)	0.37 (0.41)
14	27.89 (27.91)	28.20 (28.55)	28.21 (28.18)	28.55 (28.95)	0.32 (0.27)	0.35 (0.40)
18	27.58 (28.14)	27.93 (28.78)	27.90 (28.36)	28.24 (29.11)	0.32 (0.22)	0.31 (0.33)

The net heat gain at various latitudes is computed as the difference between average SST during 1977-2006 and during 1947-1976. It is observed that the warming occurred at various latitudes are not uniform in both AS and BoB and exhibits a decreasing trend towards higher latitudes. The maximum heat gain of 0.42°C and 0.41°C are observed at the equator in BoB and AS respectively. The minimum heat gain of 0.32°C in AS and 0.31°C in BoB is reported at 18°N (Table 3.2). The maximum net heat gain (0.44°C) during monsoon was observed at the equator in AS which exhibited a decreasing trend towards higher latitudes and the minimum heat gain (0.22°C) was recorded at 18°N. Thus variable heat gain in AS leads to stronger spatial gradient in temperature. The maximum net heat gain (0.43°C) during monsoon was observed at 6°N in BoB, which decreases

both towards higher latitudes and equator, while reaching a minimum of 0.33°C at 18°N. The net heat gain at higher latitudes in BoB is higher during monsoon than that of the annual value and vice versa in AS (Table 3.2).

Webster, *et.al.* (2005), Holland and Webster (2007) and Elsner *et.al.* (2008) reported an increase in frequency of the high intensity cyclones (cyclone category 4 and 5) associated with an increase in SST. The present study could not attempt the same due to the unavailability of cyclone category information before 1970. An interesting observation is the decreasing trend in net heat gain in SST towards higher latitudes in annual and monsoon SST, which in turn leads to a higher spatial gradient in SST. However there is no significant change in the pattern of SST before and after the year 1976. Hence the noticable reduction in the cyclone frequency in the North Indian Ocean cannot be attributed to the increase in SST alone.

3.7 Sea Level Pressure

The monthly averaged sea level pressure (SLP) during the period 1947- 2004 is analysed to identify the possible relation with the change in cyclone frequency. The SLP is extracted (0°, 5°, 10°, 15° and 20°N) along two transects (70°E in AS and 90°E in BoB), which exhibits more fluctuation in BoB than that of AS (Fig. 3.5).

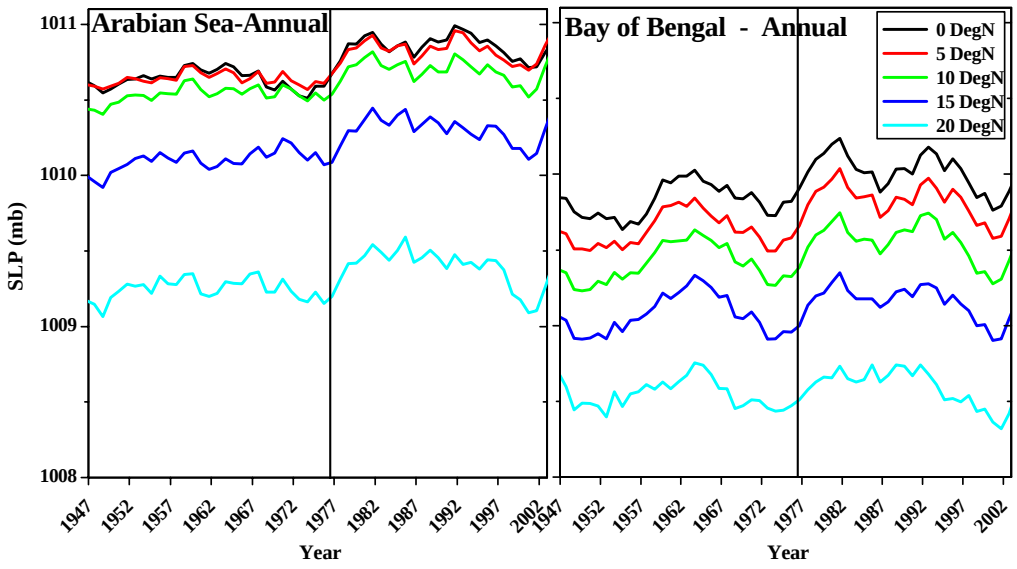

Fig. 3.5: The inter-annual variability of annual average SLP at various latitudes along two transects (70°E in AS and 90°E in BoB). The vertical line indicates the year 1976.

The spatial gradient in SLP increases towards higher latitudes in AS and BoB. However the SLP in AS remains nearly the same between 0^{o}-10^{o}N and exhibits large difference between 15^{o}-20^{o}N (Fig. 3.5). An intriguing observation is the considerable increase in SLP after the year 1975 in both AS and BoB. BoB exhibits a cyclic trend (around 15 years) which is not evident in AS. The increase in SLP in BoB during mid 1970's is accompanied with a change in trend as well. The SLP reaches maximum around the year 1982 followed by a net decreasing trend for the remaining period in AS and BoB. The distribution of monsoon SLP in AS and BoB does not exhibit any significant feature during the reporting period (Fig. 3.6).

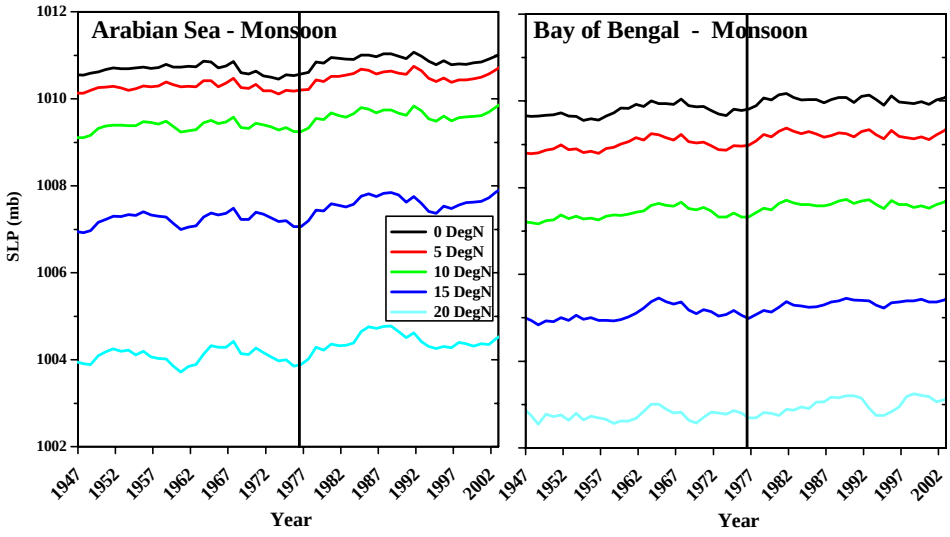

Fig. 3.6: The inter-annual variability of monsoon SLP at various latitudes along two transects (70^{o}E in AS and 90^{o}E in BoB). The vertical line indicates the year 1976.

Trenberth (1990) and Miller *et al.* (1993) reported sudden decrease in winter pacific mean sea level pressure during mid 1970, associated with climate change in 1970's, and is attributed to change in cyclone frequency in Northern Hemisphere. Contrary to that, AS exhibits a sudden increase in SLP around 1975 whereas that in BoB is accompanied with a change in trend as well. The changes in SLP during mid 1970's in AS and BoB might have contributed to the significant change in cyclone frequency appeared after the year 1976.

3.8 Results and Discussion

The cyclones exhibit significant inter-annual variability in both AS and BoB. The cyclone frequency in BoB is much higher than that of AS. However there is no significant correlation between the frequency of cyclones in AS and BoB. One striking feature is the substantial decrease in the annual average cyclones in BoB (from 12.6 to 3.6) and AS (from 2.3 to 1.4) after the year 1976. AS exhibited 39.1% reduction in cyclone activity whereas that in BoB is 71.4%. The cyclone frequency considered under the reporting period does not exhibit any significant cyclic oscillation.

The intra-annual variability of tropical cyclones in North Indian Ocean is more prominent than the inter-annual variability. The intra-annual occurrence of cyclones during the period 1947-1976 and 1977-2006 differs significantly, particularly for the BoB basin. The first half exhibits an active cyclone season in BoB during May to December with maximum frequency during post monsoon. The second half (1977-2006) exhibit a different picture with two cyclone seasons namely, before and after the southwest monsoon with nearly cyclone free monsoon season. The significant difference in inter-annual and intra-annual variability between the first half and second half could be due to the transition in atmosphere-ocean climate system during mid 1970's.

The origin and dissipating point of cyclones in North Indian Ocean during the period 1947 to 1976 exhibit large variability in space and time. The originating area varies between 5^{o} and 20^{o}N with the march of seasons. The cyclones originate below 10^{o}N during January, February and December whereas the originating area is between 5^{o} and 15^{o}N during April and November. The originating area is spread across a wide area above 5^{o}N during the peak cyclone season (May, June and October); more specifically, cyclones originate above 15^{o}N during July, August and September.

The cyclone genesis during the period 1977 to 2006 exhibited significant decrease in cyclone frequency specifically during southwest monsoon. Another interesting feature is the southward shift in originating area during January, May and June in BoB and during June in AS. McCabe *et al.* (2001) reported a northward shift of cyclone tracks and higher

cyclone frequency in higher latitudes in northern hemisphere associated with global warming. Contrary to that, the AS and BoB exhibits southward shift in cyclone track.

The analysis of long term SST in AS exhibits higher variability with strong SST gradient than that of BoB. The warming occurred at various latitudes are not uniform in both AS and BoB and exhibits a decreasing trend towards higher latitudes. The lower net heat gain at higher latitudes in AS and BoB leads to a stronger spatial gradient in SST and this would affect cyclone formation. Higher monsoon SST at higher latitudes in BoB could have contributed to the cyclone formation during monsoon. It can be inferred that variable net heat gain, especially the lesser heat gain at higher latitudes may lead to changes in cyclone formation over a long period in AS and BoB.

The detailed analysis of SST at selected points could not reveal any drastic change during 1976 and hence does not exhibit any direct relation with change in cyclone frequency. However the analysis of SLP in AS and BoB exhibits significant increase after 1975, which could have contributed to the change in cyclone frequency. This indicates a momentous role of local SLP bring about a change in cyclone frequency for northern Indian Ocean.

CHAPTER-IV

Upper Ocean Response to Cyclones in Arabian Sea

4.1 Introduction

Arabian Sea (AS) is unique with many characteristics, including a complex air-sea interaction system, often driven by local as well as remote forcing mechanisms. The seasonal reversal of winds and the associated response(s) in ocean currents is just one among the interesting features observed in AS. The warm pool in the South Eastern AS displays the long lasting warmest water in the world which collapses by the onset of southwest monsoon (Sanilkumar *et al.* 2004). The onset of southwest monsoon in AS is mostly accompanied by a cyclone passage, which brings out intriguing responses in the upper ocean.

AS experiences two cyclone seasons – one before and another after the southwest monsoon – with nearly equal chance of occurrence. This chapter deals with the characteristics of selected cyclones in AS during the period 1997 to 2006 and specifically addressed with emphasis on the upper ocean response(s) consequent to cyclone passage.

4.2 Data and Method

The cyclone track data from Unisys website during the period 1997 to 2006 has been utilized to identify the characteristics of the cyclone. The time series buoy data for a period of two or more weeks starting with 3 to 5 days before the passage of cyclones and till the end of visible response are utilized in this study. TMI-SST at the location of maximum intensity (Fig. 4.1) is retrieved for a period of 30 days starting from 10 days before the day of maximum intensity. The Hovmoller diagrams of TMI-SST and normalized wave spectra were utilized to identify the variability in ocean response.

The upper ocean response to passage of a cyclone is immediately visible as a change in wave, surface current and temperature pattern which is studied in detail using various methods such as progressive vector diagram, rotary spectral analysis and power spectral analysis. Progressive vector diagram shows the extent of oscillations and mean flow whereas rotary spectrum exhibits the frequency of oscillations in current observation. Power spectrum analysis of temperature profile is used to find out the depth up to which the oceanic response has penetrated.

4.3 Cyclones in AS during 1997 to 2006

The details of cyclone passage during the study period are analyzed and five of them are selected based on the availability of buoy data (Table 4.1). One cyclone under the category cy-1 during post monsoon, one tropical storm and three cy-3 cyclones during pre-monsoon are studied in detail to understand the variable oceanic response.

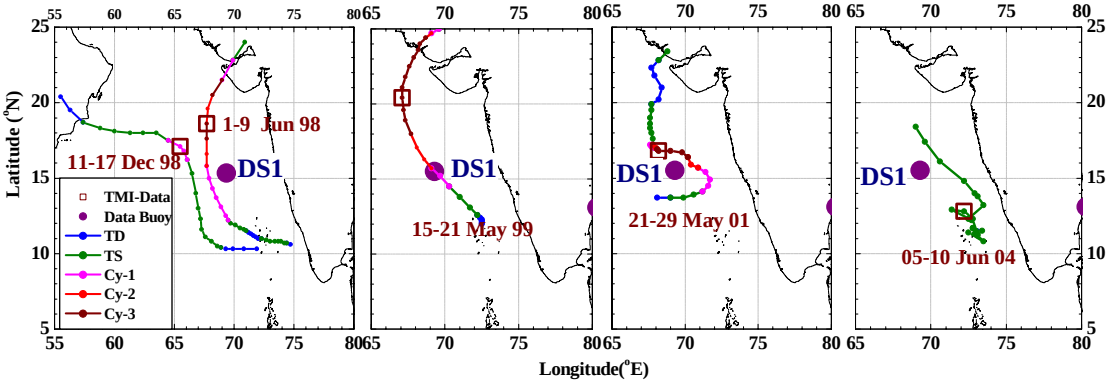

Fig.4.1: Cyclone tracks, data buoy location and TMI-SST extraction point during various AS Cyclones

All these cyclones are formed in the area between 10^{o}-13^{o}N, 67^{o}-75^{o}E, in which two cyclones of the pre-monsoon period (June 1998 and May 1999) were noticed to follow nearly the same track (Fig. 4.1). The cyclones during the pre-monsoon period made net movement towards north and made landfall on the northwest coast of India (except the tropical storm), whereas the one in post monsoon period moved towards northwest and made landfall on the coast of Oman. The tropical storm observed in June 2004 dissipated before land fall.

Table 4.1: Details of cyclones utilized in this study

Sl. No.	**Basin**	**Type**	**Duration**	**Data Availability**
1.	AS	Cy-3	1-9 June1998	DS1& TMI
2.	AS	Cy-1	11-17 December 1998	DS1& TMI
3.	AS	Cy-3	15-21 May1999	DS1& TMI
4.	AS	Cy-3	21-29 May 2001	DS1& TMI
5.	AS	TS	05-10 June 2004	DS1& TMI

Noticeable, the buoy location is on the right side of the track except during May 2001 and June 2004. The track was closer to the buoy location (nearly under the track) during May 1999 and far away during December 1998. The cyclone remained near to the buoy location for a longer duration during May 2001. The cyclone approached the buoy as category 1 cyclone (cy-1) during June 1998 and May 1999 whereas the cyclone intensified further into category 2 (cy-2) during May 2001 near the buoy location. The cyclone category was tropical storm near the buoy location during December 1998 and in June 2004.

4.4 Observations of Wind, Sea Level Pressure and Air Temperature

The met-ocean observations from the data buoy during the passage of various cyclones provided crucial information regarding the cyclone characteristics and its response in the upper ocean. The wind and air pressure are the major pre-cursors of the approaching cyclone. The wind direction exhibited slow rotation during the passage of cyclones

except for the TS in 2004 (Fig. 4.2). The direction of rotation is clockwise when the buoy location is on the right side of the track (during June 1998, December 1998 and May 1999) whereas the rotation is anticlockwise when the buoy is on the left side of the track (during May 2001). The wind direction could not completely regain the pre-cyclonic condition and exhibited deviations except for the cyclone in December 1998.

The wind speed at the buoy site before the cyclone passage is less than 10m/s except during June 2004 cyclone (Fig. 4.2). Therefore the approach of the cyclone is considered when the wind speed exceeds 10m/s. Sharp increase in wind speed is observed at all these occasions which recorded a maximum of 24.64m/s in June 1998, 17.54m/s December 1998, 35.49m/s in May 1999, 23.74m/s in May 2001 and 22.31m/s in June 2004. The higher wind speed (above 10m/s) continued for a period of nearly 13 days during June 2004. The wind speed immediately returned (~2 days) to the pre-cyclonic condition in May 1999, which recorded the highest wind speed. The higher wind speed is observed for longer duration (~6 days) during May 2001whereas the cyclones in 1998 exhibited higher wind speed for ~3days. The wind speed of 35.49m/s in May 1999 is the highest wind speed ever reported in the North Indian Ocean (Rajesh *et al.*, 2005) associated with a cyclone passage and corresponds to a wind stress of $3.52 N/m^2$.

Sea level pressure (SLP) observation during the passage of cyclone is available except during May 1999. The decrease in SLP associated with the cyclone passage, varies with cyclone characteristics and exhibits direct correlation with the maximum wind and duration of high wind speed. It is observed that the SLP before the cyclone passage is ~1010mb during pre-monsoon and ~1015mb during post-monsoon. A critical value of SLP is decided for pre-monsoon (1005mb) and post monsoon (1010mb) season based on the initial SLP to identify the duration of the cyclone. The longest duration of cyclone influence is depicted in June 2004 as seen in the duration of high wind. Similarly the gradual decrease/increase in air pressure which recorded the lowest value of 992.97mb in May 2001 also indicates longer duration of high wind speed. However there are no SLP observations corresponds to the highest wind speed of 35.49m/s in May 1999. The

minimum air pressure recorded at the buoy site was 997.4mb in June 1998, 1004.68mb in December 1998, 992.97mb in May 2001 and 999.38mb in June 2004.

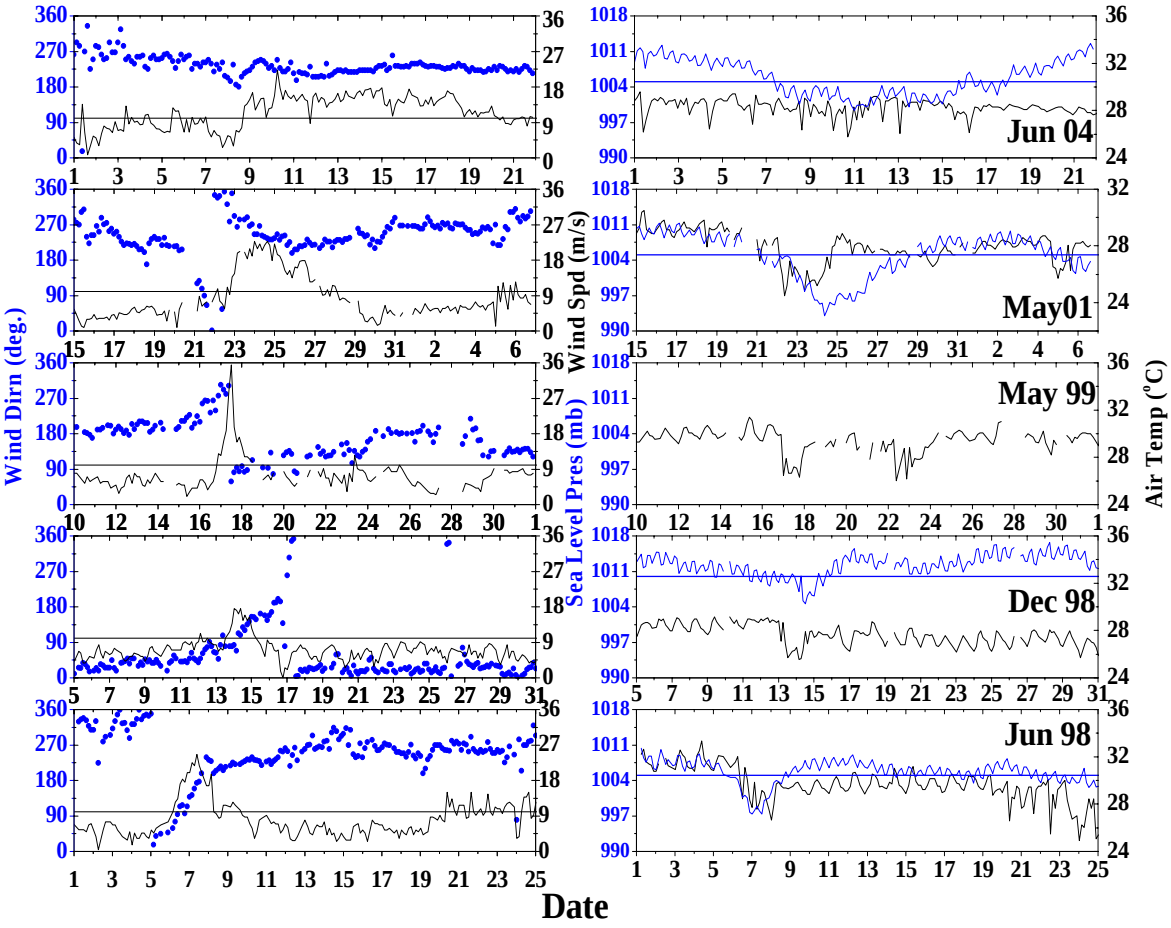

Fig. 4.2: Wind, sea level pressure and air temperature observations during the passage of cyclones in AS. The horizontal lines at 10m/s, 1005/1010mb are used as an indicator for duration of cyclones

The air temperature observations exhibit the rapid decrease which lasted for a day associated with cyclone passage. The minimum air temperature at the time of cyclone passage was 26.64^{o}C in June 1998, 25.55^{o}C in December 1998, 26.5^{o}C in May 1999, 24.49^{o}C in May 2001 and 25.78^{o}C in June 2004. The air temperature exhibited minimum value before reaching the minimum SLP during all cyclone events and exhibited lot of fluctuations. This could be due to the intense rain associated with the cyclone passage; unfortunately the rain measurements are not available at the location.

4.5 Wave Observations

The wave observations exhibited calm sea conditions before the cyclone passage. Sharp increase and a gradual decrease in wave height are observed during most of the cyclones. The maximum value of significant wave height recorded are; 7.66m in June 1998, 5m in December 1998, 6.41m in May 1999, 7.81m in May 2001 and 6.72m in June 2004 (Fig. 4.3). The narrow peak in high wind speed during May 1999 is repeated in wave height as well. Similarly the sustained high wind speed during May 2001 and June 2004 corresponds to high waves for longer duration. An interesting observation is that the highest wind speed (35.49m/s) in May 1999 does not correspond to the highest wave height whereas the maximum value of 7.81m is observed for a much smaller wind speed of 23.74m/s in May 2001. This indicates the importance of duration of wind in generating oceanic response in waves (Young, 1988; Young and Burchell, 1996 and Young, 2003).

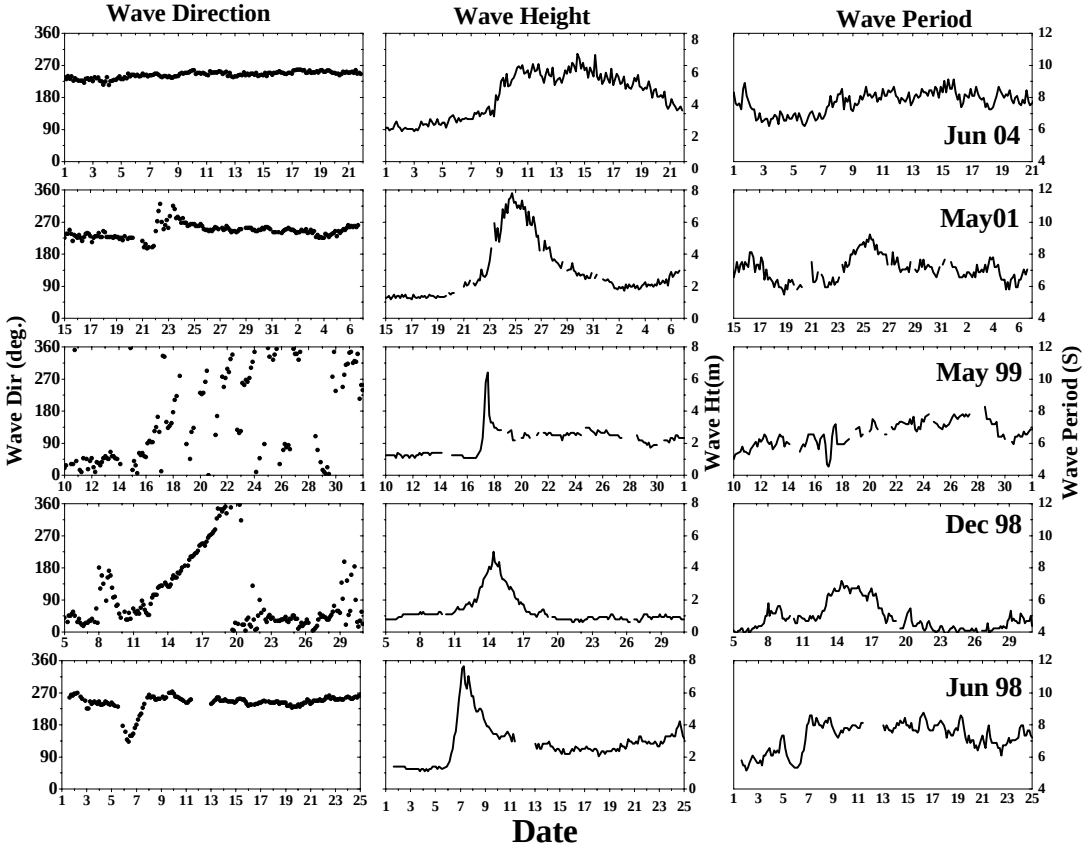

Fig. 4.3: Wave observations during the cyclones in AS

The mean wave direction exhibits clockwise rotation during June 1998, December 1998, May 1999. Slight anticlockwise rotation in wave direction is observed during May 2001, whereas the wave direction did not exhibit any significant change during June 2004. The rotation in June 1998 and May 2001 are more rapid and didn't make complete cycle.

The mean wave direction made a slow and a single cycle during December 1998 whereas that of May 1999 made many rotations in short period. The buoy was on the right side and closer to the track during May 1999, which might have lead to the clockwise rotations in wave direction and resulted in churning up of sea surface. The chaotic sea state combined with sudden rise and fall of wave height indicates a dangerous sea condition near the cyclone track. The buoy was located farthest from the cyclone track during December 1998, which could be the reason for the slow rotation in wave direction.

4.5.1 Wave Spectra

The wave spectrum exhibits the distribution of wave energy as a function of frequency and direction. 1-D frequency spectra are available during June 2004 and are utilized to identify the spectral pattern during the passage of cyclone (Fig. 4.4).

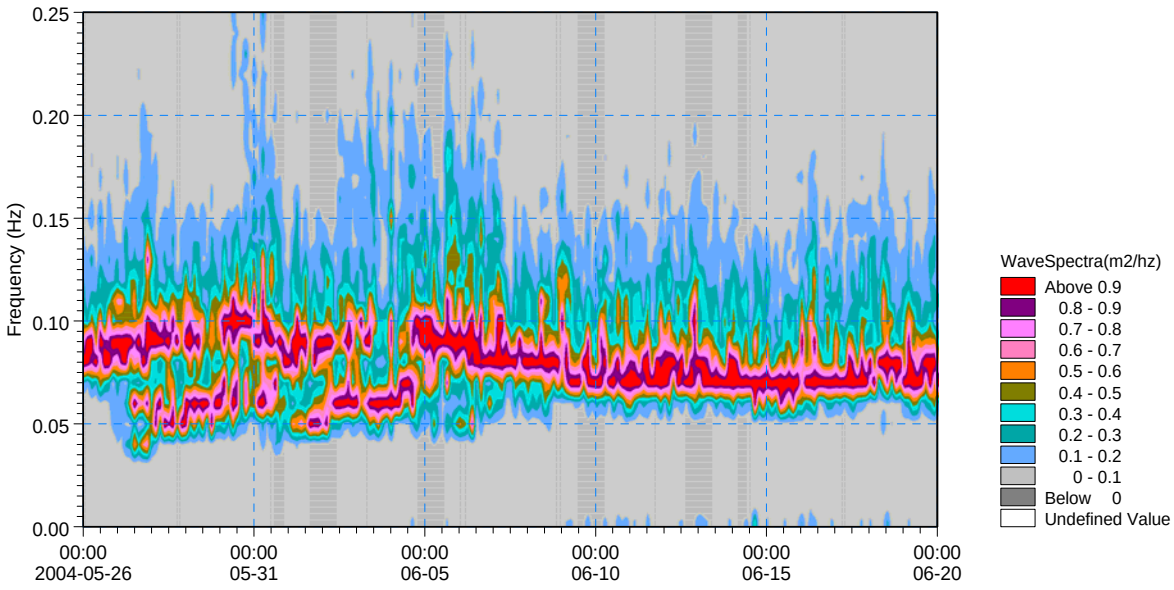

Fig.4.4: Wave spectra before, during and after the passage of cyclone in June 2004

The spectra are in general single peaked except for the period 27 May to 04 June 2004. Single peaked spectra with spectral peak around 0.09Hz (11s) is observed in the beginning. Double peaks in spectra started appearing from 27 May 2004 with a shift in spectral peak around 0.06 Hz (16s). The shift in spectral peak from 11s to 16s indicates the dominance of swell component generated by the distant cyclone. The double peaks in wave spectra represent the contribution from both locally generated sea and the long swells (Fig. 4.4).

The double peak in wave spectra remained till 04 June with major peak shifting between sea and swell component. The wave spectra shifted to single peak on 05 June and the spectral peak exhibits gradual shift from 0.1hz to 0.08Hz during 06 to 9 June. The spectral energy exhibits considerable increase as the cyclone approaches the buoy location. The cyclone was closer to the buoy location on 09 June and exhibits spectral peak at 0.08Hz (12.5s). The spectra remained single peak at 0.08Hz for the remaining period. The cyclone dissipated on 10 June immediately after crossing the buoy location. The wave spectra indicates the prevalence of long swells reaching the buoy location before the cyclone, which changed to sea dominated single peak wave spectra during the cyclone passage.

4.6 Surface current

The surface current observations at the buoy location during the passage of cyclones indicate clockwise rotation with significant increase in current speed (Current speed data is not available during December 1998 and both current speed and direction are not available during May 2001). The clockwise rotation observed at the buoy site made complete circles with a period of ~2days and continued for a longer duration even after the passage of cyclones (Fig. 4.5). This indicates the dissipation of kinetic energy as inertial currents which propagate to greater distance (Lien *et al.,* 1996). The current direction resumed the pre-cyclonic condition after the clockwise rotation.

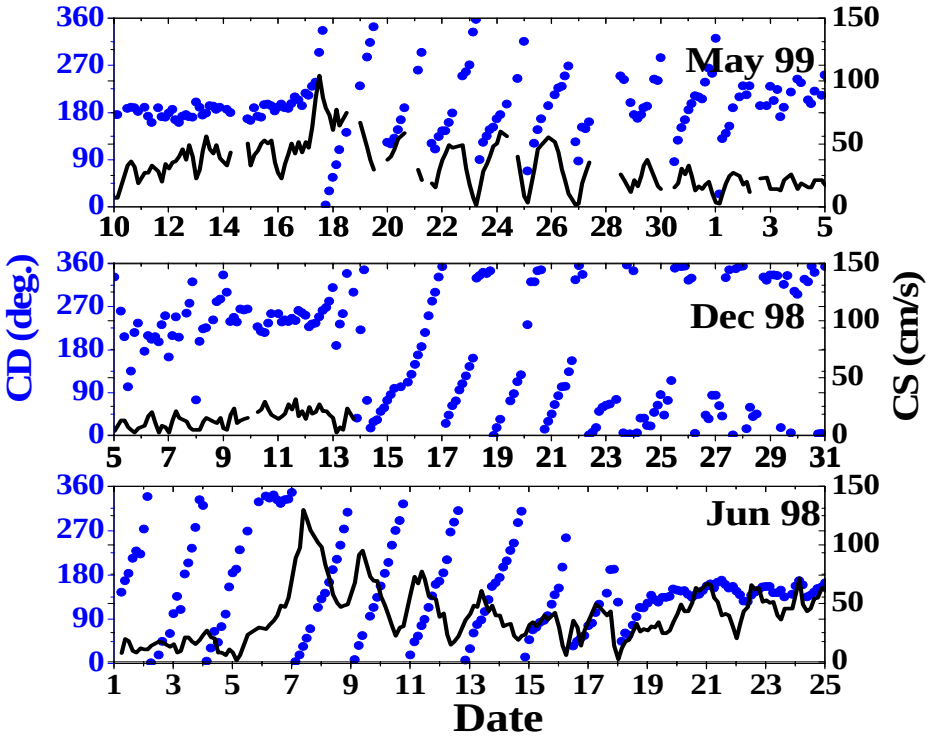

Fig. 4.5: Surface current observations during the passage of cyclones in AS

The rotation started as an immediate response to the cyclone passage during December 1998 and in May 1999 whereas the clockwise rotation started before the cyclone passage in June 1998. The response generated by the passage of a tropical storm in Central AS during 27-29 May 1998 combined with the impact of cyclone during 1-9 June 1998 might have forced the clockwise rotation in the surface current much before the arrival of the June 1998 cyclone at the buoy site.

There was a rapid increase in the current speed forced by the cyclonic wind, which increased to a maximum of 130.1cm/s in June 1998 and 104.3cm/s in May 1999. The buoy was located on right side of the track during June 1998, December 1998 and in May 1999, which favored significant increase in current speed. An interesting observation is that the strong wind in May 1999 could produce only lesser current speed than that of the weaker wind in June 1998, which indicates the complex oceanic response during cyclone passage (Fig. 4.5). Similar to that of current direction, higher amplitude oscillation with a period of ~2days is observed in the current speed during June 1998 and in May 1999.

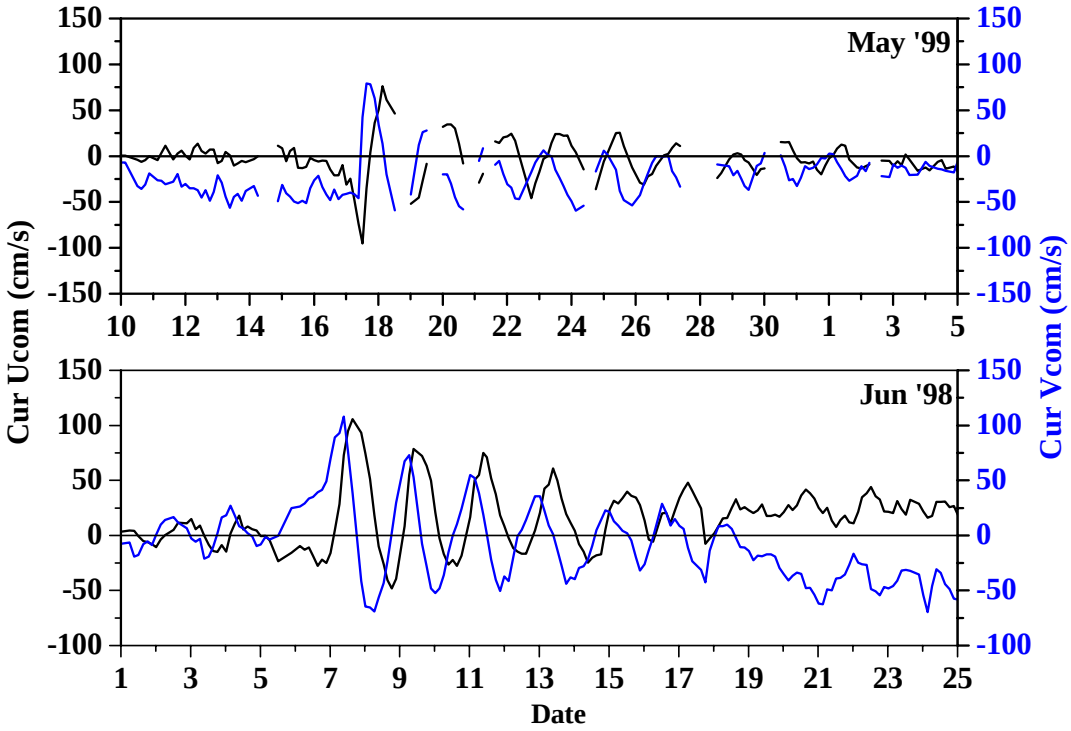

Fig. 4.6: Surface current vectors during the passage of cyclones in AS

The clockwise rotation in current direction indicates the inertial oscillation generated by the cyclone. The current vectors during the cyclone passage are studied in detail to understand the oceanic response in surface currents and the inertial oscillation. The amplitude of eastward component and northward component are nearly equal during both the observations (Fig. 4.6). A phase lag of eastward component behind northward component is observed. Phase lag of northward component behind east ward component is reported during inertial oscillation in southern hemisphere (Rivas and Piola, 2005). Maximum amplitude is observed during June 1998 followed by May 1999. However the higher amplitude observed during June 1998 than that of May 1999 again supports the combined effect of response to forcing mechanisms other than the intensity of local wind. Gonella (1971) reported that the most important factor that governs the amplitude of the inertial oscillation is duration of the wind compared to inertial period. The duration of the strong wind in May 1999 is less compared to that of June 1998 which exhibited high wind for longer duration.

4.6.1 Progressive vector Diagrams

The progressive vector diagrams indicate the inertial oscillations associated with cyclone passage. Well-defined circular oscillations are generated by the strong wind forcing associated with cyclones during June 1998 and in May 1999 (Fig. 4.7). The progressive vector diagram during June 1998 shows mean eastward flow with five well defined clockwise rotations during the first two weeks, thereafter the flow is towards southeast. The theoretical period of the inertial oscillation at the point of observation is 45.3hr and the inertial radius corresponding to the highest current speed is 33.2km while the corresponding observed values are 45.0hr and 30.0km respectively.

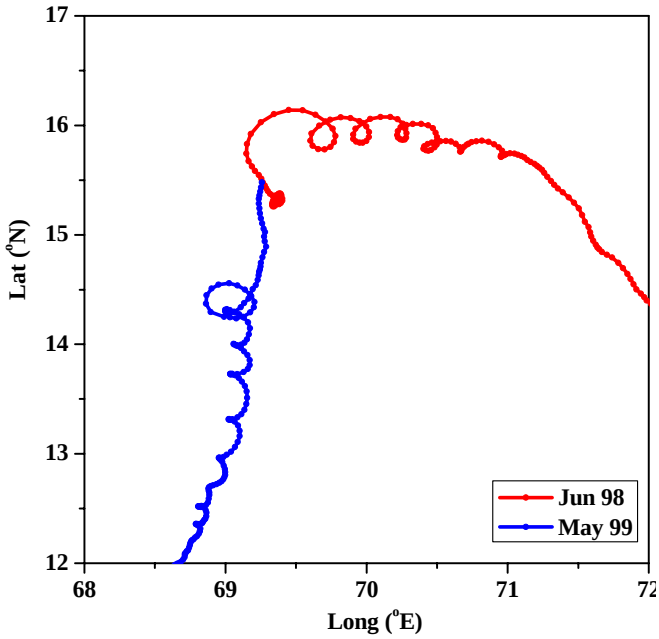

Fig. 4.7: Progressive vector diagram during the passage of cyclones in AS

The progressive vector diagram during May 1999 shows the mean flow towards south. Only one well defined inertial circle is observed during this period. The inertial oscillation started on 15 May 1999 and lasted till 27 May. The inertial period corresponding to the latitude of observation is 44.84 hrs whereas the observed period is 45 hrs. The inertial radius corresponding to the maximum current speed of 104.3 cm/s is 26.73km whereas the observed value is 29.0km. The difference between the observed and the computed values could be due to the coarse sampling interval of three hour.

4.6.2 Rotary spectra

The rotary spectral analysis of the surface current vectors indicates the characteristics of inertial oscillation generated by the cyclones. A minimum sample size of 10 times the local inertial period centered during the period of inertial oscillation is used for this analysis which helps the better identification of the inertial frequency. The rotary spectrum analysis exhibits significant peak at the inertial band in the negative rotary component (S^-), which agrees well with the theories of clockwise rotation in the northern hemisphere (Fig. 4.8). There is significant difference between the positive and negative components where the negative component dominates the spectrum in inertial band. The rotary coefficient, which indicates the strength of the inertial oscillation at the time of inertial peak, is negative with high magnitude. It shows that the inertial oscillation observed at the buoy site is nearly circular in clockwise direction. The inertial peak is observed slightly higher or lower than the local inertial frequency. The coarse sampling interval of 3.0hour limits the identification of exact inertial peak.

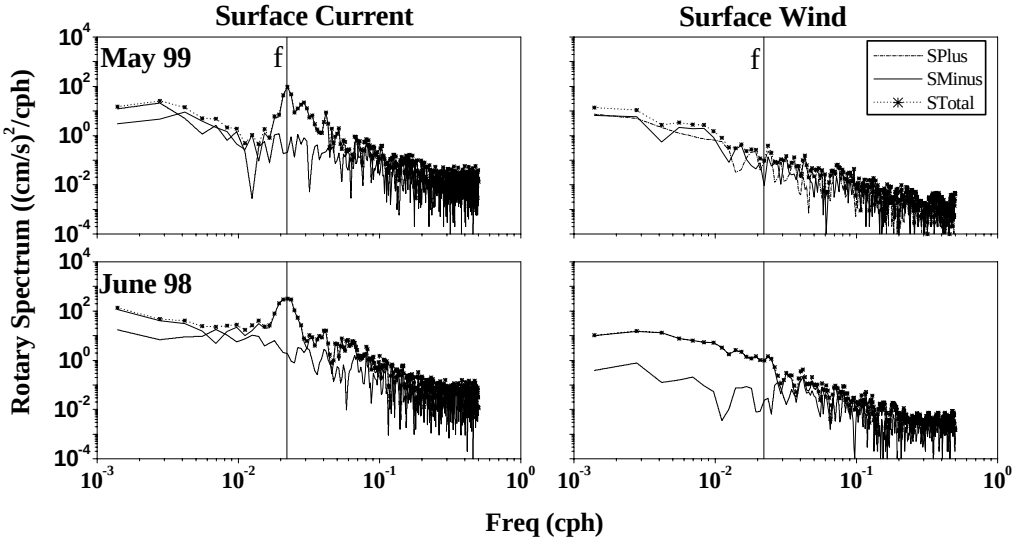

Fig. 4.8: Rotary spectrum of surface current and wind during the passage of June 1998 and May 1999 cyclones in AS

The rotary spectrum analysis of the current in both the observations shows spectral peaks at inertial frequency with dominant negative rotary component (S^-). The observations during June 1998 and in May 1999 exhibit inertial peak at 0.533cpd (45.0 hr). The

inertial frequency for the latitude of observation is 0.5298cpd (45.3 hr) during June 1998 and that of May 1999 is 0.5352cpd (44.84hr). The inertial period during June 1998 exhibits slightly lesser value than the theoretical period and hence shows a blue shift whereas that of May exhibits a higher value and hence a red shift (Fig 4.8). Jacobs *et. al.* (2001) reported that the blue shift in inertial oscillation is due to the presence of internal waves. The difference between the observed and local inertial peak are less. Gonella (1971) suggested that the difference in period/frequency is smallest when the transfer of momentum is at a maximum due to the homogeneity of the surface layer. The slight difference shows that the transfer of momentum is at maximum during both the observations.

The rotary spectrum of the wind observations at DS1 during inertial oscillations in June 1998 and in May 1999 does not indicate any significant spectral peak at the inertial frequency (Table 4.2). However there is significant difference between the clockwise and anticlockwise components. The dominance of negative rotary component suggests the presence of clockwise oscillation, which is also observed in the time series observations.

Table 4.2: Inertial characteristics observed at DS1 during cyclone passage

Period	Surface Current			Surface Wind		
	Phase Diff. at Inertial Peak	Rotary Coefft	Percentage of Energy	Phase Diff at Inertial Peak	Rotary Coefft	Percentage of Energy
Jun'98	94.01	-0.99	56.14	86.08	-0.952	6.38
May'99	88.99	-0.996	48.99	104.08	-0.80	2.32

Spectral analysis of current during the cyclone passage in June 1998 and May 1999 indicates rotary coefficient of -0.99 and -0.996 respectively at inertial peak. The corresponding energy values are 56.14% in June 1998 and 48.99% in May 1999 which reveals the dominance of inertial oscillation with ~50% energy in inertial band. The phase difference at spectral peak is 94.01deg and 88.99 deg during June 1998 and May 1999 respectively. The rotary coefficient of -0.99 with a phase difference of ~90deg and ~50% energy in the inertial band indicates the presence of strong inertial oscillation.

4.7 Mixed Layer Temperature

4.7.1 Sea Surface Temperature

Significant drop of SST is observed during the passage of cyclones in AS. The SST before the passage of cyclone showed the presence of warm water of more than 30^{o}C during June 1998 and in May 2001, whereas the pre-cyclonic SST is ~29^{o}C and ~28^{o}C during May 1999 and in December 1998 respectively (Fig. 4.9). The reduction in SST is highest during May 2001 and lowest during December 1998.

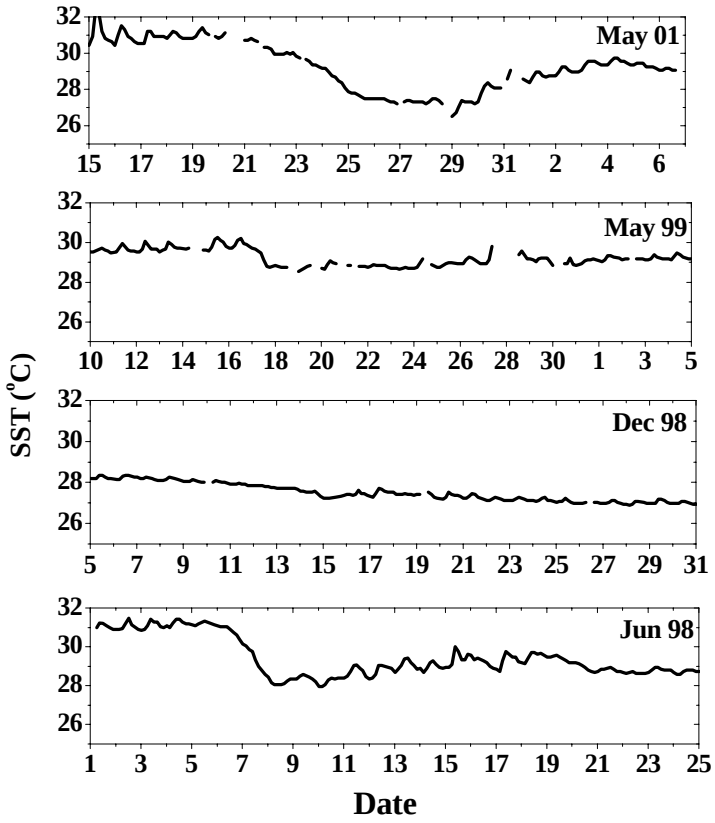

Fig. 4.9: SST during the passage of cyclones in AS

The SST just before the cyclone passage is 31.33^{o}C during June 1998. The wind induced mixing and Ekman pumping brought down the SST as low as 28.06^{o}C within three days during June 1998. The monsoon onset in 1998 was associated with the cyclone passage. The SST could not regain the pre-cyclonic condition and remained with an average of 29^{o}C during the monsoon season.

The SST observations during December 1998 did not exhibit much variation. The values exhibit a steady decreasing trend during the entire reporting period. The SST before the cyclone passage was 28.18^{o}C, which gradually reduced to 27.23^{o}C after the cyclone passage. Weaker wind forcing of a short duration could be the reason for less reduction in SST during December 1998.

The SST before cyclone passage was 29.96^{o}C on 16 May 1999, which reached a minimum of 28.55^{o}C on 17 May. Even though the cyclone was intense with wind speed of 35.49m/s near the buoy, the cooling observed in SST is only 1.41^{o}C, much less than that observed in June 1998. Even though the wind forcing was strong, the short duration could be the reason for the comparatively lesser cooling in SST.

The maximum SST observed at the location was 30.92^{o}C on 19 May 2001. SST dropped by 4.4^{o}C, reaching a minimum of 26.52^{o}C on 29 May (Fig. 4.9). Even though the wind forcing was not as high as that of June 1998 and May 1999, the continuous high wind stress from 23rd to 27th enhanced the mixing of the water column and resulted in the significant drop of SST. This supports the importance of duration of strong wind in ocean response.

It is observed that the reduction in SST greatly depends on the duration of the strong wind (Price, 1981). The buoy was on the right side, closer to the track during May 1999 and again, was on the right side of the track during June 1998 as well in December 1998. But the maximum reduction in SST is observed during May 2001; in this case, the buoy was located on the left side of the track. It is also noted that the lesser cooling in SST associated with cyclone passage is coincident with lower pre-cyclonic SST.

4.7.2 Subsurface Variability in Temperature

Time series observations of temperature profile during June 1998 show the pre-monsoon warming of SST to more than 30^{o}C and the sudden deepening of the mixed layer associated with the passage of cyclone. The mixed layer depth (MLD) is computed as the depth at which a reduction of 0.5^{o}C from SST is observed (Levitus, 1982). The pre-

cyclone MLD at the buoy site was ~20m which became ~50m by 9 June due to the intense mixing associated with cyclone passage. It also exhibits near inertial oscillation in the deeper layers after the cyclone passage (Fig. 4.10).

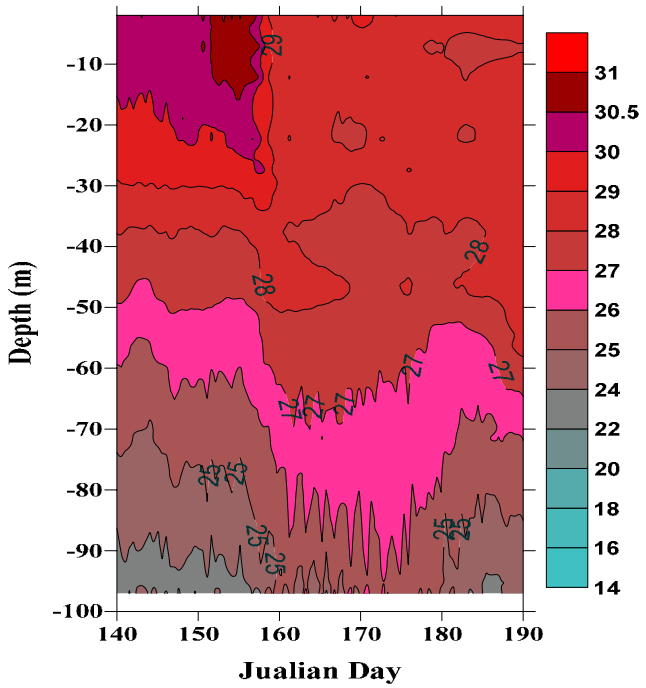

Fig. 4.10: Vertical distribution of temperature before, during and after the passage of cyclone in June 1998

The response to the wind stress during the forced stage and that of wind stress curl during the relaxation stage brought about substantial cooling of the SST and mixed layer resulting in significant increase in the MLD (Price *et al.*, 1994). Very high pre-cyclonic SST combined with a very thin MLD could have been the reason for the significant deepening of MLD in AS. The energy of the mixed layer currents are dispersed as near inertial frequency internal waves and inertial currents which lasted for two weeks.

The temperature observations exhibit the warming of seawater during the pre-monsoon period, which acquires a maximum of more than 31^{o}C and collapses after the cyclone passage at the buoy site (Fig 4.10). A sudden decrease in temperature up to a depth of 27m and increase in temperature at deeper levels due to the wind induced mixing associated with cyclone passage is observed.

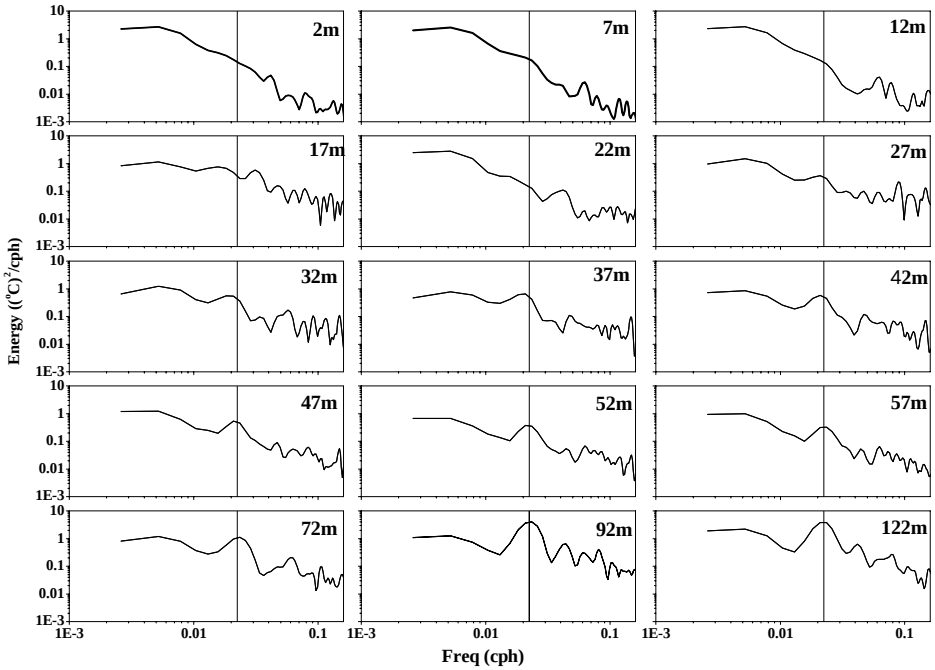

Fig. 4.11: The power spectrum of temperature profiles during the cyclone in June 1998. The vertical line indicates the local inertial frequency

The power spectra of temperature profile during June 1998 exhibit the penetration of inertial energy to deeper layers. Oscillations with near inertial period are observed after the cyclone passage with an increase in amplitude with depth (Fig. 4.11). Significant peaks in the inertial band are observed at deeper depths with maximum inertial energy at 97m and later starts decreasing as observed at 122m. Dickey *et al.* (1998) reported similar near inertial temperature oscillations set up by the hurricane Felix, which was initially increasing with depth reaching a maximum value at the seasonal thermocline below the mixed layer.

The temperature up to 22m depths does not exhibit any significant inertial energy. However significant energy in the diurnal and semidiurnal bands are observed. The spectrum at 27m during June exhibits the first indication of inertial signal and lower energy in diurnal and semidiurnal bands. The inertial peak closer to the local inertial frequency shows higher exchange of momentum during wind forcing associated with the cyclone passage during June 1998.

4.8 Spatial and Temporal Variability in Temperature

The TRMM/TMI SST was available during the passage of various AS cyclones, which showed the spatial/temporal response due to the cyclone. TMI-SST at the location of maximum intensity is retrieved for a period of 30 days starting from 10 days before the day of maximum intensity (Table 4.3). The data is extracted over a longitudinal band of 7.5degree with 2.5 degree on the left side and 5degree on the right side of the location of maximum intensity. The data set also exhibits the pre-cyclone warming, the sudden drop associated with cyclone passage and the build up of SST after the cyclone.

Table 4.3: TMI data extraction details during AS cyclones

Sl. No.	Starting date of TMI Data	Type	Max. Wind (kt)	Location of Max. Intensity	
				Long. (^{o}E)	Lat.(^{o}N)
1.	29 May1998	Cy-3	100	67.7	18.6
2.	06 December 1998	Cy-1	65	65.5	17.1
3.	10 May1999	Cy-3	110	67.1	20.4
4.	15 May 2001	Cy-3	110	68.2	16.8
5.	29 May 2004	TS	45	72.2	12.8

The cyclone during June 1998 attained maximum intensity (cy-3) at 18.6^{o}N, 67.7^{o}E on 8 June 1998 with maximum wind speed of 100kt. The SST before the cyclone passage was 30.9^{o}C, which reduced to 25.65^{o}C after the cyclone passage (Fig. 4.12). The maximum drop of 5.25^{o}C is observed on the right side (at 68.25^{o}E), 66km away from the cyclone track. The buoy observations displayed less reduction in SST, since the system was not extensively intensified when it crossed the buoy location. The cooling of 5.25^{o}C in SST was observed on 9 June, a day after the cyclone passage. The SST on the left side of the track returned to the pre-cyclone condition very quickly. However the SST remained less than 30.0^{o}C for a longer period on right side of the track with maximum cooling, shifting further rightward.

The cyclone attained maximum intensity (Cyclone-1) at 17.1°N, 65.5°E on 15 December 1998 with a maximum wind speed of 65kt. The TMI-SST exhibited maximum drop of 2.4°C, which is observed at 66°E, 55km away on the right side of the track (Fig. 4.12). The cooling remained at this location for a longer period compared to earlier events. The DS1 buoy was far away (330km) from the cyclone track and the observed cooling was only ~1°C. However this exhibits the wide spread effect of cyclone passage. It can also be inferred that post monsoon cyclones in AS produce noticeable cooling even though the magnitude of cooling is less than that of pre-monsoon cyclones.

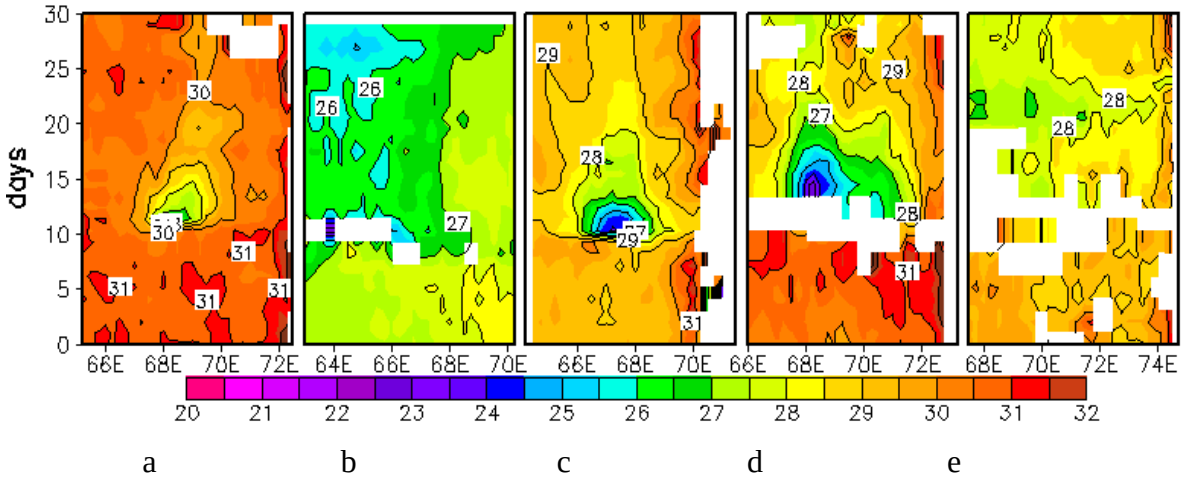

Fig. 4.12: 30 days Hovmoller diagram of SST before, during and after the passage of AS cyclones in a) Jun'98, b) Dec'98, c)May'99, d)May'01 and e) Jun'04

The cyclone during May 1999 attained maximum intensity (Cyclone-3) at 20.4°N, 67.1°E on 19 May 1999 with maximum wind speed of 110kt. The TMI-SST from 10 May to 08 June 1999 exhibit the intense cooling associated with the cyclone passage and its spatial coverage (Fig. 4.12). It can be noted that the maximum cooling of 5.5°C was observed at 72km (67.75°E) away on the right side of the track. The spatial and temporal coverage of the cooling is extensive which lasted for 10 days over a longitudinal belt of 275km. However the buoy reported lesser cooling due to lower intensity (Cyclone-1) of the cyclone near the buoy location.

The Arabian Sea cyclone in May 2001 is peculiar for being practically stationary at a location for a longer period after intensifying into cyclone-3. The cyclone during May 2001 attained maximum intensity (Cyclone-3) at 16.8^{o}N, 68.2^{o}E on 24 May 2001 with maximum wind speed of 110kt. TMI-SST was more than 30.6°C before the cyclone passage and started decreasing as the cyclone intensified (Figure 4.12). The maximum cooling of 7.5^{o}C with lowest SST of 22.8°C was observed around 68.25^{o}E near the cyclone track; this is attributed to the slow transition towards northeast during that period. Price (1981) also reported less rightward bias in cooling for slow moving cyclones.

The cyclone during June 2004 did not intensify beyond the category of tropical storm. The time series SST for the Hovmoller diagram is extracted along the longitudinal belt at 12.8^{o}N, 72.2^{o}E. The corresponding maximum wind speed is only 45kt. The cooling observed at this location is much less compared to other cyclones, attributed to the low intensity.

The AS had experienced three cyclones (June 1998, May 1999 and May 2001) with similar intensity (cy-3); however the associated cooling indicates a different picture. The maximum cooling observed during May 2001 (7.5^{o}C) is much higher than that of June 1998 (~5.25^{o}C) and May 1999 (~5.5^{o}C). A lag of approximately one day is observed between maximum cyclone intensity and maximum cooling in AS, again with maximum lag during May 2001. This indicates the role of factors other than the intensity in determining the oceanic response. The May 2001 cyclone belong to the category of slow moving cyclones with a speed of 2.34m/s whereas the speed of the other systems were 4.93m/s (June 1998) and 3.59m/s (May 1999). This supports the findings of Price *et al.* (1981) on higher upper ocean responses to slow moving cyclones.

4.9 Results and Discussion

The upper ocean response(s) to cyclones in AS, importantly, exhibits significant variability. The importance of (relative) location and proximity to cyclone track are evident in various met-ocean parameters. The wind direction exhibits only one rotation with period increasing with distance from the cyclone track whereas the speed decreases

as it move away from the track. The waves are in resonance with wind on both sides of the track and exhibits higher response on the right side of the track. The current direction rotates with near inertial period, whereas the period of rotation in wave direction increases as it moves away from the track as observed during December 1998. The wave spectra during the cyclone indicates double peak before the arrival of the storm and exhibits single peak during the cyclone passage. The double peak indicates the co-existence of sea waves and long swells. The single peak during the cyclone passage indicates the dominance of sea waves over long swells.

The wave height and current speed depends on the relative location of observation and the duration/cyclone translation speed with maximum response to slow moving cyclones. The inertial oscillation is observed in surface current and in the mixed layer temperature. The inertial peak closer to the local inertial period indicates maximum transfer of energy during the cyclone passage. The inertial energy increases with depth in temperature and reaches maximum at depth of 97m and thereafter the inertial energy decreases. This indicates the propagation of inertial energy into deeper layers below the mixed layer which reaches maximum at thermocline region (Dick *et al.,* 1998 and Lien *et al.,* 1996).

Significant effect on the upper ocean due to the passage of a cyclone is the noticeable cooling in the SST. The time evolution of the enhanced wind mixing and the resulting drop in SST is demonstrated in the moored buoys and satellite observations. It is observed that the intensity of cyclones are more during pre-monsoon in AS. The Cyclones during the post-monsoon season also generate noticable response in upper ocean, but to a lesser magnitude. The presence of warm SST (> 28^{o}C) before the cyclone formation and the cooling due to intense mixing brings out significant changes in upper ocean. Maximum buoy observed cooling is 4.4^{o}C at DS1 associated with AS cyclone during May 2001. The highest wind speed observed at the buoy site was 35.49m/s at DS1 during AS cyclone in May 1999, which could produce a cooling of 1.41^{o}C only. The May 2001 cyclone belong to the slow moving whereas the May 1999 cyclone belongs to the category of moderate speed cyclone. It supports the fact that slowly moving cyclones

induce higher response than that of fast moving cyclones. It is also observed that the cooling in AS during a post monsoon cyclone is significant.

The detailed analysis of the oceanic response during various cyclones indicates the major factors that control the upper ocean response. The duration of the strong wind and the cyclone translation speed are important factors controlling the oceanic response(s). It is observed that the most important factor controlling the SST response is the duration of the strong wind. Another important factor is the relative location with the cyclone track, with maximum response near right side of the track. The oceanic response closer to the track reports chaotic sea state with waves from all directions combined with sudden rise and fall of wave height. However the corresponding oceanic response exhibits lesser response in wave height, cooling and current speed. The asymmetric response of surface wind is well depicted in the buoy observations and the period of rotation of wind increases with distance from the track. The cyclone passage generates near inertial currents which contributes to the mixed layer dynamics.

CHAPTER-V

Upper Ocean Response to Cyclones in Bay of Bengal

5.1 Introduction

Bay of Bengal (BoB), the semi-enclosed basin in the north Indian Ocean exhibits unique characteristics with seasonal reversal of wind and ocean currents and a low salinity surface layer. The large influx of fresh water from rivers and the low lying coast line with a narrow continental shelf further adds to its complexity in response to cyclones. The loss of life and property associated with the strong winds, torrential rains and storm surges also accounts for higher impacts than that of AS. Most of the disastrous cyclones in the history of India belong to the BoB basin. The BoB is an area of higher incidence of cyclones compared to AS (Dube et al., 1997) and is considered to be the most perilous cyclone basin in terms of storm surge with an estimated death toll of 3,00,000 in 1970 and 1,38,000 in 1991 associated with severe cyclone (Lander and Guard, 1998). The cyclones in BoB exhibit large variability in frequency and the recent records exhibit a reduced frequency (described in chapter III) and higher intensity. This chapter addresses the oceanic response to cyclones during the period 1997 to 2006. Cyclones during pre and post monsoon ranging from the category of Tropical Storm to Cyclone-5 are analyzed in detail to identify the characteristics of oceanic response.

5.2 Data and Method

The cyclone track data from Unisys website during the period 1997 to 2006 has been utilized along with buoy data, ARGO and TMI-SST. Time series observations of met-ocean data from moored data buoys DS3-A & DS3-B (Central Bay of Bengal), DS4-A & DS4-B (Northern Bay of Bengal) and DS5-A & DS5-B (Southwest Bay of Bengal), SW6, MB10, MB11, MB12 and OB8 in BoB are utilized in this study (Table 5.1). All parameters derived from buoy data have been studied for a period of two or more weeks including pre and post cyclone period. The TMI data at the location of maximum intensity is retrieved for a period of 30 days starting from 10 days before the day of maximum intensity. The Hovmoller diagram is prepared from this data set to identify the reduction in SST. The temperature and salinity profiles from ARGO floats are utilized to understand the vertical variability during the passage of cyclones. Three profiles each during the passage of cyclones in May 2003 and April 2006 are utilised in this study. The normalized wave spectra are utilized to identify the oceanic response in waves associated with cyclones.

5.3 Cyclones in BoB during 1997 to 2006

The characteristics of tropical cyclones in BoB during the period 1997 to 2006 are addressed with an emphasis on the ocean response to cyclones. During the study period, a total of 30 cyclones were reported in BoB, out of these, 20 (66%) belong to the categories of tropical depression/storm and only one under the category of highest intensity cyclone-5. There were 5cyclones under category cy-1, one cy-2 and 3 cy-3 cyclones. No cyclones under the category cy-3 are reported during the study period. Two cyclones each under the categories cy-2 and cy-4 and one cyclone each under the categories TS, cy-2 and cy-5 during the reporting period are studied in detail to understand the variability in response to differential forcing (Table 5.1).

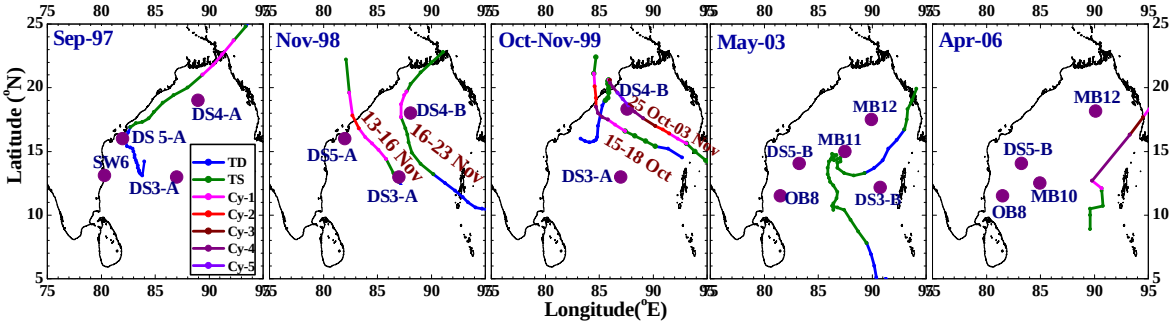

Fig. 5.1: Cyclone tracks and buoy locations during various cyclones in BoB

Unlike the cyclone observations in AS, there are many data buoys near the cyclone track in BoB, which falls on either side of the track and provide a rich data set to identify the variable response to cyclone passage. However, most of these buoys are on the left side of the track. Maximum of five data buoys were present during the passage of the TS during May 2003, followed by four data buoys during the cyclones in 1997 and in 2006. There are observations from three data buoys in 1998 and two data buoys during 1999 cyclones. Among the network of data buoys DS5-A and DS4-A (cy-1 in September 1997), DS3-A (cy-2 in November 1998), DS4-B (cy-1 in November 1998), DS4-B (cy-5 in October 1999) and MB11 (TS in May 2003) were closer to the cyclone track and hence exhibit higher oceanic response.

Table 5.1: Details of cyclones and buoy data utilized in this study

Sl. No.	Basin	Type	Duration	Data Availability
1.	BoB	Cy-1	19-27 September 1997	DS3-A, DS4-A , DS5-A & SW6
2.	BoB	Cy-2	13-16 November 1998	DS3-A, DS4-B, DS5-A & TMI
3.	BoB	Cy-1	16-23 November 1998	DS3-A, DS4-B, DS5-A & TMI
4.	BoB	Cy-4	15-18 October 1999	DS3-A, DS4-B & TMI
5.	BoB	Cy-5	25 October-3 November 1999	DS3-A, DS4-B & TMI
6.	BoB	TS	8-19 May 2003	DS3-B, DS5-B, MB11, MB12, OB8, TMI & ARGO
7.	BoB	Cy-4	24-29 April 2006 (Cyclone MALA)	DS5-B, MB10, MB12, OB8, TMI & ARGO

The cyclones generated in BoB during pre-monsoon season (May 2003 and April 2006) moved towards northeast (parallel to the east coast) and made landfall at Bangladesh/Myanmar coast whereas that of post-monsoon moved towards northwest (shore normal) and made landfall along the east coast of India except the one that occurred in September 1997. The cyclone during September 1997 moved parallel to the coast and made landfall in Bangladesh coast (Fig. 5.1). Two cyclones formed in BoB during November 1998. The first cyclone moved towards northwest, attained the strength of cyclone-2 and made landfall. The second cyclone during 16 to 23 November 1998 developed from the remnants of tropical storm 'Chip' from the Western Pacific, initially moved towards northwest. The cyclone intensified into category cy-1, re-curved and made landfall on Bangladesh coast (Source: cyclone report from IMD and Unisys).

Two cyclones again formed in BoB during October 1999. The first cyclone intensified into cy-4, moved northwestward and crossed Orissa coast as cy-2. The second cyclone during 25 October to 3 November 1999 is very peculiar for its southward movement and happens to be the deadliest Indian Ocean tropical cyclone since 1971. The cyclone made landfall just weeks after the first cyclone hit a nearby area. It slowly weakened, moved southward and re-emerged into the Bay of Bengal, and later, dissipated over the open waters (Source: cyclone report from IMD and Unisys). The data buoy DS4-B was near to the track of the cyclones in October 1999, but this buoy was equipped only with a wave sensor and unfortunately, could not record any other observations. Another buoy DS3-A in the central BoB was operational during both the cyclones. The observations from these two buoys, especially the wave data from DS4-B indicate the intensity of the cyclone.

The tropical depression formed in the southeast BoB during May 2003, initially moved in a northwestward direction. Later the system re-curved and started moving towards northeast and crossed the Myanmar coast on 20 May 2003. Five data buoys in BoB picked up the signals of this cyclone passage. The cyclone re-curved near the MB11 location in the central BOB, enabling it to pick up the responses for a prolonged period. Interestingly, this cyclone approached the DS3-B buoy twice during its passage and the

buoy observations evidently show corresponding responses (Source: cyclone report from IMD and Unisys).

A tropical storm formed in the central BoB in April 2006 was named as MALA, which moved northeastward and made landfall over Myanmar and quickly dissipated. This cyclone is the third intense cyclone to form in April, while the other two were in 1991 and 1994 (Source: cyclone report from IMD and Unisys). Four data buoys (DS5-B, MB10, MB12 and OB8) deployed in the BoB and three Argo floats captured the signals of cyclone passage.

5.4 Sea Level Pressure and Air Temperature Observations

A drop in sea level pressure (SLP) is the pre-cursor of a cyclone; being the first indicator, this is very important and the gradient obviously shows the severity of the cyclone. SLP exhibited almost uniform distribution with semidiurnal oscillations at all buoy locations except during cyclones. A sudden drop in SLP during the passage of cyclone(s) and immediate regain of normal atmospheric conditions are observed.

SLP dropped more than 10mb within a day and recorded a minimum of 995.7mb and 994.9mb at locations DS4-A and DS5-A during the passage of the cyclone in September 1997 (Fig. 5.2). The SLP observations showed the passage of two cyclones within a period of 10 days during November 1998 and in October 1999. The SLP reached a minimum of 998.63mb (at DS4-B) on 20 November 1998, 1001.86mb (at DS3-B) on 18 October 1999 and 1003.47mb (at DS3-B) on 29 October 1999.

SLP observations at buoy locations were around 1007mb just before the cyclone in May 2003. The average pressure drop observed is of the order of 7mb with a maximum drop of 11mb at MB11, reaching a minimum of 994.4mb on 14 May 2003. SLP observations exhibited gradual decrease during April 2006 without any significant drop associated with cyclone passage (Fig. 5.2).

The air temperature exhibits significant diurnal oscillation at all buoy locations. The sudden fluctuations in air temperature could be due to the intense local rains associated

with cyclone passage. The air temperature was high at DS4-A location than that of DS5-A before the passage of cyclones in September 1997 and in November 1998. The pre-cyclonic air temperature exhibited significant difference between DS3-A, DS4-A, DS5-A and SW6, which became nearly uniform after the cyclone passage. The observation of air temperature is available only at DS3-A location during the cyclones in October 1999, which did not exhibit much variability, probably because of the large distance from the track (Fig. 5.2).

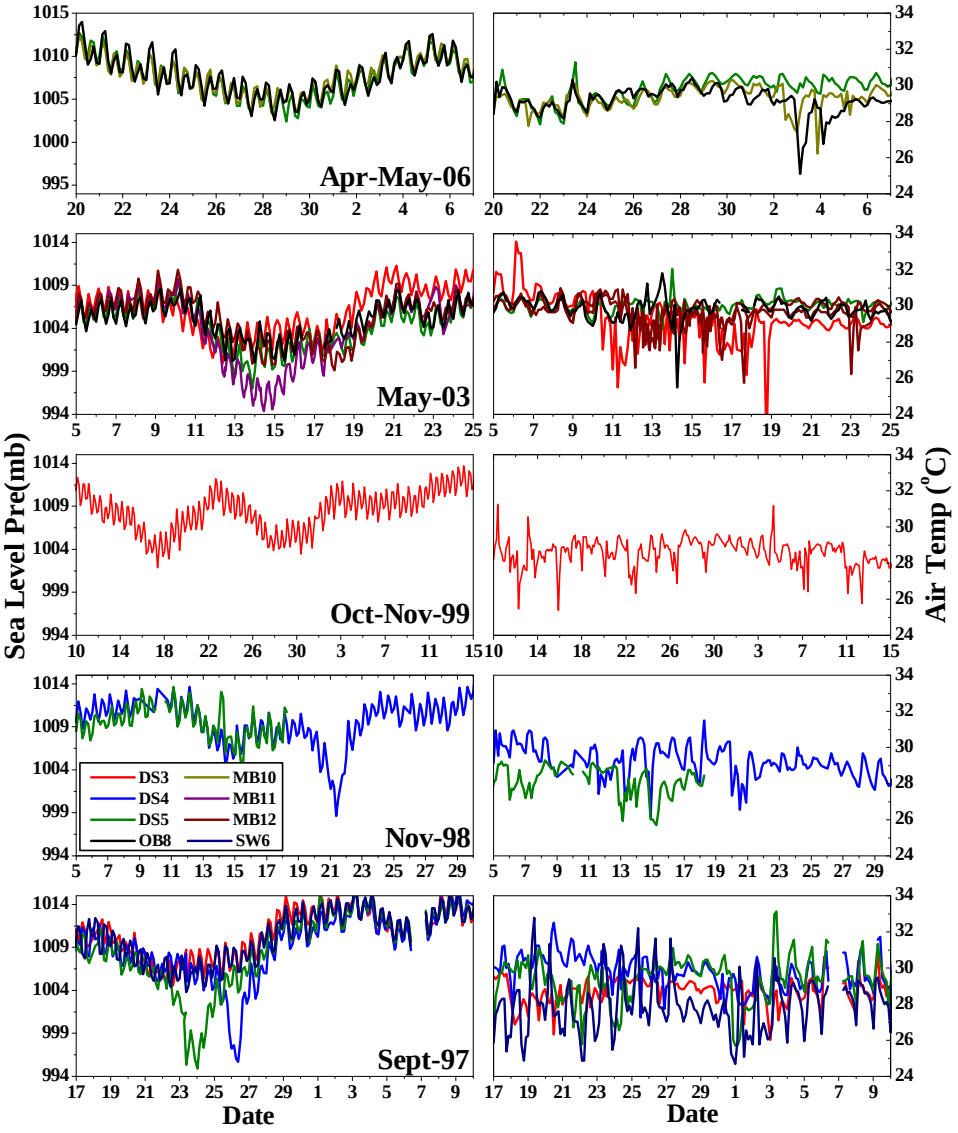

Fig. 5.2: Air pressure and air temperature observations during the passage of various cyclones in BoB

The air temperature exhibited large fluctuations at all buoy locations during the passage of cyclone in May 2003 for a longer period, which could be due to the local rains associated with the cyclone passage. The air temperature at all locations was almost uniform before the passage of the cyclone in April 2006. The MB10 and OB8 location exhibited temperature fluctuations during the cyclone passage whereas that at DS5-B continued without any significant fluctuations in air temperature.

5.5 Surface Wind Observations

The intriguing observation(s) on surface wind, during the passage of cyclones, is highlighted by the relative rotation (clockwise/anticlockwise) in wind direction on either side(s) of the cyclone track (right/left). The wind direction at DS4-B buoy during the cyclones in November 1998 and DS3-A buoy during the Orissa super cyclone in October 1999 made complete circles. Rotation in wind direction is observed at other locations too associated with cyclone passages, but did not exhibit a complete circle (Fig. 5.3).

The DS3-A and DS4-A buoys were on the right side and DS5-Aand SW6 buoys were on the left side of the track during the cyclone in September 1997. Even though the buoys were closer to the track, none of these made complete rotation in wind direction, since the cyclone did not intensify beyond the tropical storm stage near the buoy locations. Clockwise rotation at DS4-A and anticlockwise rotation at DS5-A and SW6 were observed whereas no change in wind direction was observed at DS3-A. The cyclone track was initially towards DS5-A buoy; the cyclone approaching the buoy turned northeast and thence the location happens to be on the left side of the track. This change in cyclone track is reflected as slight clockwise rotation, followed by anticlockwise rotation in wind direction at DS5-A. The maximum wind speed observed is 22.54 m/s on 24 September 1997 at DS5-A followed by 20.05m/s on 26 September at DS4-A location (Fig. 5.3).

The DS4-B buoy was on the right side and DS5-A buoy was on the left side of the track during the passage of cyclones in November 1998. DS4-B buoy exhibited two complete clockwise circles, whereas that of DS5-A exhibited an anticlockwise rotation during the first cyclone in November. The DS5-A observations are not available during the second

cyclone in November 1998. An interesting feature is the period of rotation at DS4-B, ~6 days during the first cyclone and ~4 days during the second cyclone. The DS4-B buoy was located far away from the cyclone track during the first cyclone and was nearer to the track during the second cyclone, which contributed to the variable period of rotation. The cyclone intensified to cy-1 near DS4-B buoy location which resulted in complete circular rotation. It may be noted that the passage of first cyclone did not produce any significant increase in wind speed. The wind speed reached a maximum of 17.96m/s at DS4-B during the second cyclone in November 1998.

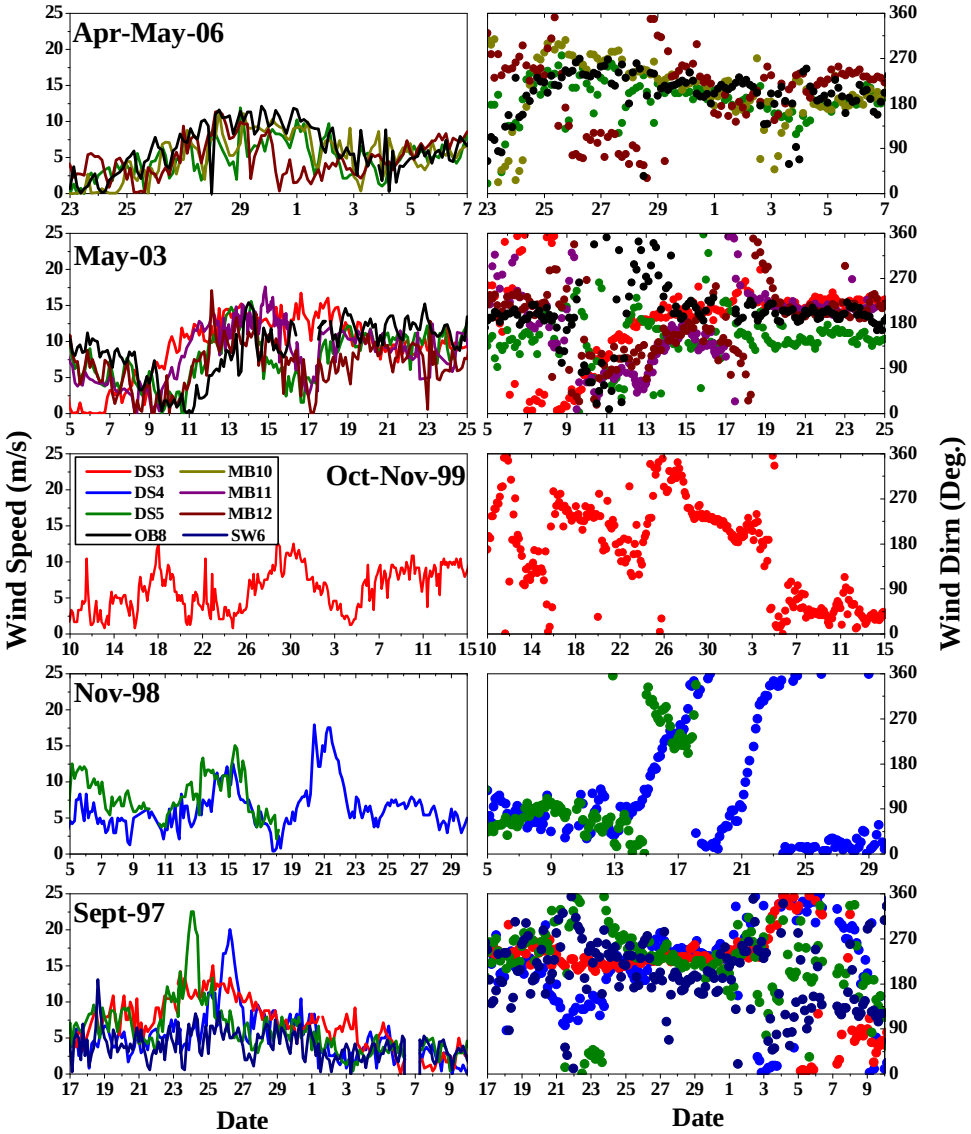

Fig. 5.3: Surface wind observations during the passage of various cyclones in BoB

The DS3-A buoy was located on the left side of the track and exhibited anticlockwise rotation during the cyclones in October 1999. The buoy was closer to the track during the first cyclone and displayed an incomplete rotation and a complete anticlockwise rotation during the second cyclone. The differential intensity (TS and cy-2 during first and second cyclone respectively) near the buoy location could be the reason for the variable response in wind direction. The buoy observation indicates only slight increase in wind speed during the passage of cyclones. Even though the peaks are comparable, the duration of high wind speed is longer during the passage of second cyclone at this location (Fig. 5.3).

Wind observations are available at five buoy locations (DS3-B, DS5-B, MB11, MB12 and OB8) during the cyclone in May 2003. The buoy DS3-B was on the right side of the track and the other buoys were on the left side of the track. The wind direction at DS3-B exhibited clockwise rotation and that at OB8 and DS5-B exhibited anticlockwise rotation. The data buoys MB11 and MB12 initially exhibited clockwise rotation and later, anticlockwise rotation. The change in cyclone track (initially towards northwest and then later towards northeast) resulted in change in relative positions of the buoys and variable response to wind rotation. The wind observations did not exhibit much change in magnitude except for the slight increase during the cyclone passage (Fig. 5.3). The buoys MB11 and DS3-B exhibited higher wind speed for a longer period. The maximum wind speed observed was 17.58m/s at MB11 location, 17.07m/s at MB12 location and 16.69m/s at DS3-B location.

All buoys (DS5-B, MB10, MB12 and OB8) were located at considerable distances on the left side of the track during the passage of cyclone in April 2006 and hence exhibited lower responses (Fig.5.3). The wind observations displayed moderate wind throughout the reporting period with slight increase during cyclone passage. Anticlockwise rotation in wind direction is observed only at MB12 location.

5.6 Wave Observations

The immediate response to cyclone wind forcing at ocean surfaces is seen as an increase in wave height. Similar to that of wind, the asymmetry on either side of the track is well depicted in wave observations. However a complete rotation was observed only at DS4-B during the second cyclone of November 1998, which was located very close to the track on the right side. Significant increase in wave height was also observed during the passage of all cyclones at all locations.

The data buoys (DS3-A, DS4-A and DS5-A) show the rapid increase in wave height coinciding with the cyclone passage in September 1997 (Fig.5.4). Even though the wind forcing was stronger, the wave height observed at DS5-A (4.22m) is less than that at DS4-A (6.25m). Similarly, DS3-A location exhibited comparatively higher wave height even in the absence of strong wind forcing. The variable response in wave height indicates the importance of relative location of the buoys on either side of the track. The wave direction at DS3-A and DS4-A did not exhibit any significant fluctuations during the passage of the cyclone. There was an anticlockwise rotation in wave direction at DS5-A site which indicates the resonance with wind direction. The average wave period after the passage of the cyclone shows waves with higher periodicity, which signifies the contribution from the swells generated by distant cyclones.

Wave direction at DS4-B site during the passage of November 1998 cyclones exhibits clockwise rotations. A slight clockwise rotation during the passage of first cyclone is followed by nearly complete clockwise rotation during the second cyclone. The rotation in wave direction continued after the passage of cyclones as semicircular between 0 to 180 degrees. The DS5-A buoy on the left side of the track exhibited anticlockwise rotation during the passage of the first cyclone. The DS4-B site exhibited significant increase in wave height reaching a maximum of 4.53m on 21 November whereas DS5-A wave height remained as such. The wave period observations showed nearly uniform variation at both locations.

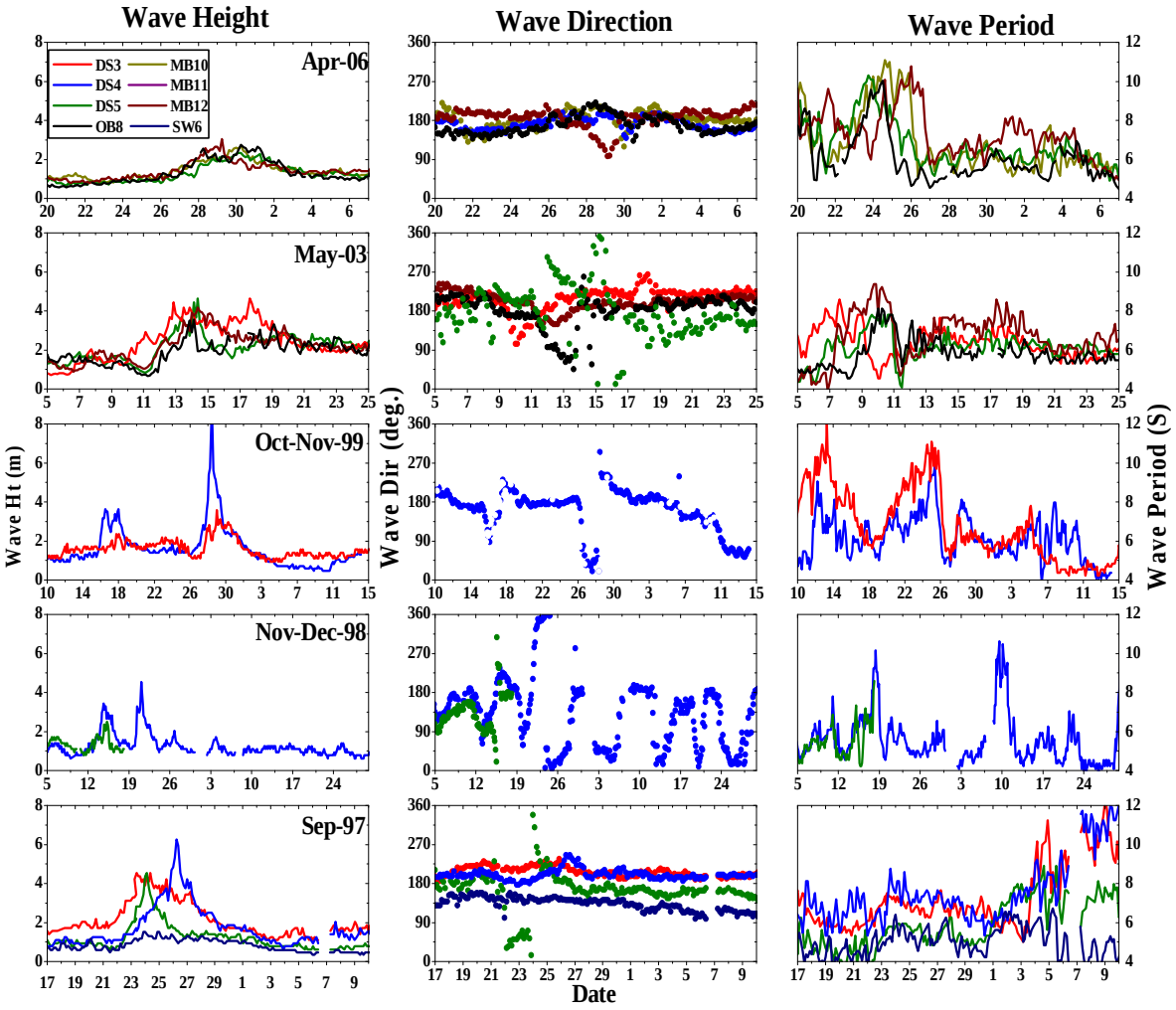

Fig. 5.4: Wave observations during the passage of various cyclones in BoB

DS3-A and DS4-B buoys recorded wave observations during the passage of cyclones in October 1999. During the first cyclone, DS3-A does not exhibit any significant change in wave height whereas DS4-B exhibited swift increase to a maximum of 3.63m. Inadvertently, wave direction was not available at DS3-A location. During the occurrence of the second cyclone, there was a sharp increase in wave height at both locations. The DS4-B buoy recorded 8.44m on 28 October 1999, which is the highest deep ocean wave height observed in the North Indian Ocean, as on date (Rajesh *et al.*, 2005). DS4-B exhibited a slight clockwise rotation during the passage of first cyclone followed by an anticlockwise rotation during the second cyclone. At this instance, even though the

DS4-B buoy was very close to track during the second cyclone, the position being on the left side, resulted in an incomplete rotation. The wave period exhibited nearly uniform variation at both the buoy locations. The sharp decrease in wave period indicates the dominance of sea waves during the passage of cyclones.

The wave observations exhibited a slight increase in wave height during the passage of cyclone in May 2003 (Fig. 5.4). The DS3-B buoy had recorded two peaks in wave height of 4.5m and 4.65m on 12 and 17 May 2003, respectively. The buoy DS3-B on the right side of the track exhibited a slight clockwise rotation. The DS5-B and OB8 buoys on the left side of the track exhibited slight anticlockwise rotation whereas the MB12 buoy on the left side of the track did not indicate any significant change in wave direction.

The wave observations exhibited calm sea conditions except a slight peak of wave height not more than 3m during the cyclone in April 2006. The wave direction remained nearly southwesterly at all locations except the mild anticlockwise rotation at MB12 during the passage of cyclone (Fig. 5.4).

5.6.1 Wave Spectrum

The wave spectral data is available during May 2003 (DS3-B and OB8) and April 2006 (DS5-B) which exhibits the variability of wave energy during the cyclone passage (Fig. 5.5). The rapid increase in wave period around 11 May indicates the passage of cyclone near the buoy location (Young, 2003). The presence of single peaked spectra for a longer duration separated by a short duration of double peaks at DS3-B clearly indicates that the location is under the influence of cyclone for a longer period. The spectra then exhibits double peak from 20 May till the end of month, May 2003. The first peak in swell region is centered on 0.05Hz and the second peak in sea band slowly varies from 0.1Hz to 0.15Hz and then returns to 0.1Hz by the end of May. During the occurrence of double peaks, the major peak is in the sea band, which indicates the dominance of local wind.

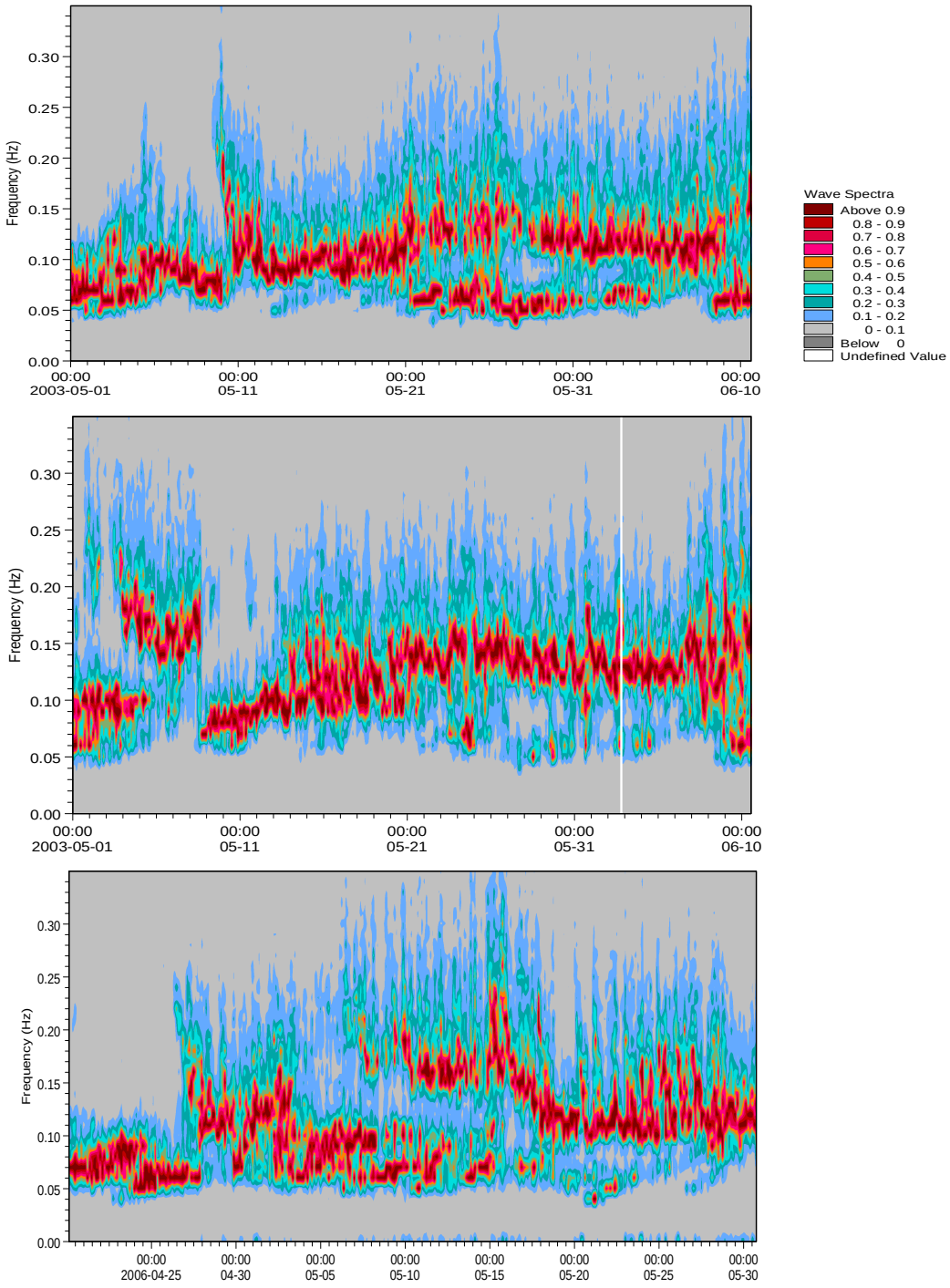

Fig. 5.5: Wave spectra during the passage of May 2003 [DS3-B(top), OB8(Middle)] and April 2006 [DS5-B(Bottom)] cyclones in BoB

Wave spectra at OB8 also exhibit the impact of cyclone passage during May 2003 (Fig. 5.5). OB8 also exhibits single peaked spectra at lower frequencies at the beginning of May 2003, which indicates the dominance of long swells at the location. The spectra then exhibit double peaks during the days 03 - 06 May, followed by single peaks at higher frequency. The sudden shift from high frequency to lower frequency single peak spectra during 09 May 2003 indicates the presence of the swells reaching the location from a distant storm. Unlike the DS3-B, the cyclone passage is indicated by single peaks in swell region. The location of the buoy far away from the cyclone track is the reason for the less dominance of single peak at higher frequencies during cyclone passage. The spectral peak then exhibits a gradual shift from 0.07Hz to 0.15Hz and this continues upto 05 June, 2003. The spectra also exhibits occasional double peak from 22 May to 05 June with major peaks in the sea band and with lesser contribution from swell waves. The spectra, thereafter, from 05 June onwards exhibit distinct double peaks with significant contribution from both the bands.

Wave spectra at DS5-B exhibits pre-cyclonic single peaks (0.07Hz) followed by double peaks for a short period and again single peaks in higher frequency (~0.12Hz) during 20 to 30 April 2006. The single peaks immediately after the passage of cyclone exhibit wide spectra with peaks shifting between 0.05Hz and 0.15Hz indicate the contribution from both sea and swells. The spectra then exhibit double peaks during 07-22 May indicating the presence of swells generated by a distant cyclone. An interesting feature is that the buoy exhibits swell dominated double peaks for a significant period of time followed by sea dominated double peaks (Fig. 5.5). It indicates the importance of swells from the distant cyclone at this location for a longer duration.

5.7 Surface Current Observations

The surface current observations at the buoy locations do exhibit interesting features. The data buoy DS4-A exhibits clockwise rotation in current direction followed by rapid increase in current speed after the passage of cyclone in September 1997 (Fig. 5.6). The DS4-A buoy recorded a maximum of 148.8 cm/s on 26 September 1997. The oscillation

exhibit a periodicity of ~36 hour which matches the inertial period of the location and lasted for ~20 days. DS5-A also recorded a clockwise rotation in current direction which resumed as eastward flow immediately after one cycle of rotation. DS3-A buoy does not exhibit any significant change in current speed/direction during the cyclone passage.

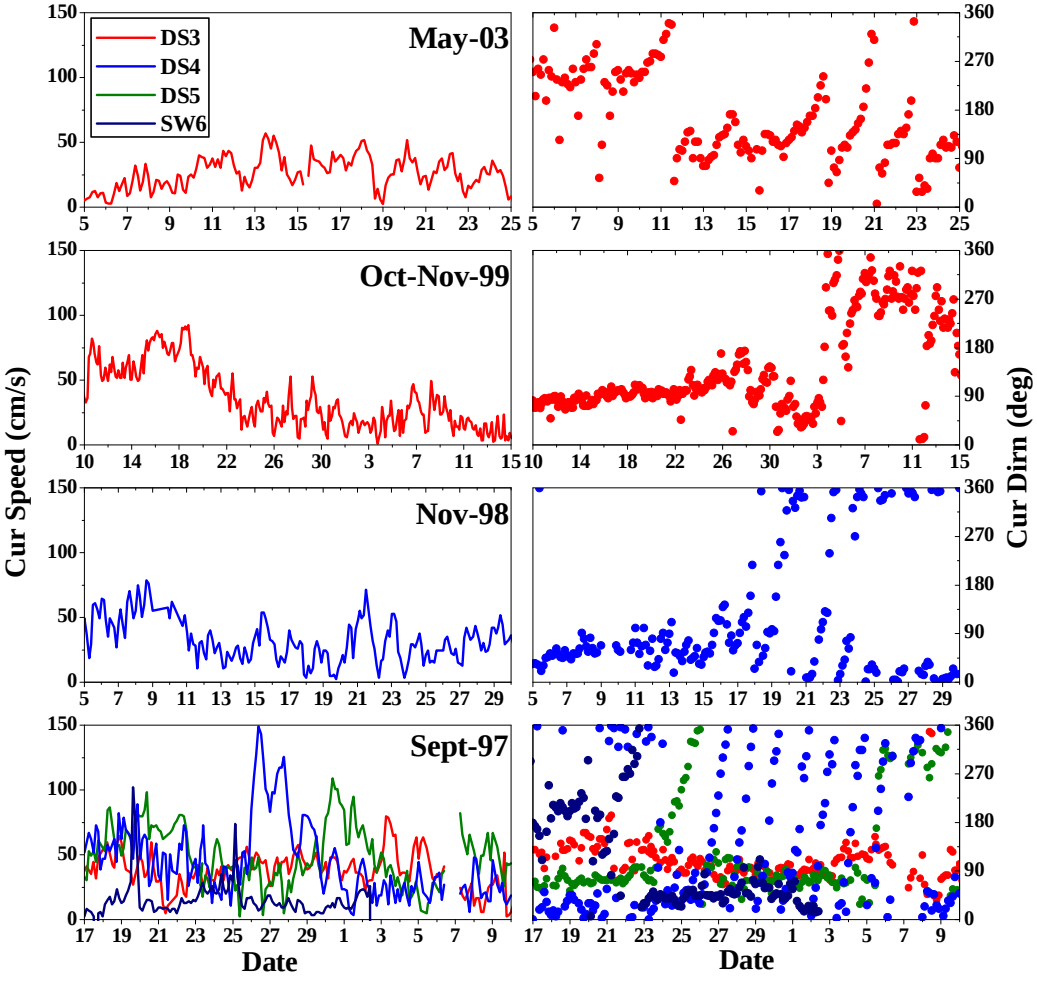

Fig. 5.6: Surface current observations during the passage of various cyclones in BoB

Surface current observations are available only at DS4-B location during the cyclones in November 1998, which exhibits clockwise rotation associated with the passage of the second cyclone (Fig. 5.6). The clockwise rotation exhibited only two complete cycles and weakened immediately after the cyclone passage. The current speed remains more or less uniform with an average speed of 45cm/s. The wind direction exhibits complete clockwise rotation during both the cyclones, which indicates strong resonance between

wind and current. However the wind speed observed at this location is comparatively weak during November 1998 cyclones (12.53m/s and 17.96m/s respectively).

The surface current observations are available only at DS3-A location during the passage of cyclones in October 1999, which exhibits moderate values including the prevalence of the cyclone. The current speed was around 50cm/s before the cyclone passage which reduced to an average of 25cm/s after the passage of first distant cyclone and continued till the end of observation (Fig.5.6). The first cyclone does not generate any significant change in current direction. During the passage of the second cyclone, the current direction exhibited a clockwise rotation. The surface current observations are available only at DS3-B buoy during the cyclone in May 2003, without any significant change in current speed. The current direction exhibited clockwise rotation associated with cyclone passage in May 2003.

Clockwise rotation in current direction is observed during passage of cyclones in BoB, which indicates the inertial oscillation generated by the cyclone. Detailed analysis of current vectors is carried out to delineate the properties of inertial oscillation. Significant oscillation in current vectors is observed only at DS4-A location during September 1997, which lasted for more than a week with nearly equal eastward and northward components (Fig. 5.7). A phase lag in eastward component behind northward component signifies the clockwise rotation. The current vectors at DS3-A do not exhibit any oscillation and that of DS5A exhibit a slight oscillation only.

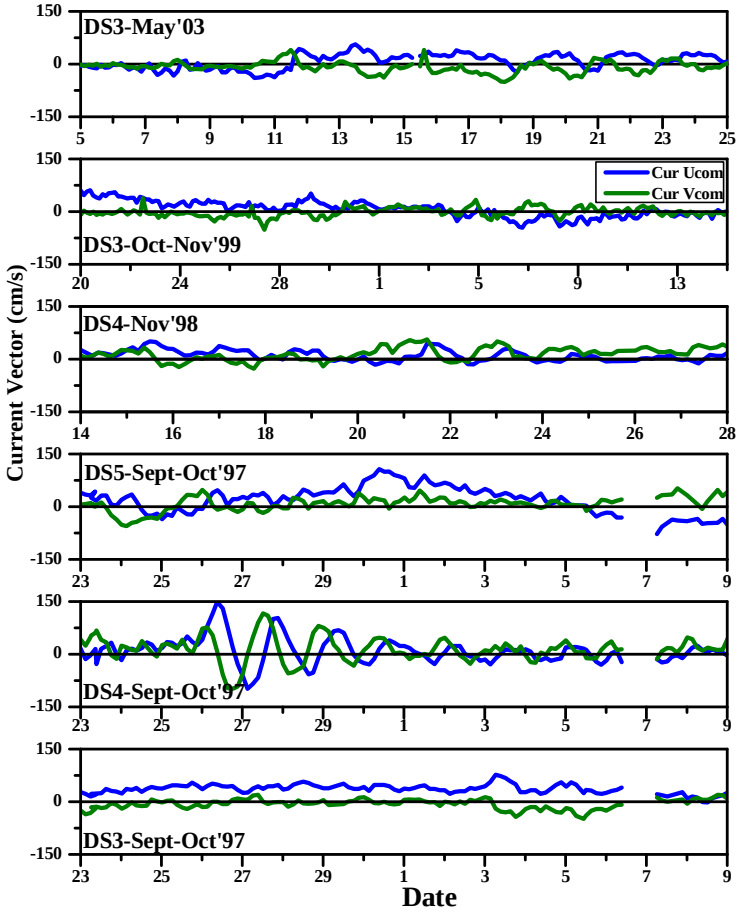

Fig. 5.7: Surface current vectors during the passage of various cyclones in BoB

The current vectors during November 1998 exhibit a weak oscillation at DS4-B location. Even though the wind forcing and the relative location of the buoy were most favorable for generating inertial oscillation, the absence of strong wind and currents inhibit the generation of significantly long lasting inertial oscillation. The current vectors during October 1999 and May 2003 exhibit weak oscillations too.

5.7.1 Progressive Vector Diagram

The Progressive Vector Diagrams (PVD) indicate the mean flow in surface current during the passage of cyclone. PVD of DS4-A during September 1997 exhibit clockwise rotation with mean flow towards northeast. The PVD displays well defined seven circles with decreasing radius, which reveals the transient nature of the oscillation. The inertial oscillation started on 25 September 1997 was noticed upto 19 October 1997 (Fig. 5.8).

The observed inertial period is 36 hours whereas the computed inertial period for the same latitude was 36.75 hours. The observed radius of oscillation corresponding to the highest current speed is ~25.00km where as the computed radius is 31.33km at DS4-A location. PVD at DS5-A exhibited a single clockwise rotation during September 1997. Even though the track was very close to the buoy, the location on the left side of the track along with lesser intensity of the cyclone is attributed as a reason for lesser response at DS5-A. The DS3-A buoy was quite far away from the track and hence the PVD exhibited southeastward flow without any significant change associated with cyclone.

PVD at DS4-B during the first cyclone in November 1998 exhibits east-northeast flow without any oscillation. However the surface current during the second cyclone is towards north with semicircular clockwise rotation. The buoy was on the right side of the track during the two cyclone passages and was very close to the track during the second cyclone in November 1998. The cyclone intensified into category one (cy-1) with clockwise rotation in wind direction.

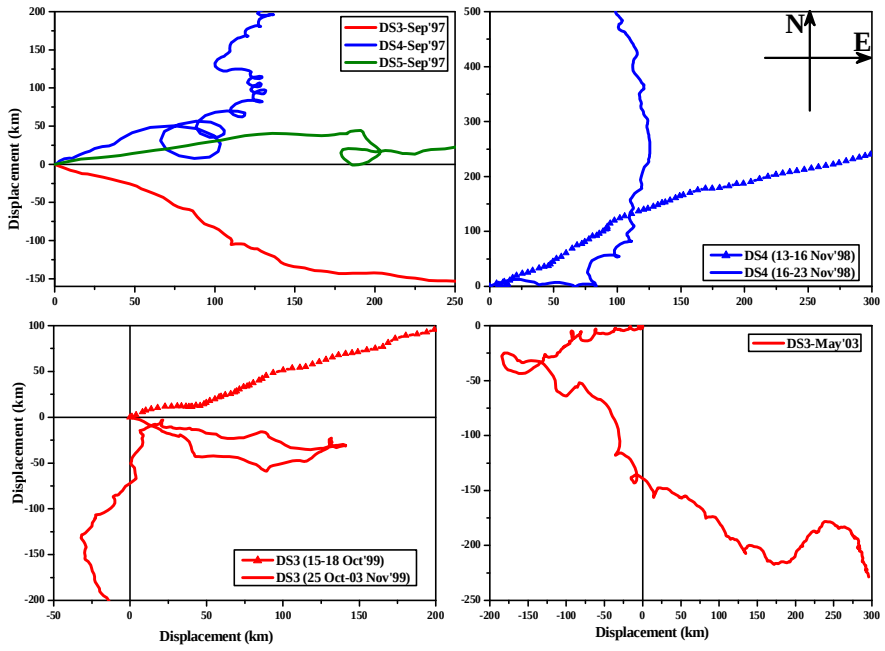

Fig. 5.8: Progressive vector diagram of surface current during the passage of various cyclones in BoB

The buoy DS3-A was on the left side at a considerable distance from the cyclone tracks during the passage of cyclones in October 1999. The PVD during the first cyclone exhibited steady northeastward flow without any inertial oscillation. However the PVD during the second cyclone (Orissa super cyclone) exhibited peculiar feature(s) which moved east - southeast and then turned to move towards the opposite direction. PVD exhibited slight clockwise rotation with a mean southerly flow. The location being on the left side and the large distance from the track could be the reason for lesser response at this location.

PVD at DS3-B exhibited an initial mean flow towards southwest and also displayed a clockwise circle during May 2003. The mean flow exhibited sudden shift in direction from southwest to southeast with slight clockwise rotation. The change in mean direction resulted from the change in cyclone track which passed closer to the buoy twice during its course in May 2003.

5.7.2 Rotary Spectrum

The rotary spectra during the passage of various cyclones indicate the intensity and variability of inertial oscillation at different locations (Fig. 5.9). The rotary spectrum analysis exhibited significant peak at the inertial band in the negative rotary component (S^-) with marginal difference between the positive and negative components, except at DS5-A during September 1997. The rotary coefficient, which indicates the strength of the inertial oscillation at the time of inertial peak, is negative with high magnitude and a phase difference of ~90degree, which indicates that the inertial oscillation observed at the buoy site is nearly circular in clockwise direction.

Strong inertial oscillation is observed at DS4-A location during September 1997 as indicated by the peak at 36hr (very close to local inertial period of 36.75hr) with high energy. DS3-A exhibits peak at 45hr whereas the local inertial period is 53.25hr. DS3-A and DS4-A exhibit peak at inertial band with blue shift whereas no peak is observed at DS5-A near inertial band.

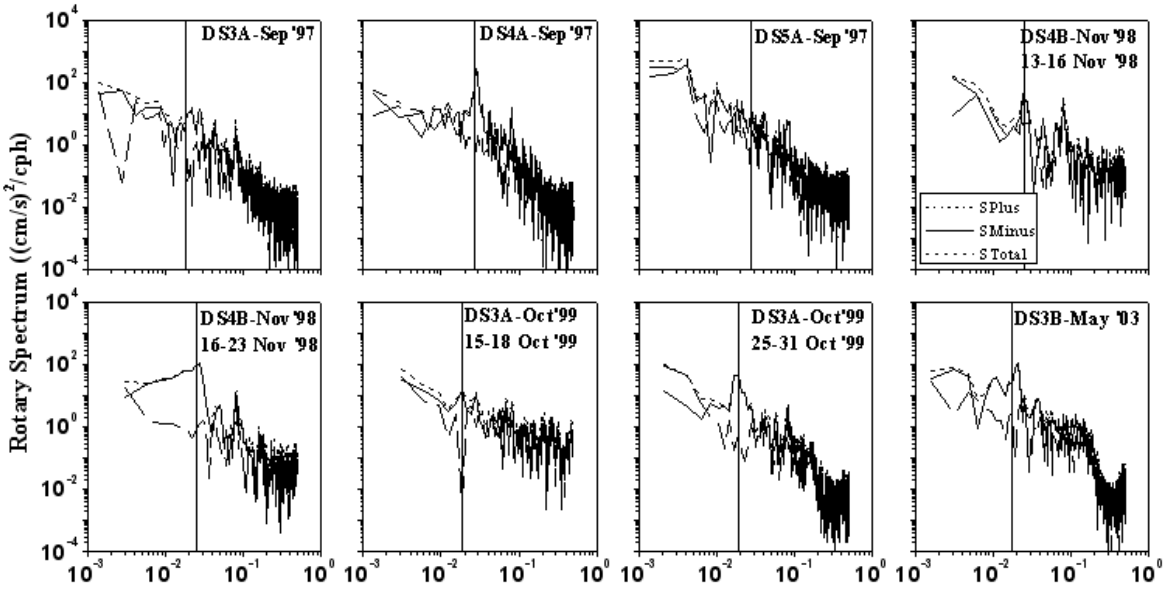

Fig. 5.9: Rotary spectra of surface current during the passage of various cyclones in BoB. The vertical line indicate the local inertial frequency

The rotary spectra during the cyclones in November 1998 exhibited distinct peaks at inertial band. The inertial peak during the first cyclone in November 1998 displays a narrow peak with significant energy at 40.5hr, whereas that of second cyclone exhibits a wider peak at 36hr corresponding to a local inertial period of 36.75hr. The energy in the second cyclone is higher and the shift is less which indicates higher inertial oscillation. The wider peak signifies the distribution of energy over a band around the inertial frequency.

The rotary spectra during the cyclones in October 1999 exhibited peaks at 54hr (October 1999a) and 53.33hr (October 1999b) very close to the local inertial period of 53.25hr with a slight red shift. However the inertial peak during the second cyclone exhibits higher energy than that of first cyclone. May 2003 cyclone exhibits dominant peak at 48.10hr against local inertial period of 56.91hr which indicates considerable blue shift.

Table 5.2: Inertial characteristics observed during cyclone passages

Period	Location	Phase Diff. at Inertial Peak	Rotary Coefft	Percentage of Energy	Local Inertial Period (hour)	Observed Inertial Period (hour)	Shift (hour)
Sep '97	DS3-A	91.48	-0.999	10.10	53.25	45	-8.25 (Blue)
Sep '97	DS4-A	94.17	-0.995	52.40	36.75	36	-0.75 (Blue)
Sep '97	DS5-A	107.72	-0.574	2.16	43.43	--	--
Nov '98a	DS4-B	124.96	-0.800	14.91	36.75	40.5	+3.75 (Red)
Nov '98b	DS4-B	81.37	-0.986	57.05	36.75	36	-0.75 (Blue)
Oct '99a	DS3-A	91.70	-0.999	12.35	53.25	54	+0.75 (Red)
Oct '99b	DS3-A	92.24	-0.980	17.55	53.25	53.33	+0.08 (Red)
May '03	DS3-B	86.14	-0.948	29.53	56.91	48.1	-8.81(Blue)

The high energy at DS4-A during September 1997 accounts for more than 50% of the total energy (Table 5.2). Even though the November 1998b accounts for the highest energy, the wider peak at inertial band indicates the distribution over a wider range whereas that of September 1997 is concentrated in the inertial frequency alone. The distribution of energy during May 2003 also accounts for considerable contribution from inertial band. Near circular clockwise rotations are indicated by the ~90 degree phase difference and ~ -0.99 rotary coefficient. The maximum transfer of energy is observed at DS3-A during the second cyclone in October 1999 as indicated by the minimum difference between observed and local inertial frequency (Gonella, 1971). The cyclones during October 1999a, September 1997 and November 1998b also accounts for higher transfer of momentum. The shift in inertial frequency could be due to presence of mean flow pattern which leads to [Doppler] shift in inertial frequency (White, 1972). The considerable blue shift observed at DS3-A during September 1997 and DS3-B during May 2003 could be due to the mean southeastward flow prevailing at that location. The dissipation of inertial oscillation energy by turbulent mixing downward from the surface layer is another reason for lowering of inertial frequency (Pollard, 1970) observed at buoy locations.

5.8 Variability in Temperature and Salinity

The variability in mixed layer characteristics are considered as one of the most important indicator(s) of the oceanic response associated with cyclone passage. The thermohaline variability inferred from moored buoys, ARGO floats and TMI-SST is utilized to quantify the mixed layer response.

5.8.1 Sea Surface Temperature

The sea surface temperature variation during any cyclone passage depicts the response of the upper ocean to the cyclone. Rapid decrease in SST associated with cyclone passage with significant reduction in diurnal oscillation indicates significant mixing forced by strong cyclonic winds over the ocean surface.

The pre-cyclonic SST at DS4-A is much higher than that of other locations and exhibited maximum decrease during the passage of cyclone in September 1997 (Fig. 5.10). Price (1981) reported that the cyclone generated strong mixed layer currents leads to strong entrainment and high response in mixed layer and SST. Dickey *et al.* (1998) reported that the inertial oscillation is accompanied by large-amplitude temperature oscillations at inertial period leading to vertical displacements of isotherms in the mixed layer which results in enhanced mixing and cooling. The combined effect of cyclone and strong inertial oscillation resulted in the abrupt decrease of 2.25^{o}C at DS4-A. Higher wind speed observed at DS5-A site had recorded a decrease of 1.07^{o}C only in SST. This emphasizes the role of relative location and proximity to the cyclone track in upper ocean response. Large diurnal oscillations are observed in SST just before the cyclone passage. SST almost regained the pre-cyclonic conditions within a period of 10 days at DS3-A and DS5-A, whereas the DS4-A remained cooler as a consequence of larger reduction in SST. The pre-cyclone SST at SW6 exhibits much low values (~27^{o}C) and it exhibited a slight decrease of ~0.5^{o}C. However the SST at all locations including SW6 attains near homogenous values (inside one degree), spread over a wide oceanic area, within one week of the cyclone. It reveals nearly uniform SST near the track after cyclone passage.

Only DS4-A buoy has salinity observation reported, exhibiting a pre-cyclonic value of < 27psu. The salinity exhibited a swift increase of 4.0psu which mirrors the decrease in SST associated with cyclone passage. The significant increase in salinity shows the intensity of the cyclone as well as the difference in salinity between the surface layer and the high salinity sub-surface layer. This supports the presence of thin barrier layer with low salinity in BoB (Vinayachandran, *et al.*, 2002). The high salinity remained in the location for a longer period.

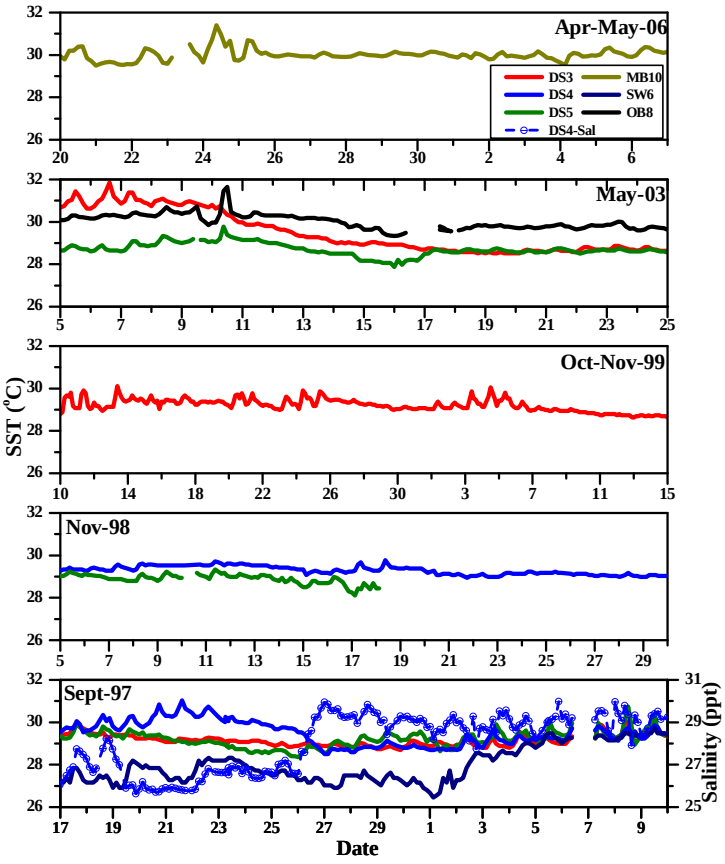

Fig. 5.10: SST and Salinity observations during the passage of various cyclones in BoB

The SST observations during cyclone in November 1998 did not exhibit any significant variation. The SST at DS4-B remains nearly the same (29.3°C) throughout the reporting period (Fig. 5.10). DS5-A exhibited a slight decrease on 17 November 1998. It is intriguing to note that there is very little response in SST associated with cyclone passage at these locations.

The SST observations are available only at DS3-B during the cyclones in October 1999, which did not exhibit much variation except for the reduction in diurnal oscillation during the passage of cyclones. The location of the buoy, far away, on the left side of the track is the reason for low upper ocean response.

The SST observations showed large diurnal variation (except at DS5-B) just before the passage of the cyclone in May 2003 (Fig. 5.10). There was a sharp decrease in SST at all locations with maximum decrease at DS3-B location associated with the passage of cyclone. Lowest pre-cyclonic SST and minimum cooling was observed at DS5-B location. DS3-B exhibited highest SST before the cyclone passage and was located on the right side of the track and exhibited a maximum cooling of 2.25^{o}C at the buoy location.

The SST observations are available only at MB10 location during the passage of cyclone in April 2006, which exhibited large pre-cyclonic diurnal oscillations. There was considerable reduction in the diurnal oscillation after the cyclone passage (Fig. 5.10). The location did not exhibit any significant reduction in SST and retained an average value of 30^{o}C. The large distances from the cyclone track could be the reason for such mild response at this location.

5.8.2 Subsurface variability in temperature and salinity

The subsurface response in temperature and salinity was studied utilizing the data from temperature profiles in moored buoys (September 1997) and ARGO floats in BoB (May 2003 and April 2006) during the passage of cyclones. The temperature profile upto a depth of 120m is available at DS3-A and DS5-A locations during the passage of September 1997 cyclone. Data from three floats each during May 2003 and April 2006 cyclones, all located on the left side of the track, exhibited wide variability in temporal and spatial scales.

5.8.2.1 Moored buoy observations

The temperature profiles during September 1997 cyclone indicates cooling of surface temperature and deepening of the mixed layer associated with the passage of cyclone

(Fig. 5.11). The maximum SST before the cyclone passage was 29°C at both the locations which reduced to 28.5°C after the cyclone passage. The DS3-A location regained pre-cyclonic SST whereas the DS5-A location exhibited a warming trend reaching a maximum of 30°C within 20 days of cyclone passage. The MLD before the cyclone passage was 40m at DS3-A and 30m at DS5-A locations which deepened to 60m at DS3-A and 50m at DS5-A locations. Similar to that of MLD, the 26°C isotherm also exhibits deepening by 20m at DS3-A and DS5-A locations. The upward trend in isotherms observed at DS3-A location after the cyclone passage indicate presence of upwelling.

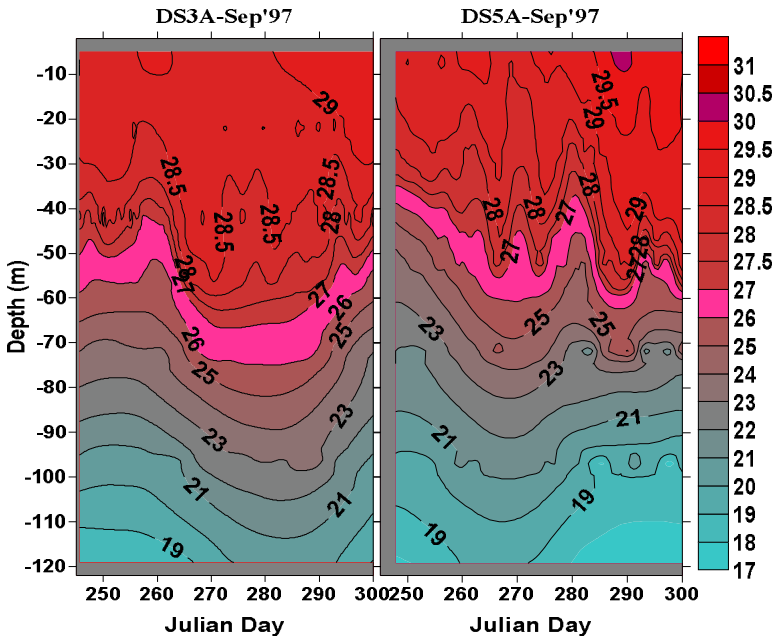

Fig. 5.11: Vertical distribution of temperature at two buoy locations (DS3-A and DS5-A) during the passage of September 1997 cyclone in BoB

The spectral analysis of temperature profiles at DS3-A and DS5-A during September 1997 does not exhibit any significant oscillation in the inertial frequency (Fig. 5.12). The location of DS3-A buoy, far away from the cyclone track could be the reason for the absence of inertial oscillation at this location. Even though the DS5-A is closer to the

track, the location being on the left side of the track and the low intensity of the cyclone has attributed to the absence of inertial oscillation.

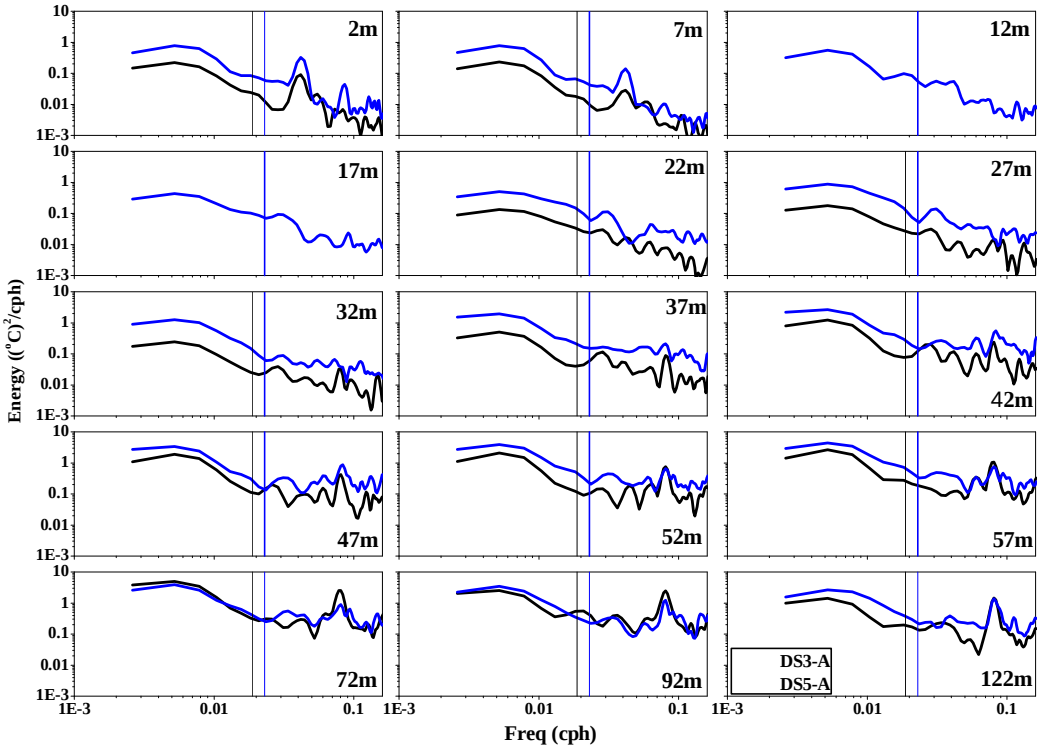

Fig. 5.12: The power spectrum of temperature profiles (DS3-A and DS5-A) during the cyclone in September 1997. The vertical line indicates the local inertial frequency

5.8.2.2 ARGO float observations

The temperature-salinity profiles exhibit presence of warm low saline water just before the passage of cyclone at all sites (Fig. 5.13) during May 2003 and April 2006. The pre-cyclonic temperature field exhibited an increasing trend throughout the layer as shown by the downward slope of the contours during the cyclone in May 2003 (Fig. 5.14). The SST was more than 30^{o}C at all locations before the passage of cyclone that cooled the waters by 0.6^{o}C at float- 2900093, 0.8^{o}C at 2900094 and a maximum of 1.1^{o}C at 2900226. The mixed layer depth before the passage of cyclone was 40m, which exhibits mild deepening after the cyclone passage. The upwelling associated with the cyclone passage is well observed from the upward slope in isotherms.

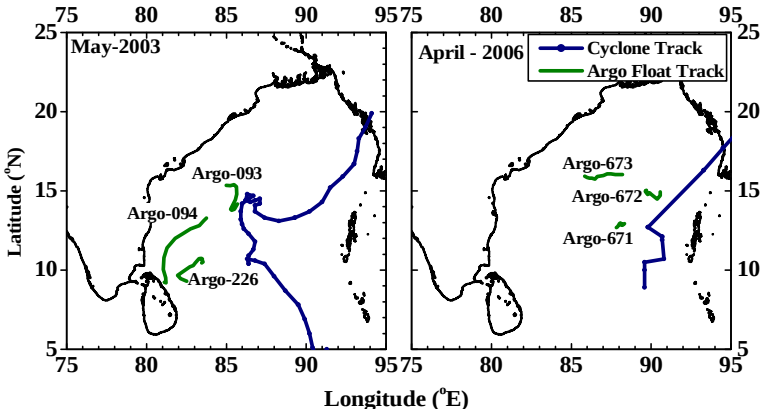

Fig. 5.13: Cyclone tracks and Argo float trajectories during May'03 and April'06 cyclones

The locations 4900671 and 4900672 exhibited comparatively less deepening of mixed layer during the cyclone passage in April 2006 followed by upward slope in isotherms indicating the upwelling (Fig. 5.14). The temperature profile at 4900673 exhibited a warming phase throughout the observational period. The large distance from the track could be the reason for lesser response at this location.

The vertical distribution of salinity during the cyclone in May 2003 exhibited variability upto a depth of ~100m, below which the salinity values remained nearly uniform (Fig. 5.14). Salinity was increasing rapidly just before the cyclone passage at all locations and immediately dropped after the cyclone passage. Minimum surface salinity of 33.26psu was observed at 2900093 and 2900226, whereas the corresponding minimum at 2900094 was 33.20psu along the track. The locations 2900226 recorded a reduction of only 0.4psu in surface salinity during the cyclone passage whereas 2900094 and 2900093 recorded a reduction of 0.6 to 0.8psu associated with cyclone passage. The salinity values remain uniform upto a depth of 40m during cyclone passage at all locations, which indicate the intensity of vertical mixing. The location of 2900093 exhibited large oscillation in surface salinity whereas that at 2900226 is nearly stable especially after the passage of cyclone. The surface salinity at 2900093 regained high salinity values by the end of May and thereafter reduced to 33.20psu in another 5 days.

Another interesting feature noteworthy in the temperature and salinity profiles is the presence of eddies, especially at 2900093 indicated by the alternate bands of high saline warmer water and low saline cooler water.

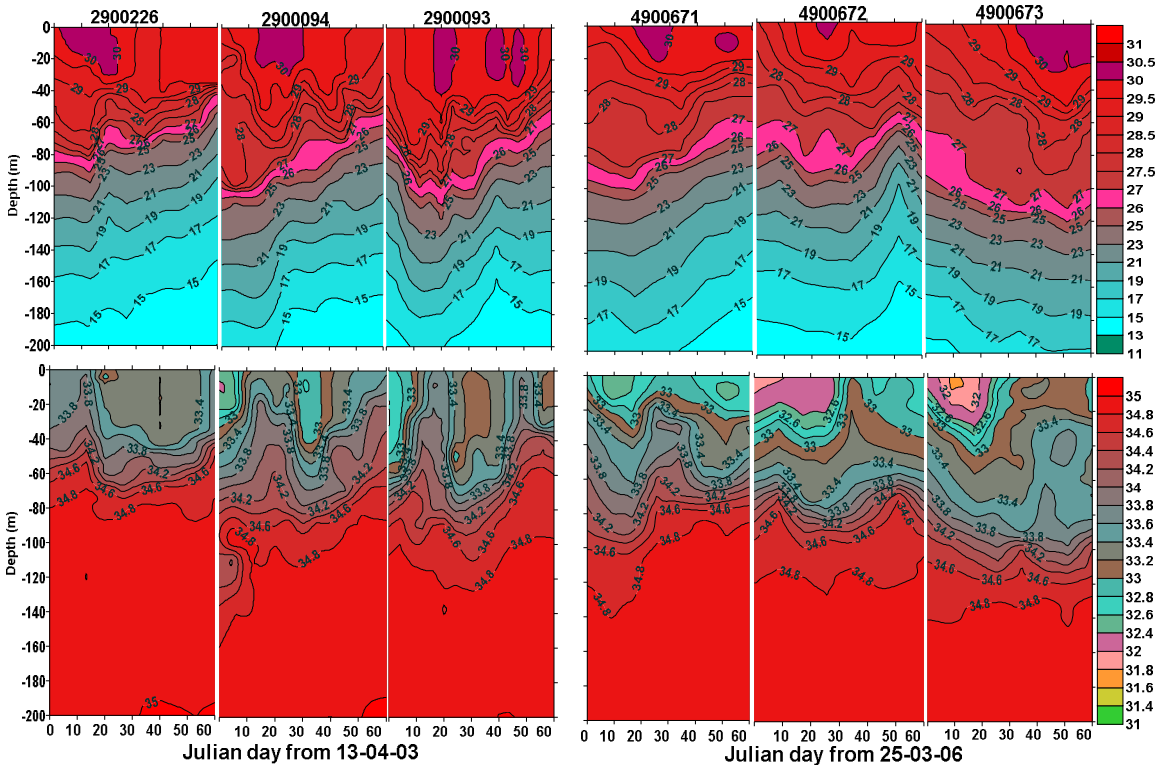

Fig. 5.14: Vertical Distribution of Temperature (top panel) and Salinity (bottom panel) from Argo Floats during the passage of BoB cyclones in May 2003 (left panel) and in April 2006 (right panel)

Presence of low surface salinity was observed with a minimum value of 31.8psu at 4900672 and 4900673 locations before April 2006 cyclone (Fig. 5.14). The mixing of less saline surface waters with deeper high saline water was observed at all locations associated with cyclone passage. The increase in salinity at 4900671 location is much less compared to that of other locations and returns back to the pre-cyclonic condition immediately after the passage of the cyclone. There was substantial increase (by more than 1psu) in salinity values during the passage of cyclone at 4900672 and 4900673. The high salinity at 4900673 sustained for a longer duration which coincided with an increase in temperature values.

5.8.3 Spatial and temporal variability in SST

TMI-SST at the location of maximum intensity is retrieved for a period of 30 days starting from 10 days before the day of maximum intensity (Table 5.3). The data is extracted over a longitudinal band of 7.5degree with 2.5degree on the left side and 5.0degree on the right side of the location of maximum intensity. Unlike the cyclones in AS, some cyclones (November 1998a, October 1999a, October 1999b and April 2006) attained maximum intensity just before landfall and made it difficult to extract the exact longitudinal band on either side of the location of maximum intensity. Hence an appropriate, longitudinal band is extracted to depict the variability in TMI-SST. The Hovmöller diagrams of SST exhibited the temporal (and spatial) cooling features and its variability associated with the passage of cyclones.

Table 5.3: TMI data extraction details during cyclones in BoB

Sl. No.	Type	Starting date of TMI-SST	Max. Wind	Location of Max. Intensity	
				Longitude(^{o}E)	Latitude(^{o}N)
1.	Cy-2	05 November 1998	85 kt	82.7	17.8
2.	Cy-1	12 November 1998	75 kt	87.7	19.7
3.	Cy-4	08 October 1999	120 kt	85.3	17.7
4.	Cy-5	19 October 1999	140 kt	87.2	19.1
5.	TS	05 May 2003	35 kt	86.2	14.4
6.	Cy-4	22 April 2006	115 kt	93.3	16.3

Maximum drop of ~1.5^{o}C in SST was observed during the passage of the first cyclone in November 1998. Since the cyclone had attained the maximum intensity just before land fall, maximum cooling occurred in shallow waters (84.5^{o}E), near the coast. The temporal and spatial coverage of the cooling was relatively less (Fig. 5.15). The passage of second cyclone in November 1998 also did not exhibit any significant drop in SST. The TMI-SST is at par with buoy observations which exhibited less impact(s) on SST.

Considering the higher intensity of cyclones during October 1999, the spatial and temporal coverage of the cooling features is comparatively low. The cooling observed after the passage of the first cyclone is 3.45°C centred around 85.5°E at a distance of 22km on the right side of the track. The cooling lasted for ~7 days over a narrow spatial band. The maximum cooling produced by the second cyclone is 4.05°C, centred around 88.0°E on the right side of the track and also at 86.0°E at left side of the track. Mahapatra *et al.* (2007) also reported regions of maximum surface cooling on the left of the cyclone track during Orissa Super Cyclone. The cyclone re-emerged into ocean waters after landfall, progressively moved southwards and finally dissipated over the open ocean. This could have added impacts on surface cooling, reflected on left side of the track. This cooling lasted for 5 days over a narrow spatial band.

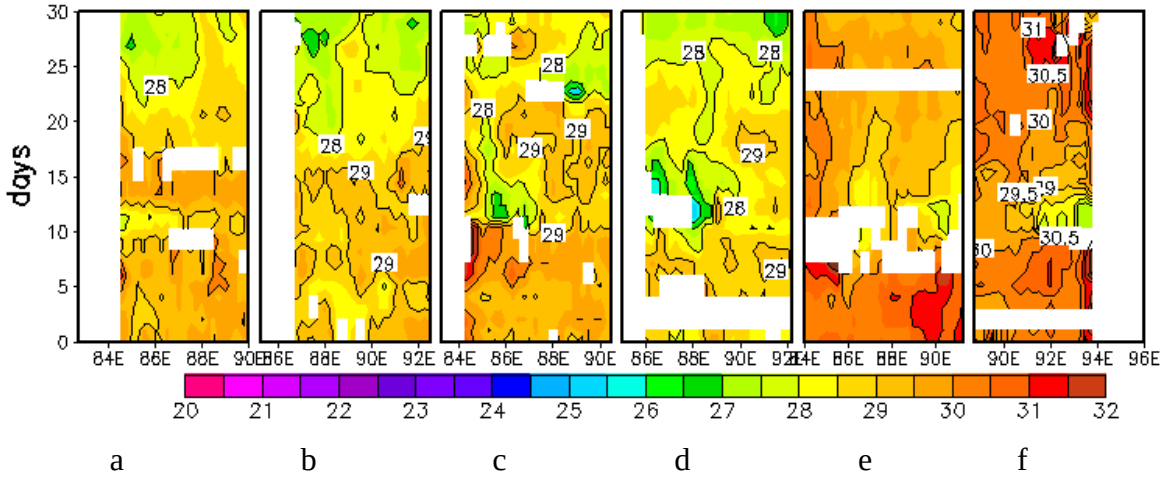

Fig. 5.15: TMI-SST during the passage of various cyclones in BoB: a) November 1998a, b) November 1998b, c) October 1999a, d) October 1999b, e)May 2003 and f) April 2006 cyclones

The pre-cyclone SST related to the first cyclone (October 1999a) was 30.15°C whereas that of second cyclone (October 1999b) was 29.10°C. The cooling associated with the first cyclone considerably reduced the pre-cyclone SST of the second cyclone which could be the reason for the lower cooling in SST during the more intense second cyclone. However Sadhuram (2004) had reported ~6°C fall in SST in Bay of Bengal after the passage of Orissa Super Cyclone (October 1999b).

The maximum cooling during the cyclone of May 2003 was 3.3^{o}C, observed at 90^{o}E followed by cooling of 2.5^{o}C around 86.25^{o}E. The cooling lasted for more than a week. Even though the system could not intensify beyond tropical storm, the associated cooling appears significant. The cooling at 86.25^{o}E indicates the less rightward bias in surface cooling associated with low cyclone translation speed. The significant cooling at 90^{o}E could be due to the curved cyclone track keeping the area under cyclone forcing for a longer duration.

The maximum cooling was 3.3^{o}C observed, at the right side of the cyclone track during the cyclone in April 2006 and this feature lasted for less than a week (Fig. 5.15). The system attained maximum intensity near the coast where relevant data is not available. Hence the exact nature of cooling could not be estimated from the satellite data.

5.9 Results and discussion

The upper ocean response to cyclones in BoB exhibits significant variability which depends on the distinctiveness of the cyclone, the time of occurrence and ocean mixed layer characteristics. The data buoy observations have helped to indicate the severity of the cyclone in terms of a drop in SLP and increase in wind speed. Maximum drop in SLP of more than 10mb within a day was observed during the passage of September 1997 cyclone, which recorded a minimum of 994.9mb and 995.7mb at locations DS5-A and DS4-A respectively. The maximum drop in SLP corresponds to highest wind speeds of 22.54m/s at DS5-A followed by 20.05m/s at DS4-A locations. The buoy DS5-A was on the left side of the track but closer than that of the DS4-A buoy, which happened to be on the right side of the track. The cyclone was initially category TD near DS5-A and later intensified to category TS near DS4-A location. The high wind speed generated by a TD at a location on the left side of the track is intriguing and this indicates significant atmospheric forcing, even on the left side of the track, as well. However the weak coupling between wind and currents on the left side resulted in a lower ocean response at this location. The clockwise rotation in wind at DS4-A location is in resonance with the clockwise rotation of the surface current which leads to higher momentum exchange as

evidenced by the higher current speed(s) and a reduction in SST. However, the rotation in wave direction was observed only at DS5-A, which reveals that the coupling between wind and wave in a cyclone field exists only over a short radius on the left side of the track. The SST values before the passage of a cyclone exhibits significant variability in BoB, which became nearly equal at all locations. This indicates significant mixing which leads to nearly uniform SST near the track after the cyclone passage.

The SLP attained a minimum of 998.63mb (at DS4-B) corresponding to a maximum wind speed of 17.96m/s during a second cyclone in November 1998. Even though the system was developed to category 'cy-1' near DS4-B, located very close to the track on the right side, the surface meteorological-ocean observations exhibited lower response compared to that of September 1997 cyclone. The wind direction exhibited complete clockwise rotations during both the cyclones of November 1998 which favored strong coupling between wind and the current. However the surface current observations exhibited a lesser amplitude and a weak inertial oscillation, lasting for a shorter duration than that of September 1997 cyclone.

Among the cyclones discussed in this chapter, highest intensity of cy-5 was recorded in respect of Orissa Super cyclone (October 1999b) followed by the cy-4 cyclones of April 2006 and October 1999a. Ocean data (except wave) related to the passage of all these cyclones are limited by the unavailability of nearby buoy observations, specifically on the right side of the track. Only wave observations are available at DS4-B location during the passage of cyclones in October 1999b, which recorded the severity of the cyclone giving rise to wave heights of 8.44m and a complete anticlockwise rotation.

Similar to that of AS, the wind and wave observations are in resonance in BoB and exhibit asymmetric pattern on either side of the track, as indicated in September 1997 (DS5-A), November 1998 (DS5-A and DS4-A), October 1999 (DS4-B), May 2003 (DS3-B, DS5-B, OB8 and MB12) and April 2006 (MB12). However, the rotation in wave direction was limited over a shorter radius of the cyclone and exhibited complete circles which were very close to the track (DS5-A in September 1997, DS4-B in

November 1998b and DS4-B in October 1999). The DS4-B exhibited peculiar oscillation in wave direction associated with the passage of the second cyclone in November 1998. The wave spectra during May 2003 and April 2006 clearly exhibited the change in spectral energy distribution during the passage of cyclones. The double peaks after the passage of cyclone indicates the swell generated from the distant cyclone. The presence of swell dominated double peaks at DS3-B and DS5-B after the cyclone passage indicates the impact of cyclone for a longer duration.

Surface current observations were available only at a few buoy locations, which exhibited inertial oscillations of varying magnitude and revealed the role of relative location(s) on either side of the track. The data buoy DS4-A exhibited clockwise rotation in current direction which lasted for ~20 days and recorded a maximum of 148.8 cm/s during September 1997. Clockwise rotation was observed during the second cyclone in November 1998 but with lesser magnitude and shorter duration. The absence of strong inertial oscillation during November 1998 even with a strong resonance with wind (indicated by clockwise rotation) could be due to the weaker wind speed. The surface current observations were available only at DS3-A location during the passage of cyclones in October 1999, which exhibited moderate values (~35cm/s). The current direction exhibited a clockwise rotation during the second cyclone in October 1999. The surface current observations were available only at DS3-B buoy during the cyclone in May 2003, without any significant change in current speed and a slight clockwise rotation in current direction.

Strong inertial oscillation was observed at DS4-A location during September 1997 as indicated by PVD and rotary spectral peak at 36hours (very close to local inertial period of 36.75hr) with high energy (52.4%). The inertial peak during the first cyclone in November 1998 displays a narrow peak with significant energy at 40.5hr, whereas that of second cyclone exhibited a wider peak at 36hr corresponding to a local inertial period of 36.75hr. The energy in the second cyclone was higher and the shift was less which indicates higher inertial oscillation. The rotary spectra during the cyclones in October 1999 exhibited peaks at 54hr (October 1999a) and 53.33hr (October 1999b), very close to

the local inertial period of 53.25hr. The shift observed in inertial frequency could be due to the prevailing mean flow conditions and turbulent mixing associated with cyclone passage (White, 1972).

The SST observations exhibited the cooling associated at specific locations as well as the spatial extend of cooling. It revealed the importance of relative location and proximity to cyclone track with higher cooling near right side of the track. The SST observations exhibited large pre-cyclonic diurnal oscillations followed by considerable reduction in the diurnal oscillation during and after the cyclone passage. The spatial mixing revealed from buoy observations associated with September 1997 cyclone is remarkable with its large spatial coverage along the eastern coastal belt of India. Maximum reduction in SST (2.25^{o}C) was observed at DS4-A associated with September 1997 cyclone. Meager response in SST at DS4-B and DS5-A located close to cyclone tracks in November 1998 is intriguing. The SST observations at DS3-B during the cyclones in October 1999, also did not exhibit much variation owing to its location, far away, on the left side of the track. DS3-B located on the right side of the track, exhibited highest SST before the cyclone passage and maximum cooling of 2.25^{o}C during the passage of May 2003 cyclone. The low cyclone translation speed also contributed to the higher cooling at this location.

The temperature profiles at DS3-A and DS5-A locations exhibited the reduction in SST and the deepening of mixed layer associated with cyclone passage. The mixed layer depth exhibited a deepening of 20m (40 to 60m at DS3-A and 30 to 50m at DS5-A) associated with cyclone passage. The Argo floats exhibited a pre-cyclone warming phase followed by cooling associated with cyclone passage. A noticeable feature is that the deepening of mixed layer lasts for a short period and returns to the pre-cyclonic condition rapidly. Another interesting feature in the temperature and salinity profiles is the presence of eddies, indicated by the alternate bands of high saline warmer water and low saline cooler water.

The TMI-SST exhibits the temporal and spatial extent of cooling associated with cyclone passage. It indicates comparatively lesser cooling than that in AS, even in the case of

high intensity Orissa Super Cyclone. The spatial and temporal extent of cooling in BoB is lesser than that of AS. A drop of ~1.5^{o}C in SST was observed during the passage of the first cyclone in November 1998 whereas that of the second cyclone in November 1998 did not exhibit any significant change in SST. The cooling observed after the passage of the first cyclone in October 1999 is 3.45^{o}C followed by a cooling of 4.05^{o}C during the second cyclone. The cooling associated with the first cyclone considerably reduced the pre-cyclone SST of the second cyclone which could be the reason for the lower cooling in SST during the more intense second cyclone. The maximum cooling during the lesser intensity (TS) slow moving (1.88m/s) cyclone in May 2003 and that of high intensity, moderate speed (4.38m/s) cyclone (Cy-4) in April 2006 was 3.3^{o}C. This reveals the importance of cyclone translation speed in cooling associated with cyclone passage.

CHAPTER-VI

Conclusion

The studies on the upper ocean responses to atmospheric forcing in the North Indian Ocean were intended to understand the responses and its variability during the passage of tropical cyclone(s). North Indian Ocean, being the smallest and most dynamic, remains the most complex among world oceans. The limited northward extent and changing wind patterns further add complexity and thus makes it unique in many oceanographic aspects which include the upper ocean responses to cyclones. The present study did reveal significant characteristics of the upper ocean response(s) in North Indian Ocean and its spatio-temporal variability associated with cyclone passage.

The cyclones in north Indian Ocean often experience large variability in frequency and intensity and exhibit significant variability in responses as well (as detailed in previous chapters). Price *et.al.* (1981) reported that the cyclone intensity and cyclone translation speed are the most important parameters, which determine the oceanic response. The detailed analysis of the observations gathered during cyclone occurrences revealed importance of various parameters, besides features on differential response between AS and BoB, the role of cyclone translation speed, asymmetric response in waves etc. The present study aims at identifying the controlling parameters that contribute significantly to oceanic response. Specifically, the factors studied in detail are intensity of the cyclone, proximity to cyclone track, cyclone translation speed and differential response between AS and BoB with an emphasis on surface cooling.

6.1 Cyclones in the North Indian Ocean

The characteristics of tropical cyclones in the North Indian Ocean during the period 1997 to 2006 exhibit higher number of occurrence under the category 'tropical depression/tropical storm' (68%). A total of 50 systems were reported of which 20 were in AS and the remaining in BoB (Table 6.1). The cyclones in AS were less intense, three occurrences in highest intensity of category 'cyclone-3', whereas three of the BoB cyclones intensified into 'cyclone-4' category and one cyclone attained the intensity of cyclone-5 during the reporting period. One cyclone under the category 'cy-2' was observed in BoB followed by 8 'cy-1' cyclones, of which 5 were in BoB and 3 in AS. There are no occurrence of cyclones under the category 'cy-3' in BoB and 'cy-2' in AS.

Table-6.1: Cyclones observed under various categories during 1997-2006

Year	Trop. Depr & Trop. Storm	Cy-1	Cy-2	Cy-3	Cy-4	Cy-5	**Total**
1997	**3** (2,1)	**1** (1)	-	-	**1** (1)	-	**5** (2,3)
1998	**3** (3)	**3** (1,2)	**1** (1)	**1** (1)		-	**8** (5,3)
1999	**4** (1,3)	-	-	**1** (1)	**1** (1)	**1** (1)	**7** (2,5)
2000	**2** (2)	**1** (1)	-	-	-	-	**3** (3)
2001	**3** (2,1)	-	-	**1** (1)	-	-	**4** (3,1)
2002	**4** (1,3)	-	-	-	-	-	**4** (1,3)
2003	**2** (2)	**1** (1)	-	-	-	-	**3** (1,2)
2004	**3** (3)	**1** (1)	-	-	-	-	**4** (4)
2005	**6** (6)	**1** (1)				-	**7** (7)
2006	**4** (2,2)	-	-	-	**1** (1)	-	**5** (2,3)
Total	**34** (14,20)	**8** (3,5)	**1** (1)	**3** (3)	**3** (3)	**1 (1)**	**50** (20,30)

Red –AS, Blue- BoB and Black Total

A maximum of 8 cyclones were observed in the year 1998 followed by 7 in 1999 and 2005. The years 1998 and 1999 reports the maximum number of high intensity cyclones. The year 1999 reports 3 cyclones under the category of cyclone-3 and above. There were two cyclone free years (2000 and 2005) for AS and only one year (2004) for BoB. It is interesting to note that the absence of cyclones in one region coincided with higher occurrence of cyclones in the other region.

6.2 Temporal and spatial variability of cyclone frequency

The cyclone frequency exhibits significant variability in spatial, inter-annual and intra-annual scale in North Indian Ocean. However there is no significant correlation between the inter-annual variability of cyclone frequency between AS and BoB. One striking feature is the substantial decrease (71.4%) in the number of cyclones in BoB (from average 12.6 to 3.6 in a year) and AS (39.1%) from average 2.3 to 1.4 in a year, after the year 1976. The significant transition in atmosphere-ocean climate system during mid 1970's could be the reason behind this phenomenon as reported for Pacific and Atlantic Oceans.

The intra-annual variability of tropical cyclones in North Indian Ocean is more prominent than the inter-annual variation. The intra-annual variability during 1977 to 2006 differs significantly from that of 1947-1976, particularly for BoB which is not as prominent in AS. The early records exhibit an active cyclone season in BoB during May to December with maximum frequency during post monsoon (September - November). The recent decade exhibited a different scenario with two cyclone seasons namely, before and after the southwest monsoon, with nearly cyclone free monsoon season. The origin and dissipating point(s) of cyclones in North Indian Ocean also reveal large variability in space and time. Also significant variability in cyclone genesis is observed before and after the year 1976. An interesting feature is the southward shift in originating area during the months of January, May and June in BoB and during June in AS.

The long term SST data at selected points in North Indian Ocean could not reveal any radical change since 1976, often distinctly noticed in cyclone frequency. However the warming phenomenon at various latitudes are not uniform in either AS or BoB but exhibits a decreasing trend towards higher latitudes. The study reports that the drastic change in cyclone frequency in Northern Indian Ocean during 1976 is not forced by the increase in SST. The recent trend emerging from this study indicates that the variable net heat gain, with lower monsoon heat gain at higher latitudes, is likely to affect the cyclone formation processes. The long term SLP at selected locations in AS and BoB exhibited

considerable increase during mid 1970's, which could have contributed to the observed reduction in cyclone frequency after 1976.

6.3 Asymmetric response in waves

The analysis of wave responses during the passage of various cyclones indicates that waves are in resonance with cyclonic wind with asymmetric response on either side of the track. As indicated from buoy observations in AS and BoB, the wave direction exhibited clockwise rotation on right side of the track and anticlockwise rotation on left side of the track. However complete circular rotation is observed only on the right side of the track, which indicates higher resonance on right side. Similar to that of wind, the period of rotation depends on the proximity to the cyclone track, which increases with distance from the track. Complete rotation in wave direction was observed at DS1 location in AS (during December 1998 and May 1999) and at DS4-B location during the second cyclone in November 1998 in BoB.

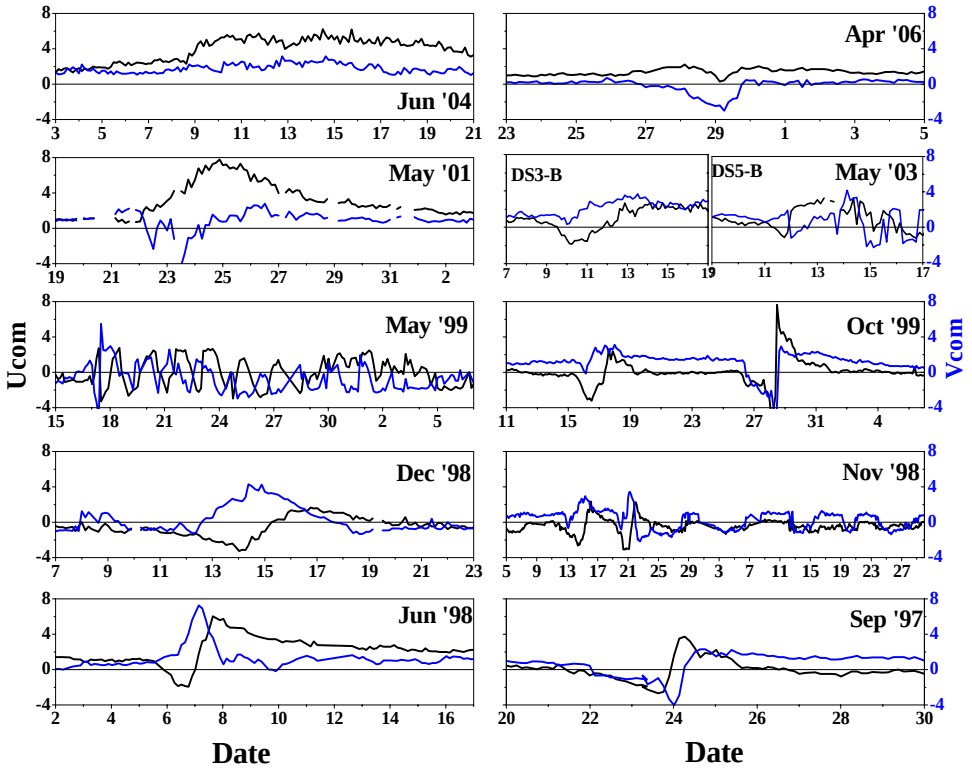

Fig.6.1: Wave velocity components during the passage of various cyclones in AS and BoB

The analysis of wave velocity components establishes the variable response on either side of the track (Fig. 6.1). The clockwise rotation is indicated by the phase lag of northward component ahead of eastward component and vice versa. Clockwise rotation during the first cyclone in October 1999 and anticlockwise rotation during the second cyclone at the same buoy location (DS4-B), signifies the importance of relative location. The successive zero crossing (Fig 6.1) indicates the time taken for the rotation which varies with distance from the track as observed at DS4-B during October 1999 cyclones.

The anomalous response in wave direction was observed during May 1999 cyclone and the second cyclone in November 1998, where the proximity to cyclone track was 27km in AS on the right side and, 102km in BoB again to the right side of the track, respectively. It was observed that waves started rotating in a clockwise direction and made several cycles similar to of inertial oscillation generated in ocean currents.

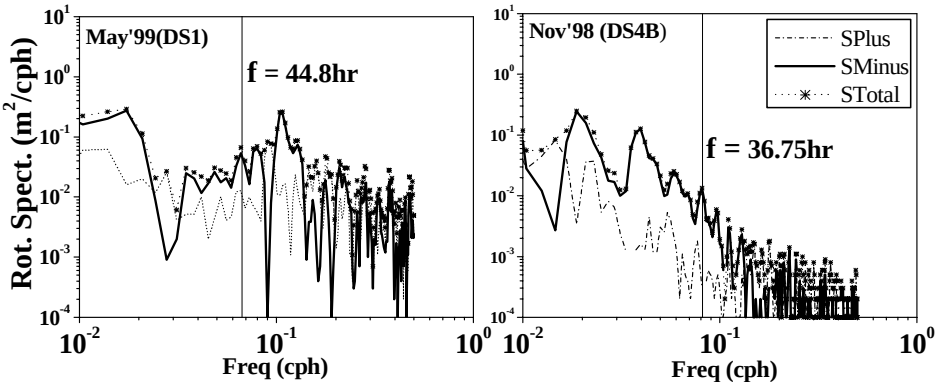

Fig.6.2: Rotary spectra of wave velocity components during May 1999 cyclone in AS and November 1998 cyclones in BoB

The wave direction exhibited nearly complete circles during May 1999 cyclone and semicircles during the second cyclone in November 1998 and lasted for a longer period. The period of rotation appears to be shorter in May 1999 and much higher during November 1998. The rotary spectral analysis of wave velocity component exhibited slight peak in the inertial band during both cyclones (Fig. 6.2). However the major peak during May 1999 corresponds to 27.8hr whereas that of November 1998 exhibited significant peaks at 159.9hr (weekly oscillation) and at 75.9hr.

It can be inferred that waves exhibit significant asymmetry on either side of the track and the response is observed at 100's of kilometers away from the track (DS1 buoy at 309km during December 1998 and DS4-B buoy at 497km away during November 1998a). The significant clockwise rotation in wave direction is observed on the right side of the track starting from near the track to far away locations. However the anticlockwise rotation in wave direction is observed over a shorter distance on the left side of the track and dissipates immediately. The response in wave height exhibits a rightward bias with maximum response at a few kilometers away from the track. The wave height also exhibited strong response near the track on the left side as observed during May 2001 in AS and during October 1999b in BoB combined with low cyclone translation speed and higher intensity of the cyclone.

6.4 Factors affecting the oceanic response

The oceanic response to cyclone passage in AS and BoB exhibits significant spatial and temporal variability, which depends on atmospheric and oceanic conditions. The study attempts to identify the major factors based on the moored buoy observations and TMI-SST, which constitute the major data set utilized for this study. The oceanic response also exhibits significant variability between AS and BoB. The cyclone characteristics near the buoy location and the buoy observed maximum responses (Table 6.2) reveal the complex nature of oceanic response to cyclones in AS and BoB.

6.4.1 Intensity of the cyclone

The intensity of the cyclone is considered as one of the important parameter(s) in determining oceanic response. The moored buoy observations and TMI-SST data during the passage of various cyclones indicate the significance of cyclone intensity in generating varied oceanic responses (Table 6.2).

The highest intensity experienced at DS1 location in AS is cy-2 during the passage of May 2001 cyclone, which accounts for the maximum cooling of 4.4^{o}C, and maximum wave height of 7.81m. The lesser intensity tropical storms during December 1998 and

June 2004 in AS could produce lesser response. Similarly the highest intensity cyclone in BoB (cy-4 cyclone in October 1999) recorded the highest wave height of 8.44m at DS4-B which establishes the role of intensity in oceanic response. The cooling observed in TMI-SST again reveals the maximum cooling corresponding to highest intensity cyclones in AS and BoB (Table 6.3). However the differential cooling produced by the same intensity cyclones in AS (cy-3 cyclones during June 1998, May 1999 and May 2001) and in BoB (cy-4 cyclones during October 1999a and April 2006) indicates the role of parameters other than cyclone intensity in oceanic response, which are discussed in the following sections.

6.4.2 Relative location and proximity to cyclone track

The studies on importance of relative location in oceanic response to cyclones (Price, 1981, Price *et al.,* 1994, Jacob *et al.,* 2000 and Morey *et al.,* 2006) reported rightward bias, owing to the asymmetry in wind field. The buoy observations scattered on either side of the track at variable distances provided the variability in oceanic response as a function of relative location and proximity to cyclone track.

There were two category cy-1 cyclones in AS during June 1998 and May 1999, in which the buoy was located on the right side of the track. The oceanic response during June 1998 (+163km) was much higher than May 1999 (+27km) in terms of wave height, current speed and cooling (Table 6.2) revealed the lower oceanic response nearly under the cyclone track. Among the two cyclones under the category TS cyclones in AS, the lesser response at DS1 during December 1998 than that of June 2004 is attributed to the larger distance from the cyclone track.

The differential response at buoy locations (DS3-A, DS4-B, DS5-A and SW6) during September 1997 cyclone in BoB clearly depicts the variable response owing to relative location and proximity to track. The higher response at DS4-A buoy (in terms of wave height, current speed and cooling) indicates strong response on the right side of the track whereas the lesser oceanic response at DS5-A even for higher wind speed, signifies weaker resonance on the left side of the track.

Table 6.2: Cyclone characteristics near the buoy location and the ocean parametric response to cyclones in AS and BoB inferred from moored buoy observations

Cyclone Period	Buoy-ID	Cycl. Category	Dist (km)	Cycl. Spd (m/s)	SLP (mb)	Wind Spd (m/s)	Wave Ht (m)	Cur. Spd (cm/s)	Drop in SST (^{o}C)
Jun-98	DS1	Cy-1	+163	3.76	997.4	24.64	7.66	130.1	3.27
Dec-98	DS1	TS	+309	5.57	1004.68	17.54	5	NA	0.95
May-99	DS1	Cy-1	+ 27	4.14	NA	35.49	6.41	104.3	1.47
May-01	DS1	Cy-2	-130	2.77	992.97	23.74	7.81	NA	4.4
Jun-04	DS1	TS	-156	0.87	999.38	22.31	6.72	NA	NA
Sep-97	SW6	TD	-345	0.64	1003.81	NA	NA	101.95	1.29
	DS3A	TD	+349	0.71	1004.69	15.04	4.53	56.25	0.39
	DS4A	TS	+151	6.1	995.7	20.05	6.25	148.8	2.25
	DS5A	TD	-35	1.94	994.9	22.54	4.53	98.44	1.07
Nov-98a	DS3A	TS	+26	4.68	NA	NA	NA	NA	NA
	DS4B	Cy-1	+497	4.14	1004.79	12.53	3.44	78.52	0.49
	DS5A	Cy-1	-166	4.78	1004.57	15.04	2.34	NA	0.83
Nov-98b	DS3A	TS	-241	6.58	NA	NA	NA	NA	NA
	DS4B	Cy-1	+102	4.58	998.63	17.96	4.53	71.42	0.74
	DS5A	TS	-640	4.44	NA	NA	NA	NA	NA
Oct-99a	DS3B	TS	-390	5.46	1001.86	12.53	2.34	92.58	0.14
	DS4B	Cy-1	+198	4.7	NA	NA	3.63	NA	NA
Oct-99b	DS3B	Cy-2	-554	4.48	1003.47	12.95	3.59	52.73	0.49
	DS4B	Cy-4	-78	4.05	NA	NA	8.44	NA	NA
May-03	DS3B	TS	+204	4.88	999.96	16.69	4.65	56.84	2.25
	DS5B	TS	-299	2.52	996.97	15.59	4.65	NA	1.23
	OB8	TS	-566	2.52	1000.02	15.4	3.56	NA	1.22
	MB11	TS	-357	1.55	994.4	17.58	NA	NA	NA
	MB12	TS	-354	4.49	999.14	17.07	4.16	NA	NA
Apr-06	DS5B	Cy-3	-911	2.63	1002.42	11.88	2.34	NA	NA
	OB8	TS	-879	2.35	1002.54	12.16	2.75	NA	NA
	MB10	Cy-1	-520	2.63	1003.77	11.41	NA	NA	0.22
	MB12	Cy-3	-473	4.94	NA	11.41	3.05	NA	NA

The DS4-B buoy was located at 198km on the right side of the track in BoB during the first cyclone in October 1999 and was on the left side (78km) during the second cyclone. The asymmetric response in wave indicates the importance of proximity to cyclone track. The DS3-B buoy located far away from the tracks did not indicate any significant change in any of the ocean parameters during both the cyclones that occurred in October 1999. Again the lesser response is observed at all buoys located far away (>500km) on the left side of the cyclone track during April 2006.

The buoy based observations on oceanic response on either side of the track reveals the proximity dependant variability in various parameters. It is observed that resonance with wind generates higher response in surface current, wave and SST on the right side of the track and it lasts for a longer duration. The maximum oceanic response is observed at a few kilometers away on right side of the track. However strong response in SST and wave is also observed near left side of the track (May 2001 in AS and October 1999b in BoB), in which the response is also contributed by the intensity and low cyclone translation speed.

6.4.3 Cyclone translation speed

The oceanic response to cyclone passage in AS and BoB revealed the importance of cyclone translation speed. The June 2004 cyclone belong to the category of TS, but generated significant wave height of 6.72m at DS1 locations in AS, which is located at 156km away on the left side of the track (Table 6.3). The response in wave is comparable to that generated by more intense cyclones on the right side of the track and is attributed to the lowest cyclone translation speed of 0.87m/s. Similarly higher response at DS1 location again on the left side of the track during May 2001 with a speed of 2.77m/s establishes the role of cyclone translation speed in AS. Again one of the reason behind the lower oceanic response during May 1999 cyclone at DS1 located near the track on the right side is attributed to the higher cyclone translation speed of 4.14m/s.

The intensity experienced at all buoy locations are only under category TS and the cyclone translation speed is low during May 2003 in BoB. Even though the buoys were

located at larger distances (>200km), the impact brought about significant drop of 2.25^{o}C in SST and caused a wave height of 4.65m at DS3-B.

Table 6.3: Surface cooling estimated from moored buoys and TMI-SST during the passage of cyclones in AS and BoB

Cyclone Period	Buoy-ID	Cyclone Response at Buoy Location						TMI-SST at Max. Cyclone Intensity				
		Cycl. Category	Dist (km)	Cycl. Spd (m/s)	pre-SST_{max} (^{o}C)	post-SST_{min} (^{o}C)	Drop in SST (^{o}C)	Cycl. Category	Cycl. Spd (m/s)	pre-SST_{max} (^{o}C)	post-SST_{min} (^{o}C)	Max. Drop in SST (^{o}C)
Jun-98	DS1	Cy-1	+163	3.76	31.33	28.06	3.27	Cy-3	4.93	30.9	25.65	5.25
Dec-98	DS1	TS	+309	5.57	28.18	27.23	0.95	Cy-1	3.62	27.3	24.9	2.4
May-99	DS1	Cy-1	+ 27	4.14	29.96	28.55	1.41	Cy-3	3.59	29.5	24	5.5
May-01	DS1	Cy-2	-130	2.77	30.92	26.52	4.4	Cy-3	2.34	30.3	22.8	7.5
Jun-04	DS1	TS	-156	0.87	NA	NA	NA	TS	2.56	29.93	27.68	2.25
Sep-97	SW6	TD	-345	0.64	28.2	26.91	1.29	Cy-1	6.61	--	--	--
	DS3A	TD	+349	0.71	29.28	28.89	0.39					
	DS4A	TS	+151	6.1	30.74	28.49	2.25					
	DS5A	TD	- 35	1.94	29.42	28.35	1.07					
Nov-98a	DS4B	CY-1	+497	4.14	29.57	29.08	0.49	Cy-2	5.39	29.4	27.9	1.5
	DS5A	CY-1	-166	4.78	29.33	28.5	0.83					
Nov-98b	DS4B	Cy-1	+102	4.58	29.77	29.03	0.74	Cy-1	3.89	29.25	28.65	0.6
Oct-99a	DS3B	TS	-390	5.46	29.47	29.33	0.14	Cy-4	3.32	30.15	26.7	3.45
Oct-99b	DS3B	CY-2	-554	4.48	29.52	29.03	0.49	Cy-5	3.54	29.1	25.05	4.05
May-03	DS3B	TS	+204	4.88	31.04	28.52	2.25	TS	1.88	31.05	27.76	3.3
	DS5B	TS	-299	2.52	29.29	28.06	1.23					
	OB8	TS	-566	2.52	30.57	29.35	1.22					
Apr-06	MB10	Cy-1	-520	2.63	30.11	29.89	0.22	Cy-4	4.38	30.6	27.3	3.3

The TMI-SST data during cyclones also exhibited the strong correlation between surface cooling and cyclone translation speed (Table 6.3). A maximum cooling of 7.5^{o}C was observed after the passage of AS cyclone in May 2001, which is more than that brought about by cyclones of same intensity (cy-3) during June 1998 (5.25^{o}C) and May 1999 (5.5^{o}C). The May 2003 tropical storm in BoB accounted for a considerable cooling of

3.3°C, same as that of the cy-4 cyclone during April-2006. The May 2001 (2.34m/s) and May 2003 (1.88m/s) cyclones belong to the category of slow moving whereas the May 1999 (3.59m/s) and April 2006 (4.38m/s) cyclones belong to the category of moderate speed cyclones. The maximum cooling observed during May 2001 cyclone is closest to the track, which indicates the reduced rightward bias for cyclones with low cyclone translation speed. This supports the fact that slow moving cyclones induce higher response than that of fast moving cyclones and this reveals that the surface cooling depends more on the cyclone translation speed than the intensity in AS and BoB.

6.4.4 Differential response between AS and BoB

The surface cooling associated with cyclone passage in AS and BoB exhibited significant variability in the degree of cooling and extent (spatial and temporal) of response. TMI-SST revealed the striking difference in surface cooling between AS and BoB (Fig. 6.3). Even though the pre-cyclonic temperature in BoB during pre-monsoon (>30.0°C) and post-monsoon (>28.0°C) are higher than that of AS (>29.0°C and >27.0°C respectively), the associated cooling in AS is much higher than that of BoB.

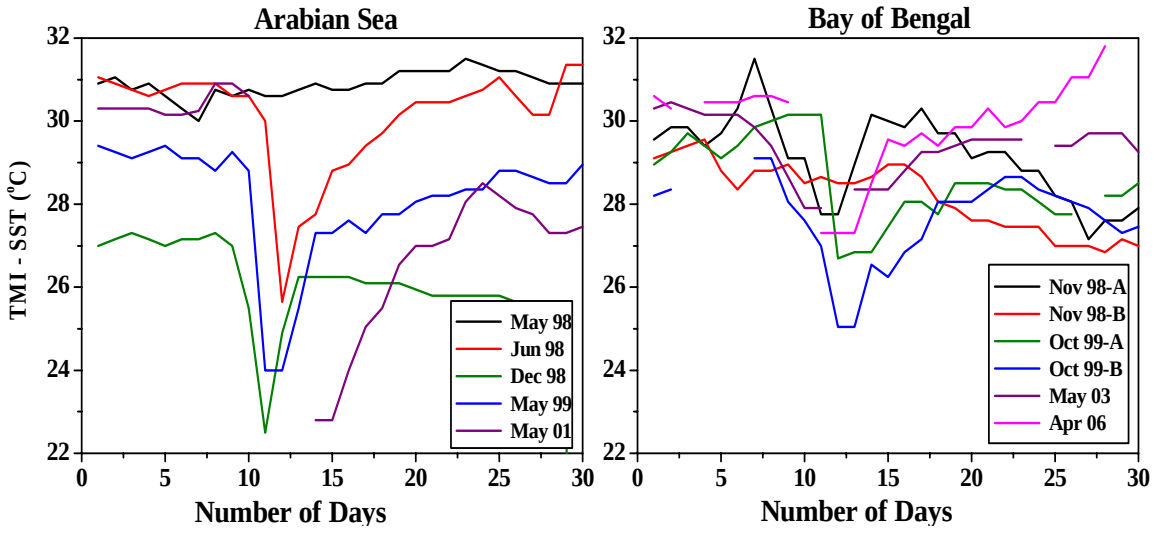

Fig.6.3: Cooling observed in TMI-SST during the passage of cyclones in AS and BoB

Category cy-3 cyclones in AS produced a cooling of more than 5^{o}C during June 1998 (5.25^{o}C), May 1999 (5.5^{o}C) and May 2001 (7.5^{o}C) whereas cy-4 cyclones in BoB could produce only 3.45^{o}C of cooling during October 1999a and 3.3^{o}C during April 2006. The TMI-SST also exhibits significant cooling for a longer duration over a wider longitudinal belt in AS whereas the spatial and temporal extent of surface cooling is limited in BoB. The occurrence of cyclones in BoB exhibited passage of a cyclone immediately after the passage of another cyclone (during November 1998 and October 1999), which is not reported in AS. It is also observed that most of the cyclones in BoB attained maximum intensity just before land fall whereas that of AS attained maximum intensity in the deep ocean (except during June 1998) and made landfall during the dissipating phase. The wide spread cooling associated with cyclone passage could be the reason which limits the immediate formation of another cyclone in AS.

6.5 Summary

The present study on upper ocean responses to atmospheric forcing (associated with cyclone passage) in North Indian Ocean revealed significant variability between AS and BoB. The analysis of cyclone frequency during 1947 to 2006 exhibited lesser frequency of cyclones in AS than that of BoB. The analysis also revealed significant reduction in cyclone frequency after the year 1976 with substantial reduction during monsoon season. The long term SST data at selected points in AS and BoB could not reveal any relation with reduction in cyclone frequency. However the SLP at same locations exhibited considerable increase during mid 1970's, which could have contributed to the observed reduction in cyclone frequency after the year 1976.

The response in waves during cyclone passage exhibited significant asymmetry on either side of the track in AS and BoB and the response is observed at 100's of kilometers away from the track. The significant clockwise rotation in wave direction is observed on the right side of the track starting from near the track to far away locations, which existed for a longer duration. However, the anticlockwise rotation in wave direction is observed over a shorter distance on the left side of the track and dissipated immediately.

Inertial oscillation is observed in surface current and in the mixed layer temperature associated with cyclone passage, which revealed the role of relative location(s) on either side of the track. The inertial peak closer to the local inertial period indicates maximum transfer of energy during the cyclone passage in both AS and BoB. The absence of strong inertial oscillation even with clockwise rotation in surface current and wind indicates the dominant role of duration of strong wind in generating inertial oscillation.

The oceanic response associated with cyclone passage reveal the variable response(s) which depends on cyclone intensity, the proximity to track and cyclone translation speed. It is observed that resonance with wind generates higher response in surface current, wave and SST on the right side of the track and it lasts for a longer duration. The maximum oceanic response is observed at a few kilometers away on right side of the track. However lesser rightward bias in the location of maximum cooling is observed for cyclones with low cyclone translation speed. The response on the left side of the track is less and is limited over a shorter distance and dissipates immediately. It is observed that the ocean response, in general, increases with intensity of cyclones. However the differential cooling produced by the same intensity cyclones in AS and in BoB indicates the dominant role of low cyclone translation speed in oceanic response.

The surface cooling exhibited strikingly differential responses between AS and BoB. The TMI-SST and buoy observations exhibited significant cooling for a longer duration in AS compared to that of BoB. The spatial extent of cooling is also much higher in AS than that of BoB. The wide spread cooling associated with cyclone passage in AS indicates the dominant role of thermal structure in oceanic response in AS than that of BoB.

------- ***-------

References

Ali, A. and J. U. Chowdhury, 1997. Tropical cyclone risk assessment with special reference to Bangladesh. *Mausam*, 48, 305–322.

Ali, A., 1999. Climate change impacts and adaptation assessment in Bangladesh, *Clim. Res.*, 12, 109–116.

Allan, R., and T. Ansell, 2006. A New Globally Complete Monthly Historical Gridded Mean Sea Level Pressure Dataset (HadSLP2): 1850-2004. *J. Climate*, 19, 5816-5842

Asnani, G. C., 2005. Tropical Meteorology, Vol. II, Praveen Printing Press, Pune, India.

Bhaskar Rao, D. V. and D. Hariprasad, 2006. Numerical prediction of the Orissa super cyclone (1999): Sensitivity to the parameterisation of convection, boundary layer and explicit moisture processes. *Mausam*, 57, 61-78.

Black, P. G., 1983. Tropical storm structure revealed by stereoscopic photographs from Skylab. *Adv. Space Res.,* 2, 115–124.

Brink, K. H., 1989. Observations of the response of thermocline currents to a hurricane. *J. Phys. Oceanogr.*, 19, 1017-1022.

Cardone, V.J., D.B. Ross and M.R. Athrens, 1977. An experiment in forecasting hurricane generated sea state. Preprints *11th Tech. Conf. Hurricanes and Tropical Meteorology*, Miami Beach, *Am. Meteor. Soc*., 688-695.

Chambers, J. M., W. S. Cleveland, B. Kleiner and P. A. Tukey, 1983. Graphical Methods for Data Analysis. Wadsworth, Belmont, Chap. 6.

Chang, S.W. and R.A. Anthes, 1978. Numerical simulations of the ocean's nonlinear baroclinic response to translating hurricanes. *J. Phys. Oceanogr*. , 8, 468-480.

Chen, C. and L. Xie, 1997. A numerical study of wind-induced, near-inertial oscillations over the Texas–Louisiana shelf. *J. Geophys. Res*, 102**,** 15583–15593.

Chintalu, G.R., P. Seetaramayya, M. Ravichandran and P.N. Mahajan, 2001. Response of the Bay of Bengal to Gopalpur and Paradip super cyclones during 15-31 October 1999. *Curr. Sci.*, 81, 283-291.

Chiswell, S., 2003. Deep equatorward propagation of inertial oscillations. *Geophys. Res. Lett.*, 30, doi:10.1029/2003GL017057.

Cione, J. J. and E. W. Uhlhorn, 2003. Sea surface temperature variability in hurricanes: Implications with respect to intensity change. *Mon. Weather Rev.*, 131, 1783-1796.

Data Buoy System Manual, 2006: National Institute of Ocean Technology, India

Deo, A.A., P.S. Salvekar and S. K. Behera, 2001. Oceanic response to cyclone moving in different directions over Indian Ocean using IRG model. *Mausam*, 52, 163-174.

Dickey, T., D. Frye, J. McNeil, D. Manov, N. Nelson, D. Sigurdson, H. Jannasch, D. Siegal, T. Michaels and R. Johnson, 1998. Upper-Ocean temperature response to hurricane Felix as measured by the Bermuda testbed mooring, *Mon. Weather Rev*., 126, 1195-1201.

Dube, S. K., Rao, A. D., Sinha, P. C., Murty, T. S. and N. Bahulayan, 1997. Storm surge in the Bay of Bengal and Arabian Sea: The problem and its prediction, *Mausam*, 48, 283–304.

Elipot S., R. Lumpkin, and G. Prieto, 2010. Modification of inertial oscillations by the mesoscale eddy field. *J. Geophys. Res*, 115, C09010, 20. doi:10.1029/2009JC005679

Elsner, J. B., J. P., Kossin, and T. H., Jagger, 2008. The increasing intensity of the strongest tropical cyclones. *Nature* 455, 92-95.

Emery, W. J. and R. E. Thomson, 1997. Data analysis methods in Physical Oceanography. Elsevier Science, New York, 431.

Emmanual, K. N., 1995. Sensitivity of Tropical Cyclones to Surface Exchange Coefficients and a Revised Steady-State Model incorporating Eye Dynamics. *J. Atm. Sci.*, 52, 3969–3976.

Faulkner, D., (2000. Rogue Waves – Defining Their Characteristics for Marine Design. Workshop on Rogue Waves 2000, 3-18. Brest, France.

Federov, K.N., A. A. Varfolomeev, A. I. Ginzburg, A. G. Zatsepin, A. Yu. Krasnopevtsev, A. G. Ostrovsky and V. E. Skylarov, 1979. Thermal reaction of the ocean on the passage of the hurricane Ella. *Okeanologiya*, 19, 9992-1001.

Firing, E., R. C. Lien and P. Muller, 1997. Observations of strong inertial oscillations after the passage of tropical cyclone Ofa. *J. Geophys. Res*., 102, 3317-3322.

Folland, C. K., and D. E. Parker, 1990. Observed variations of sea surface temperature. Climate–Ocean Interaction, Ed., M. E. Schlesinger, Kluwer, Netherlands, 21–52.

Garret, C., 2001. What is the "Near Inertial" band and why is it different from the rest of the internal wave spectrum? *J. Phys. Oceanogr.*, 31, 962-971.

Geisler, J. E., 1970. Linear theory of the response of a two layer ocean to a moving hurricane. *Geophys. Fluid Dyn.*, 1, 249–272.

Gill, A.E., 1984. On the behaviour of internal waves in the wakes of storms. *J. Phys. Oceanogr*., 14, 1129-1151.

Ginis, I. and K. Z. Dikiniov, 1989. Modelling the effect of typhoon Virginia (1978) on the ocean. *Sov. Meteorol. Hydrol*., 7, 53–60.

Goldenberg, S. B., C.W. Landsea, A. M. Mestas-Nuñez and W.M. Gray, 2001.The Recent Increase in Atlantic Hurricane Activity: Causes and Implications, *Sci.* 293,474-479.

Gonella, J., 1971. A local study of inertial oscillations in the upper layers of the ocean. *Deep Sea Res.*, 18, 775 - 788.

Gonella, J., 1972. A rotary-component method for analyzing meteorological and oceanographic vector time series. *Deep Sea Res.*, 19, 833 - 846.

Gray, W. M., 1979. Tropical cyclone origin, movement and intensity characteristics based on data compositing techniques. NEPRF CR 79- 06. U.S. Navy, pp. 126.

Hareesh Kumar, P. V., C. V. K. Prasada Rao, J. Swain and P. Madhusoodanan, 2001. Intra-seasonal oscillations in the central Bay of Bengal during summer monsoon 1999. *Curr. Sci.*, 80, 786-790.

Holland, G. J., and P. J. Webster, 2007. Heightened tropical cyclone activity in the north atlantic: natural variability or climate trend?, *Philosophical Transactions of The Royal Society* 365, 2695-2716.

India Meteorological Department (IMD), 1979. Tracks of storms and depressions in the BoB and AS (1877-1970). New Delhi, India.

India Meteorology Department (IMD), 1992. Tracks of storms and depressions in the BoB and AS (1971-1990). New Delhi, India.

Jacob, D. S., L. K. Shay, A. J. Mariano and P. G. Black, 2000. The three-dimensional mixed layer heat balance during hurricane Gilbert. *J. Phys. Oceanogr*., 30, 1407-1429.

Jacobs, G. A., J. W. Book, H. T. Perkins and W. J. Teague, 2001. Inertial oscillations in the Korea Strait. *J. Geophys. Res.*, 106, 26943-26958.

Jenkins, G. M. and D. G. Watts, 1968. Spectral analysis and its applications. Holden-Day, San Francisco.

Joseph, K. J., A. N. Balchand, P. V. Hareeshkumar and G. Rajesh, 2007. Inertial oscillation forced by the September 1997 cyclone in the Bay of Bengal, *Curr. Sci.,* 92, 795-798.

Kalsi, S. R. and K. B. Srivastava, 2006. Characteristic features of Orissa super cyclone of 29th October, 1999 as observed through CDR Paradip. *Mausam*, 57, 21-30.

Kalsi, S. R., 2006. Orissa super cyclone – A Synopsis. *Mausam*, 57, 1-20.

Krajcar, V. and M. Orlic, 1995. Seasonal variability of inertial oscillations in the Northern Adriatic. *Cont. Shelf Res.,* 15, 1221-1233.

Kumar, V. S., K. Ashok Kumar and N. M Anand, 2000. Characteristics of waves off Goa, West coast of India. *J. Coast. Res.*, 16, 782-789.

Kumar, V. S., K. Ashok Kumar and N. S. N. Raju, 2004.Wave characteristics off Visakhapatnam coast during a cyclone. *Curr. Sci.,* 86, 524-527.

Kumar, V. S., S. Mandal and K. A. Kumar, 2003. Estimation of wind speed and wave height during cyclones. *Ocean Eng.,* 30, 2239-2253.

Kumar, V. S., S. Mandal, A. M.. Manish and S. P. Rupali, 2001. Estimation of wind speeds and wave heights from tropical cyclones during 1961 to 1982, Technical Report, National Institute of Oceanography, NIO/TR-3/2001, 85 p.

Kundu, P. K., 1976. An analysis of inertial oscillations observed near Oregon coast. *J. Phys. Oceanogr.*, 6, 879-893.

Kundu, P. K., and R. E. Thomson, 1985. Inertial oscillations due to a moving front. *J. Phys. Oceanogr.,* 15, 1076–1084.

Lal D.S., 1991. Climatology, Chaitanya Publishing House, Allahabad, India.

Lander M.A. and C. P. Guard, 1998. A Look at Global Tropical Cyclone Activity during 1995: Contrasting High Atlantic Activity with Low Activity in Other Basins, *Am. Met. Soc.,* 126,1163-1173

Levitus, S., 1982. Climatological Atlas of the World Ocean, NOAA/ERL GFDL Professional Paper 13, Princeton, N.J., 173 pp. (NTISPB83-184093)

Lien, R.C., M. J. McPhaden and M. C. Gregg, 1996. High-frequency internal waves in the Upper Central Equatorial Pacific and their possible relationship to deep-cycle turbulence, *J. Phys. Oceanogr.*, 261, 581-600.

Loe, B. R., B. L. Verma, R. K. Giri, S. Bali and L. R. Meena, 2006. Recent very severe tropical cyclones over the Bay of Bengal : Analysis with satellite data. *Mausam*, 57, 37-46.

Madhu, N. V., P. A. Maheswaran, R. Jyothibabu, V. Sunil, C. Revichandran, T. Balasubramanian, T. C. Gopalakrishnan and K. K. C. Nair, 2002. Enhanced biological production off Chennai triggered by October 1999 super cyclone (Orissa). C*urr. Sci.*, 82, 1472-1479.

Mahapatra, D. K., A. D. Rao, S. V. Babu and C. Srinivas, 2007. Influence of coast line on upper ocean's response to the tropical cyclone, *Geo. Phys. Res. Letters*, 34, L17603, doi:10.1029/2007GL030410.

McBride, J. L., 1995. Tropical cyclone formation. In Global perspectives on tropical cyclone, Ed. R.L. Elsberry. WMO/TD-No. 693, TCP-38, WMO, Geneva, 63-105.

McCabe G. J., M. P. Clark and M. C. Serreze, 2001. Trends in northern hemisphere surface cyclone frequency and intensity. *J. Clim.*, 14, 2763-2768.

Menon, P. A., 1997. Our Weather, National Book Trust, India.

Miller, A. J., D. R. Cayan, T. P. Barnett, N. E. Graham and J. M. Oberhuber, 1993: The 1976–77 climate shift of the Pacific Ocean. *J. Oceanogr.*, 7, 21–26.

Millot, C. and M. Crepon, 1981. Inertial oscillations on the continental shelf of the Gulf of Lions-Observations and theory. *J. Phys. Oceanogr.*, 11, 639-657.

Mooers, C. N. K., 1975. Several effects of a baroclinic current on the cross-stream propagation of inertial-internal waves. *Geophys. Astrophys. Fluid Dyn.*, 6, 245-275.

Morey, S. L., S. Baig, M. A. Bourassa, D. S. Dukhovskoy and J. J. O'Brien, 2006a. Remote forcing contribution to storm-induced sea level rise during Hurricane Dennis. *Geo. Phys. Res. Lett.*, 33, doi:10.1029/2006GL027021.

Morey, S. L., M. A. Bourassa, D. S. Dukhovskoy and J. J. O'Brien, 2006b. Modeling studies of the upper ocean response to a tropical cyclone. *Ocean Dynamics*, 56, 594-606.

Nayak, S. R., R. K. Sarangi and A. S. Rajawat, 2001. Applications of IRS-P4 OCM data to study the impact of cyclone on coastal environment of Orissa. *Curr. Sci.*, 80, 1208–1213.

Neumann, C. J., 1993. Global overview. Chapter 1, Global guide to tropical cyclone forecasting. WMO, Geneva.

Neumann, G., and W.J., Pierson, 1966. Principles of physical oceanography. Prentice-Hall. Englewood Cliffs. 545 pp.

Panofsky, H. A. and J. A. Dutton, 1984. Atmospheric Turbulence. John Wiley and Sons, New York, pp. 397.

Pedlosky, J. and H. Stommel, 1993. Self-sustained inertial oscillations. *J. Phys. Oceanogr.*, 23, 1800-1808.

Perkins, H., 1972. Inertial oscillations in the Mediterranean. *Deep Sea Res.,* 19, 289-296.

Perkins, H., 1976. Observed effect of an eddy on inertial oscillations. *Deep Sea Res.*, 23, 1037-1042.

Pielke, Jr., R. A., C. Landsea, M. Mayfield, J. Laver and R. Pasch, 2005. Hurricanes and global warming, *Bull. of Am. Met. Soc*., 86:1571-1575.

Pollard R. T., 1980. Properties of near-surface inertial oscillations. *J. Phys. Oceanogr.,* 10, 385-398.

Pollard, R. T. and R. C. Millard Jr., 1970. Comparison between observed and simulated wind-generated inertial oscillations. *Deep Sea Res.*, 17, 813-821.

Pollard, R. T., 1970. On the generation by winds of inertial waves in the ocean. *Deep Sea Res.*, 17, 795-812.

Pond, S. and G. L. Pickard, 1986. Introductory Dynamical Oceanography. Pergamon Press. p. 64.

Poulain, P., 1990. Near-Inertial and Diurnal Motions in the Trajectories of Mixed Layer Drifters. *J. Mar. Res.*, 48, 793–823.

Poulain, P. M., D. S. Luther and W. C. Patzert, 1992. Deriving inertial wave characteristics from surface drifter velocities: Frequency variability in the tropical Pacific. *J. Geophys. Res.*, 97, 17947-17959.

Premkumar, K., M. Ravichandran, S. R. Kalsi, D. Sengupta and S. Gadgil, 2000. First results from a new observational system over the Indian seas. *Curr. Sci.*, 78, 323-333.

Press, W. H., B. P., Flannery, S. A., Teukolsky, and W. T., Vetterling, 1992. Numerical Recipes in C: The Art of Scientific Computing. Cambridge University Press, Cambridge (UK) and New York, 2nd edition.

Price, J. F., 1981. Upper ocean response to a hurricane. *J. Phys. Oceanogr*., 11, 153-175.

Price, J. F., 1983. Internal wave wake of a moving storm. Part I: Scales, energy budget and observations. *J. Phys. Oceanogr.,* 13, 949-965.

Price, J. F., T. B. Sanford and G. Z. Forristall, 1994. Forced stage response to a moving hurricane. *J. Phys. Oceanogr*., 24, 233-260.

Pudov, V. D., A. A. Varfolomeev and K. N. Federov, 1979. Vertical structure of the wake of a typhoon in the upper ocean. *Okeanologiya*, 21, 142-146.

Rajesh G., K. J. Joseph, M. Harikrishnan and K. Premkumar, 2005. Extreme observations of Meteorological and Oceanographic parameters in Indian Seas. *Curr. Sci.*, 88, 1279-1282.

Rao R. R., K. V. S. Kumar and B. Mathew, 1991. Observed variability in the current field during summer monsoon experiments. I: Northern Bay of Bengal. *Mausam*, 42, 17-24.

Rao, R. R. and R. Sivakumar, 1998. Observed seasonal variability of heat content in the upper layers of the tropical Indian Ocean from a new global ocean temperature climatology. *Deep Sea Res.*, 45, 67-89.

Rao, R.R., 1986. Cooling and deepening of the mixed layer in the central Arabian Sea during Monsoon-77 : Observations and simulations. *Deep Sea Res.*, 33, 1413-1424.

Rao, R. R., 1987. Further analysis on the thermal response of the upper Bay of Bengal to the forcing of pre-monsoon cyclonic storm and summer monsoonal onset during MONEX-79. *Mausam*, 38, 147-156.

Rao, R. R., K. V. S. Kumar and B. Mathew, 1996. Observed variability in the current field during summer monsoon experiments. Arabian Sea. *Mausam*, 47, 355-368.

Rao, R. R., R. L. Molinari and J. F. Fiesta, 1989. Evolution of the climatological near surface thermal structure of the tropical Indian Ocean. Description of mean monthly mixed layer depth, sea surface temperature, surface current and surface meteorological fields. *J. Geophys. Res.,* 94, 10801-10815.

Rao, Y. R. and K. Premkumar, 1998. A preliminary analysis of meteorological and oceanographic observations during the passage of a tropical cyclone in Bay of Bengal. Tech. Note TR001/98, National Institute of Ocean Technology, Chennai.

Reed, M., C. Turner, A. Odulo, S. E. Sorstrom and J.P. Mathisen, 1990. Final report appendices - Field Evaluation of satellite-tracked surface drifting buoys in simulating the movement of spilled oil in the marine environment, *Applied Science Associates, Inc*., ASA 88-31.

Ripa, P., 1997. Inertial oscillations and the β-plane approximations. *J. Phys. Oceanogr.,* 27, 633-647.

Rivas, A.L. and A.R. Piola, 2005. Near Inertial oscillations at the shelf off northern Patagonia. *Atlantica, Rio Grande*, 27, 75-86.

Sadhuram, Y., 2004. Record decrease of sea surface temperature following the passage of a super cyclone over the Bay of Bengal. *Curr. Sci.*, 86, 383-384.

Saji, P.K., S. C. Shenoi, A. Almeida and G. Rao, 2000. Inertial currents in the Indian Ocean derived from satellite tracked surface drifters. *Oceanologica Acta*, 23, 635-640.

Sanil Kumar K.V., P.V. Hareesh Kumar, K Jossia Joseph, J.K. Panigrahi, 2004. Arabian Sea mini warm pool during May 2000. *Current Science,* 86(1), 180-184

Salat, J., J. Tintoré, J. Font, D. P. Wang and M. Vieira, 1992. Near-inertial motion on the shelf-slope front off northeast Spain. *J. Geophys. Res.*, 97, 7277-7281.

Sanford, T. B., Black, P. G., Haustein, J. R., Feeney, J. W., Forristall, G. Z. and Price, J. F.,1987. Ocean response to a hurricane Part 1: Observations, *J. Phys. Oceanogr.,* 17, 2065–2083.

Sengupta D., B. R. Goddalehundi and D. S. Anitha, 2007. Cyclone-induced mixing does not cool SST in the post-monsoon north Bay of Bengal. *Atm. Sci. Lett.*, 9, 1 – 6.

Sengupta D., P. K. Ray and G. S. Bhat, 2002. Spring Warming of the Eastern Arabian Sea and Bay of Bengal from Buoy Data. *Geophys. Res. Lett.*, 29, 10.1029/2002GL015340.

Shay, L. K. and S. W. Chang, 1997. Free surface effects on the near-inertial ocean current response to a hurricane: A revisit. *J. Phys. Oceanogr*., 27, 23-39.

Shay, L. K., Black, P. G., Mariano, A. J., Hawkins, J. D. and Elsberry, R. L., 1992. Upper ocean response to Hurricane Gilbert. *J. Geophys. Res.,* 97, 20227–20248.

Shenoi S. S. C., D. Shankar and S. R. Shetye, 2002. Differences in heat budgets of the near-surface Arabian Sea and Bay of Bengal: Implications for the summer monsoon. *J. Geophys. Res.,* 107, doi:10.1029/2000JC000679.

Shenoi, S. S. C. and M. K. Antony, 1991. Current measurements over the western continental shelf of India. *Cont. Shelf Res.,* 11, 81-93.

Shiah F. K., S. W, Chung, S. J. Kao, G. C. Gong and K. K. Liu, 2000. Biological and hydrographical responses to tropical cyclones (typhoons) in the continental shelf of the Taiwan Strait. *Cont. Shelf Res.*, 20, 2029-2044.

Singh, O. P., T. M. Khan and M. S. Rahman, 2001a. Has the frequency of intense tropical cyclones increased in the north Indian Ocean? *Curr. Sci.*, 80, 575-580.

Singh, O. P., T. M. Khan and M. S. Rahman, 2001b. Probable reasons for enhanced cyclogenesis in the Bay of Bengal during July-August of ENSO years. *Global Planet. Change*s, 29, 135-147.

Smith, T.M., R. W. Reynolds, T. C. Peterson, and J. Lawrimore, 2008. Improvements to NOAA's historical merged land-ocean surface temperature analysis (1880-2006). *J. Climate*, 21, 2283-2296

Smitha, A., K. H. Rao and D. Sengupta, 2006. Effect of May 2003 Tropical Cyclone on physical and biological processes in the Bay of Bengal. *Int. J. Remote Sens.,* 27, 5301 - 5314.

Stramma, L., Cornillon, P. and Price, J. F., 1986. Satellite observations of sea-surface cooling by hurricanes. *J. Geophys. Res.,* 91, 5031–5035.

Thomson, R. E., P. H. LeBlond and A. B. Rabinovich, 1998. Satellite-tracked drifter measurements of inertial and semidiurnal currents in the northeast Pacific. *J. Geophys. Res.,* 103, 1039-1071.

Thrane, B.P., 1999. Information technology used in Seawatch Indonesia. Proceedings of the international seminar on application of seawatch Indonesia information system for Indonesian Marine Resources Development, March 10-11, 1999, BPPT, Jakarta.

Torsethaugen, K., and H., Krogstad, 1979. NEPTUN—A Computer Program for the Analysis of Ocean Wave Records, *Cont. Shelf Inst*., 218(1),

Trenberth, K. E., 1990: Recent observed interdecadal climate changes in the Northern Hemisphere. *Bull. Amer. Meteor. Soc*., 71, 988–993.

Trenberth, K. E., 2005. Uncertainty in hurricanes and global warming, *Sci.*, 308, 1753–1754.

Vinayachandran P. N., V. S. N. Murty and V. Ramesh Babu, 2002. Observations of barrier layer formation in the Bay of Bengal during summer monsoon, *J. Geophys. Res.*, 107, doi:10.1029/2001JC000831

Vinayachandran, P. N. and S. Mathew 2003: Phytoplankton bloom in the Bay of Bengal during the northeast monsoon and its intensification by cyclones, *Geophys. Res. Lett.*, 30, doi:10.1029/2002GL016717.

Vinayachandran P. N., J. P. McCreary, R. R. Hood and K. Kohler, 2005, A numerical investigation of the phytoplankton blooms in the Bay of Bengal during northeast monsoon. *J. Geophys. Res.*, 110, doi:10.1029/2005JC002966.

Webster, F., 1968. Observations of inertial period motions in the deep sea. *Rev. Geophys.*, 6, 473-490.

Webster, P. J., G. J. Holland, J. A. Curry and H. R. Chang, 2005. Changes in tropical cyclone number, duration, and intensity in a warming environment. *Science,* 309, 1844–1846.

Weller, R. A., 1982. The relation of near-inertial motions observed in the mixed layer during the JASIN (1978) Experiment to the local wind stress and to the quasi-geostrophic flow field. *J. Phys. Oceaogr.*, 12, 1122-1136.

White, W. B., 1972. Doppler shift in the frequency of the inertial waves observed in moored spectra. *Deep Sea Res.*, 19, 595-600.

Young, I.R., 1988. Parametric Hurricane Wave Prediction Model. J. *Waterw., Port, Coastal, Ocean Eng.* ASCE, 114, 637-652.

Young I. R. and G. P. Burchell, 1996. Hurricane generated waves as observed by satellite. *Ocean Engg.,* 23 (8), 761-776.

Young I.R., 2003. A review of the sea state generated by hurricanes. *Mar. Struct.* 16, 201–218.